Bundesministerium für Bildung und Forschung

On the Phase Front of Neutron Detection

TU München E21 Seminar: Neutronen in der Forschung und Industrie
16. November 2015

Physikalisches Institut

Ruprecht-Karls-Universität Heidelberg

Markus Köhli

U. Schmidt

ANP-PAT

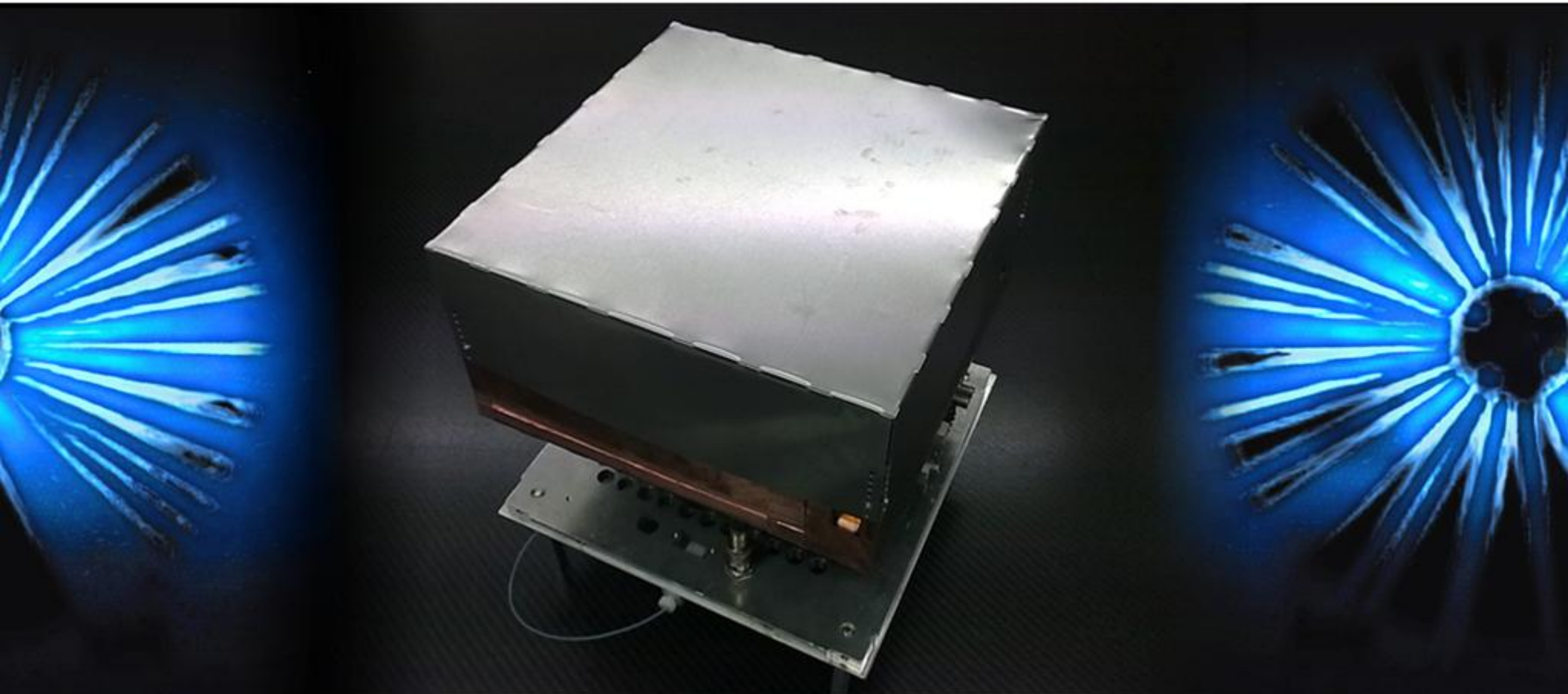

Heidelberg Research Fields

Helium-Xenon EDM
[test of Lorentz invariance]

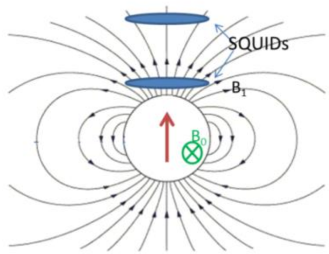

PERC and PERKEO
[V_{ud} via neutron beta decay]

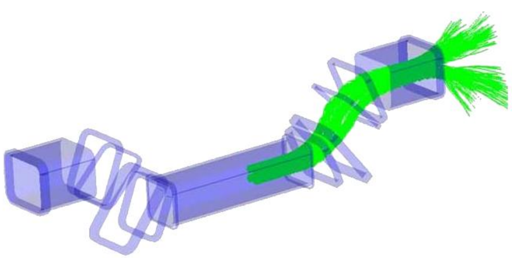

^{10}B Neutron Detectors
[large area and high time resolution]

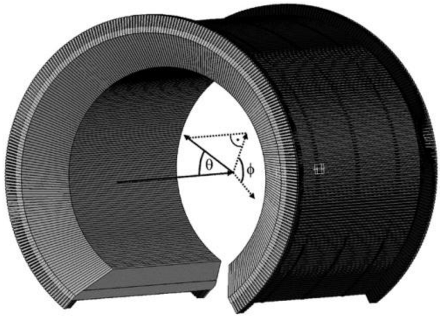

Spin Echo

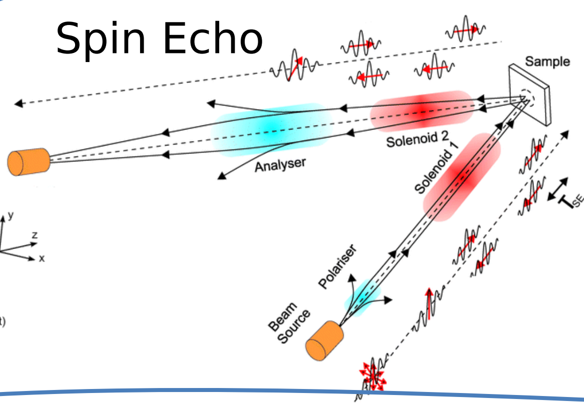

Atomic Beam Spin Echo
[Berry phase and Casimir force]

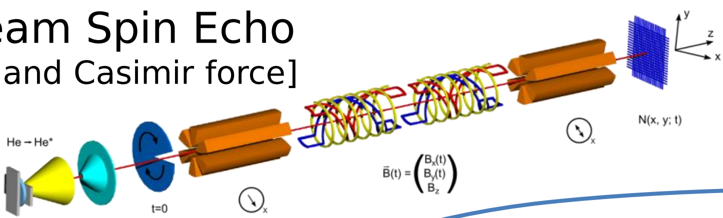

The Phase Fronts

- Cosmic Ray Neutrons (Outside the Reactor)
- Neutron Detection
- Novel Detectors
- CASCADE (at the MIRA and RESEDA spectrometer)
- Spin Echo

Heidelberg Research Fields

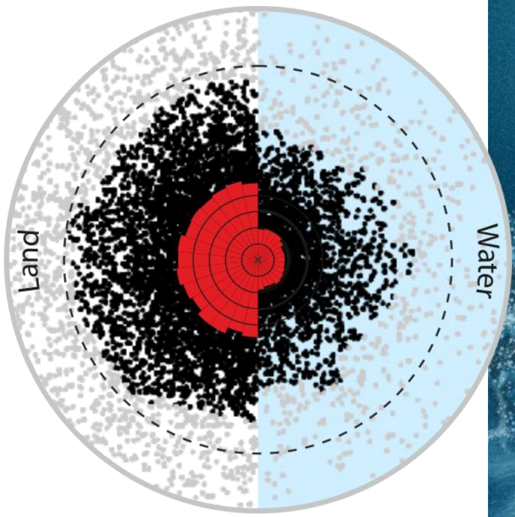

Soil moisture sensing by cosmic ray induced showers

M. Köhli, M. Schrön, U. Schmidt, P. Dietrich, S. Zacharias

HELMHOLTZ CENTRE FOR ENVIRONMENTAL RESEARCH – UFZ

TERENO

HEIDELBERG UNIVERSITY

Cosmic Radiation

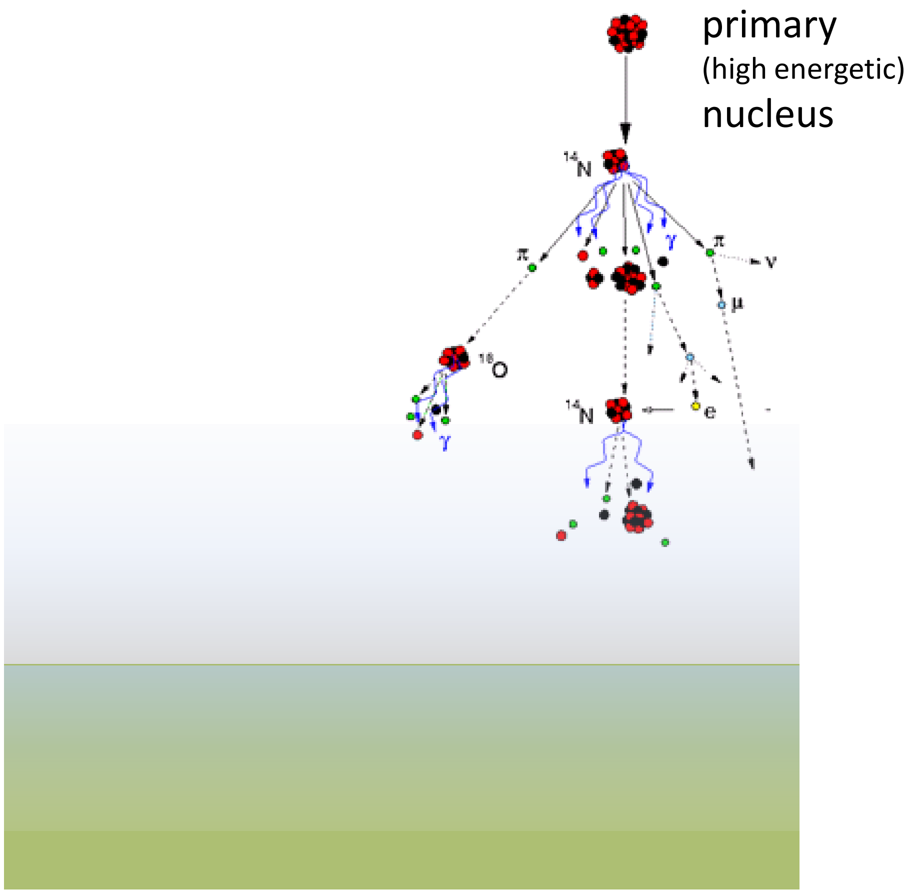

Cosmic Radiation

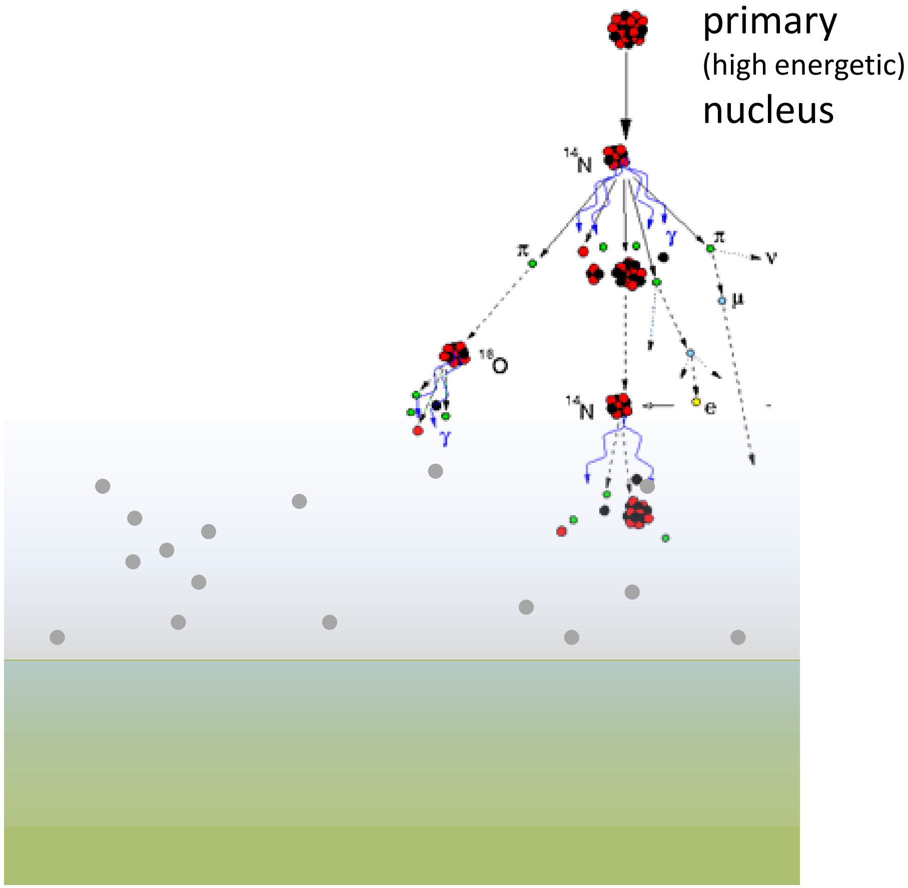

The Cosmic Ray Neutron Spectrum

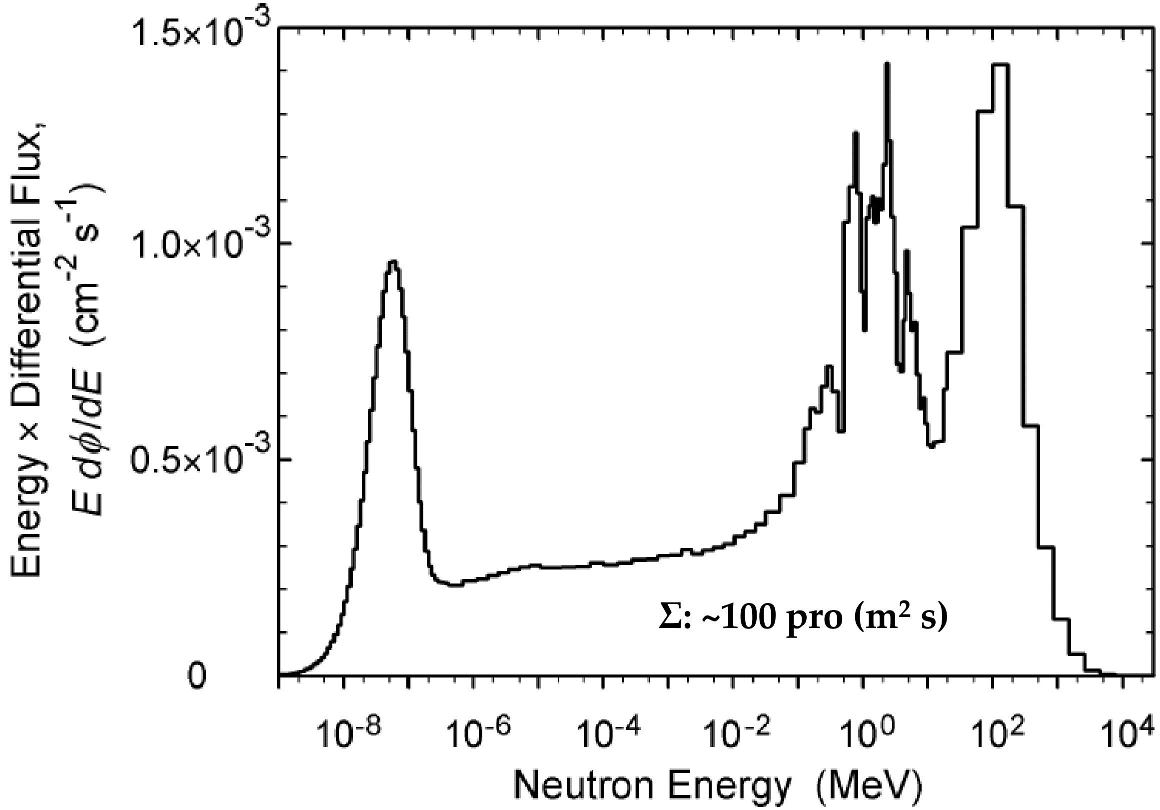

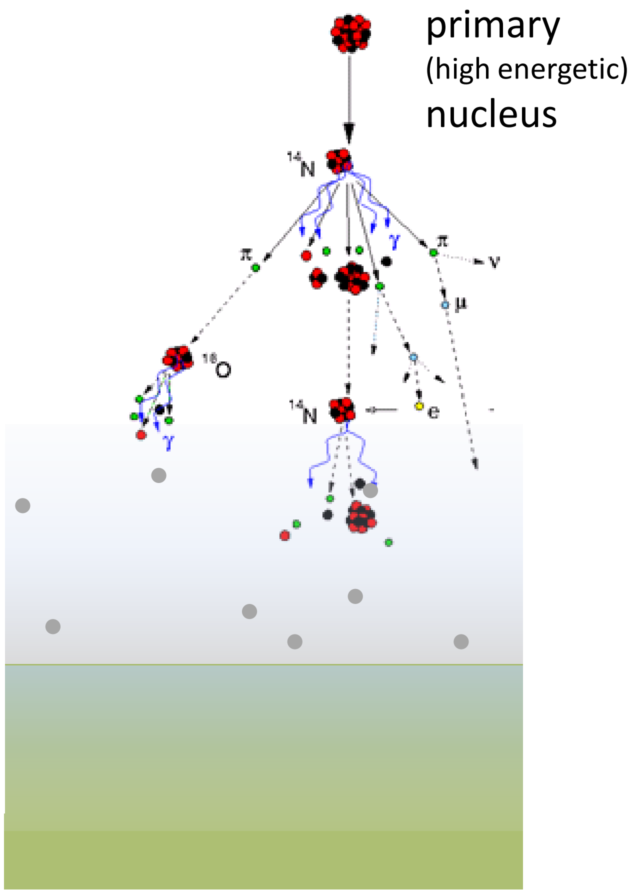

The Cosmic Ray Neutron Spectrum

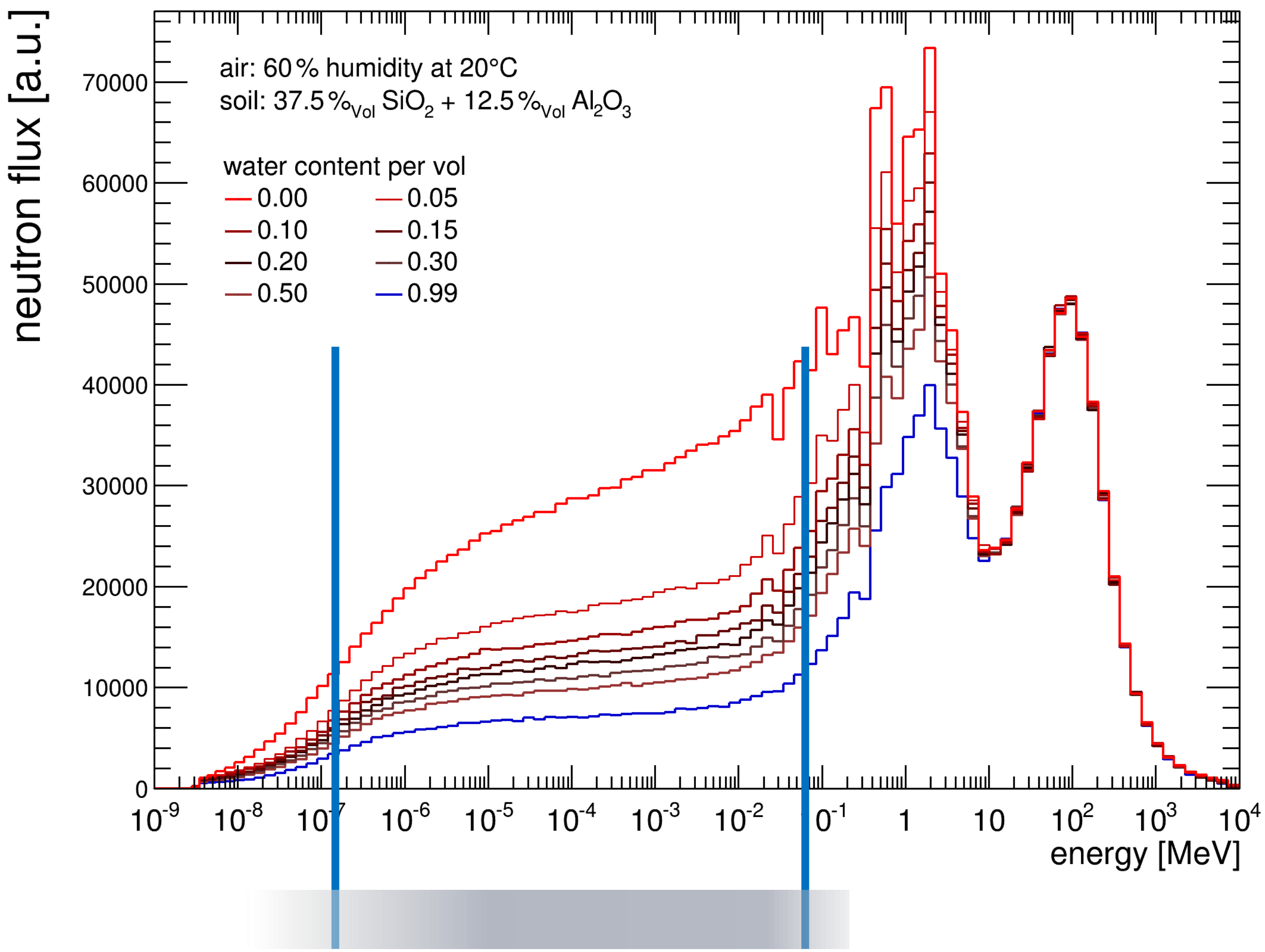

Rainfall and Neutron Background

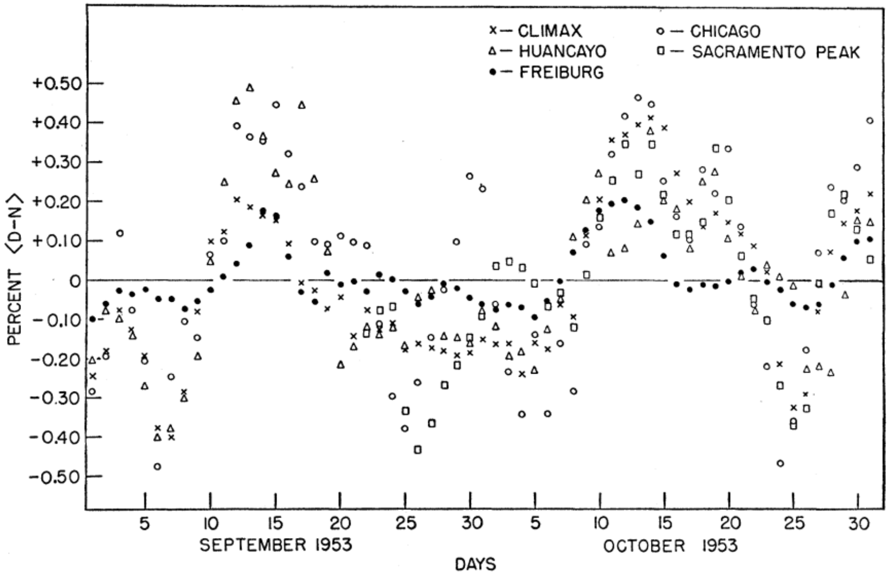

R.P. Kane, "Recurrence Phenomenon in the 24-Hour Variation of Cosmic-Ray Intensity" Phys Rev, 98, 1, 1955

Kodama et al. Application of Atmospheric Neutrons to Soil Moisture Measurements, Soil Science, 140, 1985

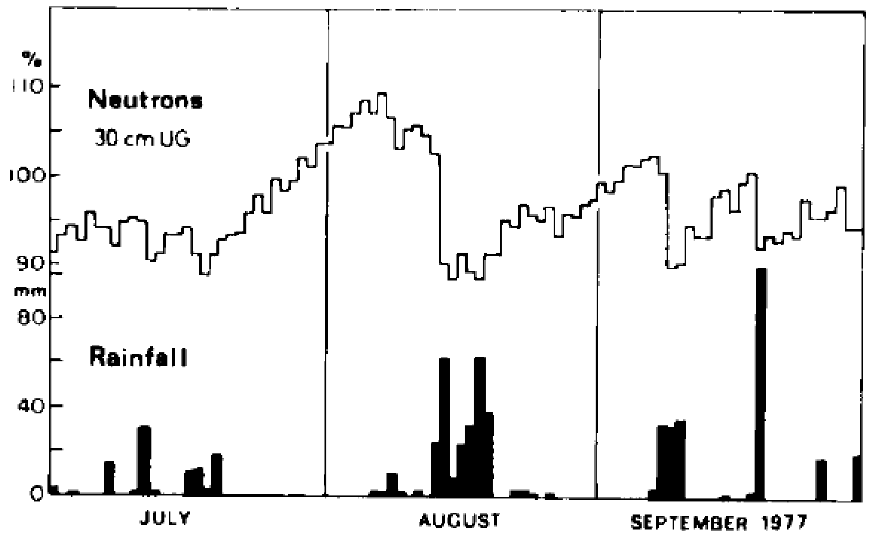

FIG. 1. Day-to-day variations of atmospheric neutron fluxes 30 cm under the ground and rainfall on the ground.

The Ship Effect

[1]

[1] https://upload.wikimedia.org/wikipedia/commons/4/42/Crossroads_Gathering_Pearl.jpg
[2] T. Kouzes et al., Cosmic-ray-induced ship-effect neutron measurements and implications for cargo scanning at borders, NIMA , 587 1, 2008 , 89-100

The Ship Effect

[1]

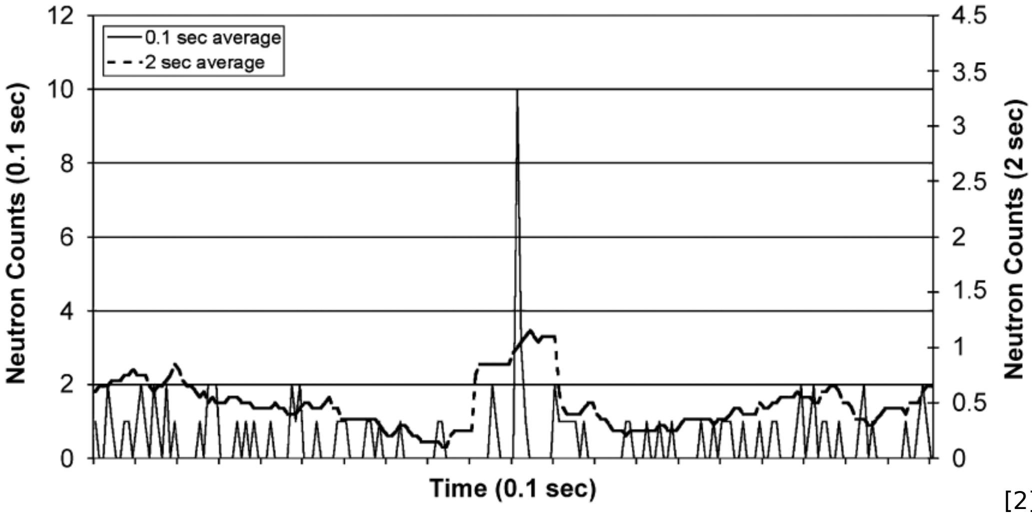

[2]

[1] https://upload.wikimedia.org/wikipedia/commons/4/42/Crossroads_Gathering_Pearl.jpg

[2] T. Kouzes et al., Cosmic-ray-induced ship-effect neutron measurements and implications for cargo scanning at borders, NIMA , 587 1, 2008 , 89-100

CRNS Campaign

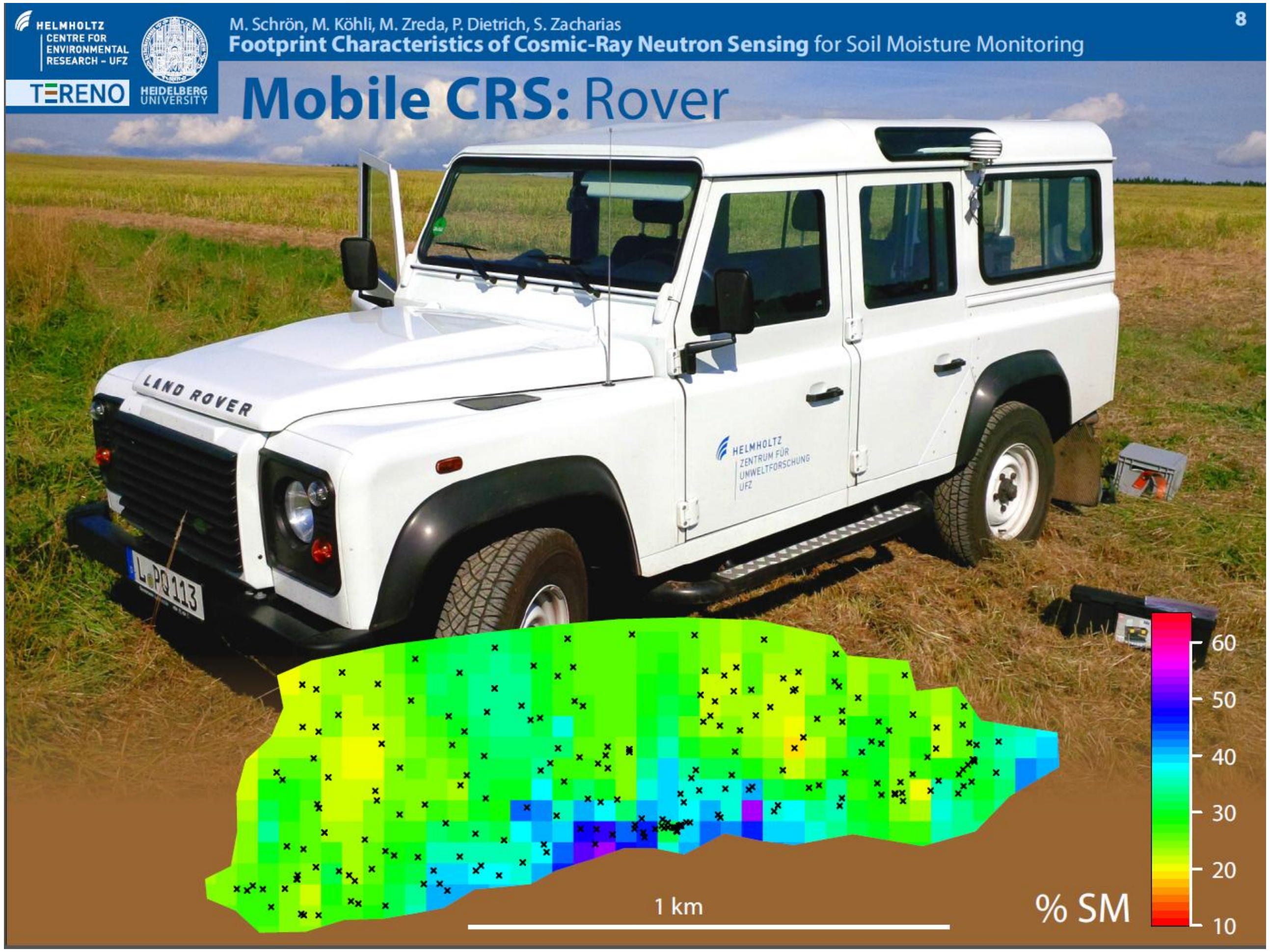

Soil Moisture Measurement Scales

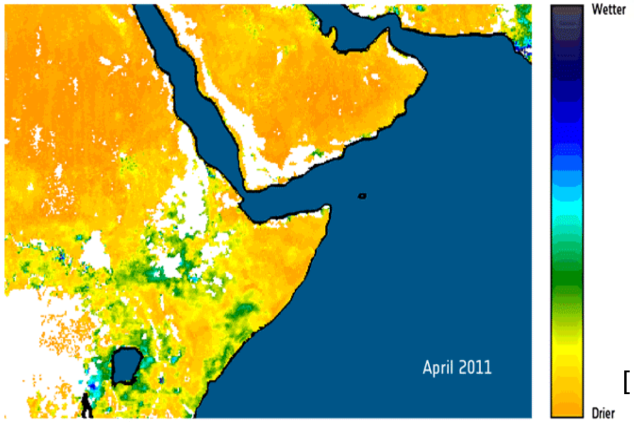

[1]

via
satellite remote sensing
(optical, microwave)

No (affordable)
technique in between

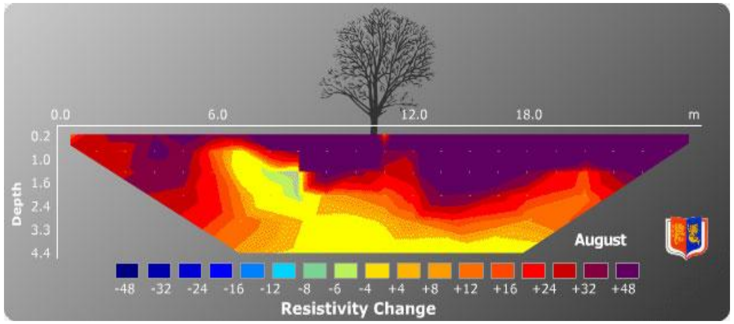

[2]

via
local techniques
(electrical resistivity, capacitance, etc)
(even neutrons...)

[1] ESA SMOS (http://www.esa.int/Our_Activities/Observing_the_Earth/SMOS/Horn_of_Africa_drought_seen_from_space)
[2] The Clay Research Group (http://www.theclayresearchgroup.org/images/ert.jpg)

Cosmic Ray Neutrons Simulation

How far do reflected neutrons travel?

- Video removed -

The Footprint

How far do reflected neutrons travel?

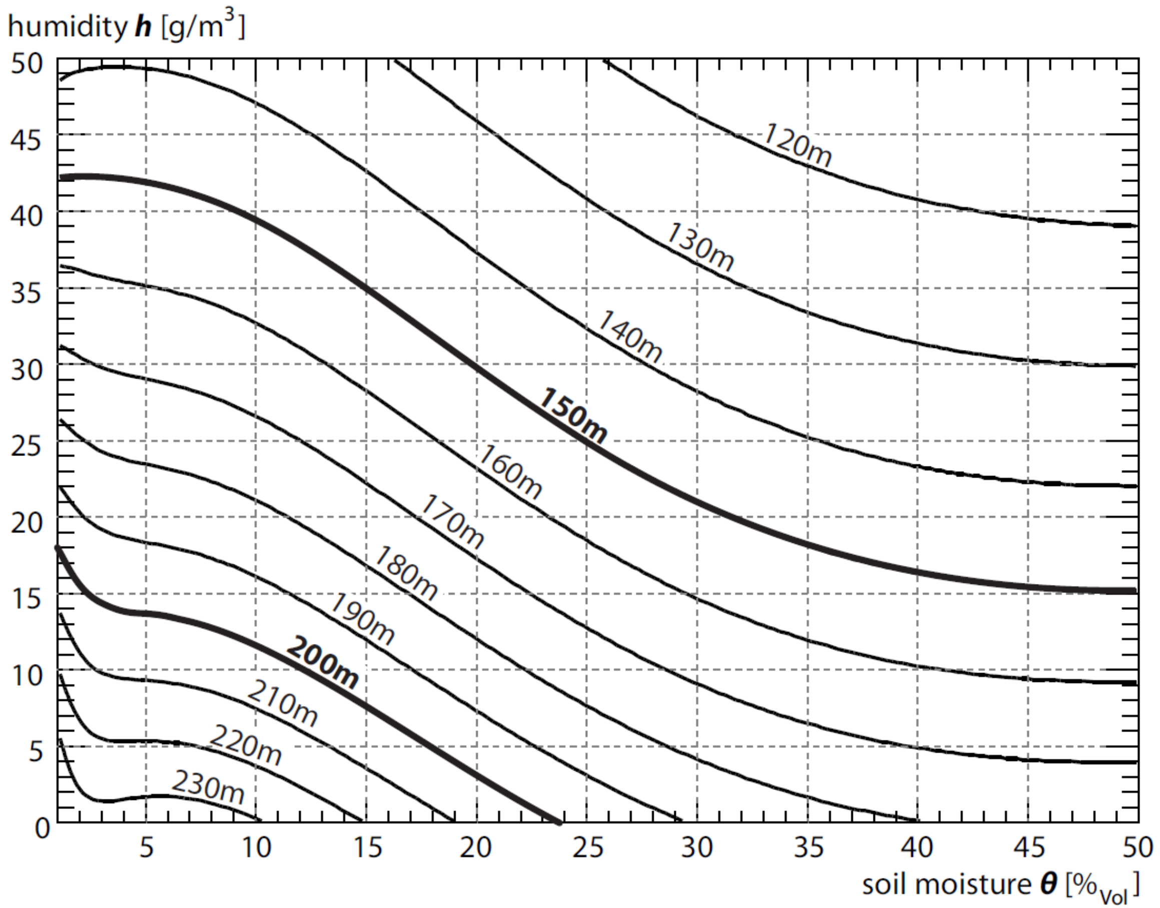

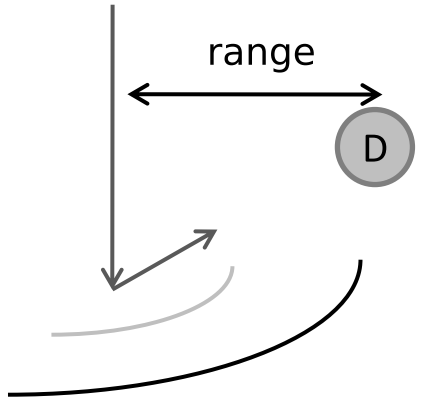

Data vs Simulation

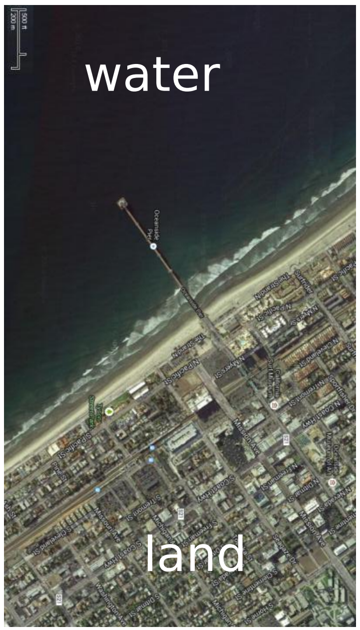

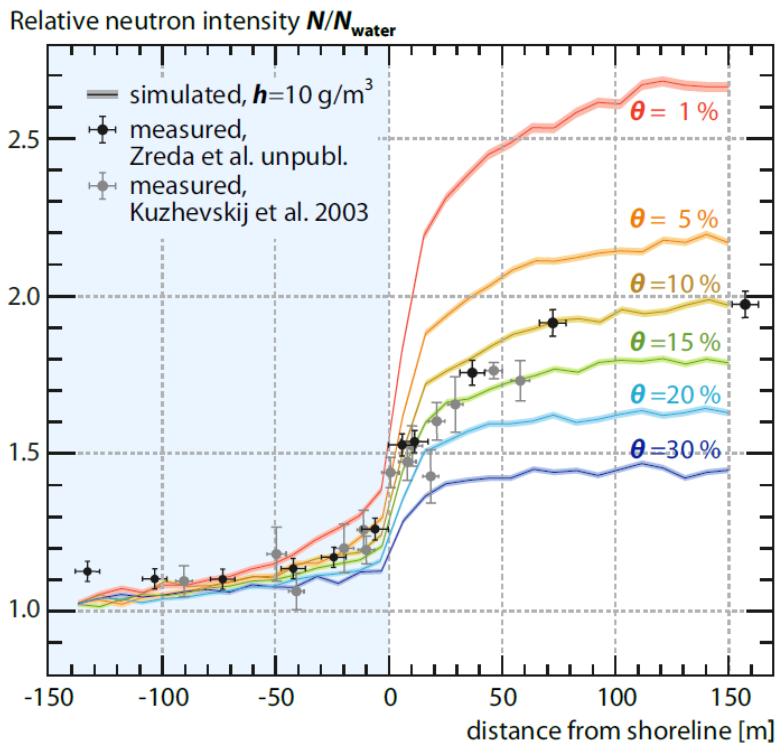

water land

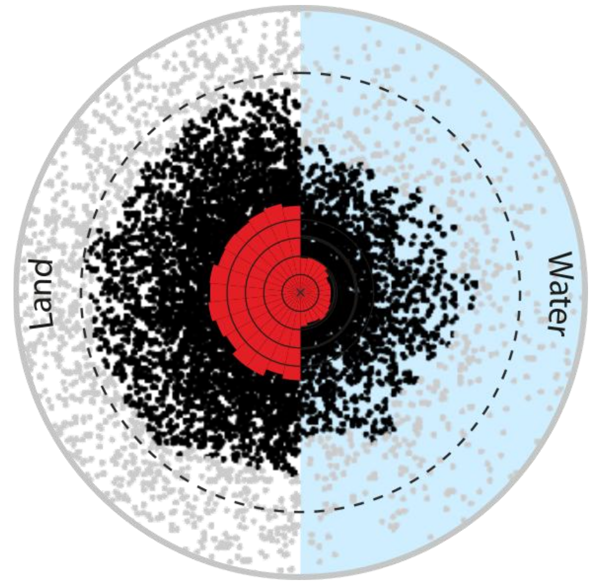

- Detected neutron origins (first contact to soil)
- Closest 86% of neutron origins for each 12° sector
- Neutron intensity for each 12° sector [arb. units]
- Footprint R_{86}(5g/m³, 5 %)=210m for homogeneous soil

Neutron Detection

Novel Detectors

Neutron Detection

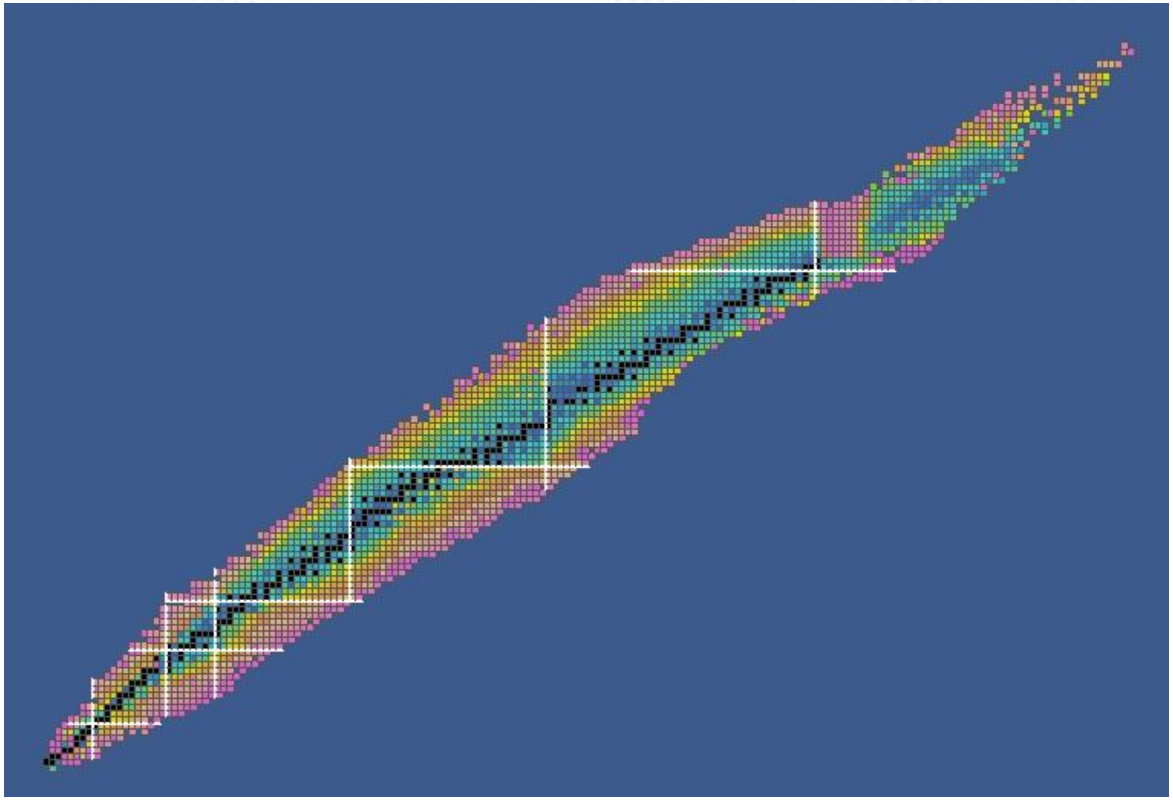

Neutron Detection

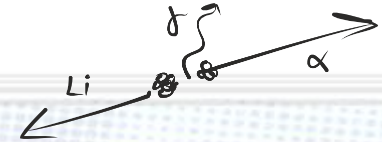

Element	Reaction		CS at 25.2 meV
^{3}He	$^{3}\mathrm{He}+\mathrm{n} \longrightarrow$	$^{3}\mathrm{H}+764\,\mathrm{keV}+\mathrm{p}$	5327 b
^{6}Li	$^{6}\mathrm{Li}+\mathrm{n} \longrightarrow$	$^{3}\mathrm{H}+\alpha+4.78\,\mathrm{MeV}$	940 b
^{10}B	$^{10}\mathrm{B}+\mathrm{n} \longrightarrow$	$^{7}\mathrm{Li}+\alpha+2.79\,\mathrm{MeV}$ (6 %)	3837 b
	$^{10}\mathrm{B}+\mathrm{n} \longrightarrow$	$^{7}\mathrm{Li}^{*}+\alpha+2.31\,\mathrm{MeV}$ (94 %)	
^{155}Gd	$^{155}\mathrm{Gd}+\mathrm{n} \longrightarrow$	$^{156}\mathrm{Gd}+\gamma+e^{-}+(30-180)\,\mathrm{keV}$	61000 b
^{157}Gd	$^{157}\mathrm{Gd}+\mathrm{n} \longrightarrow$	$^{158}\mathrm{Gd}+\gamma+e^{-}+(30-180)\,\mathrm{keV}$	254000 b
^{235}U	$^{235}\mathrm{U}+\mathrm{n} \longrightarrow$	fission fragments $+\,160\,\mathrm{MeV}$	584 b

Helium Conversion

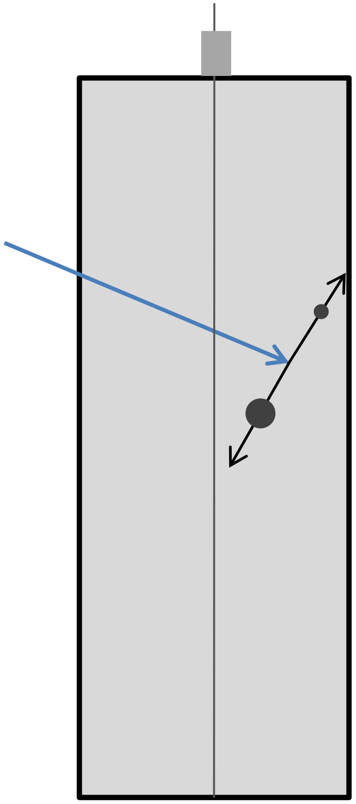

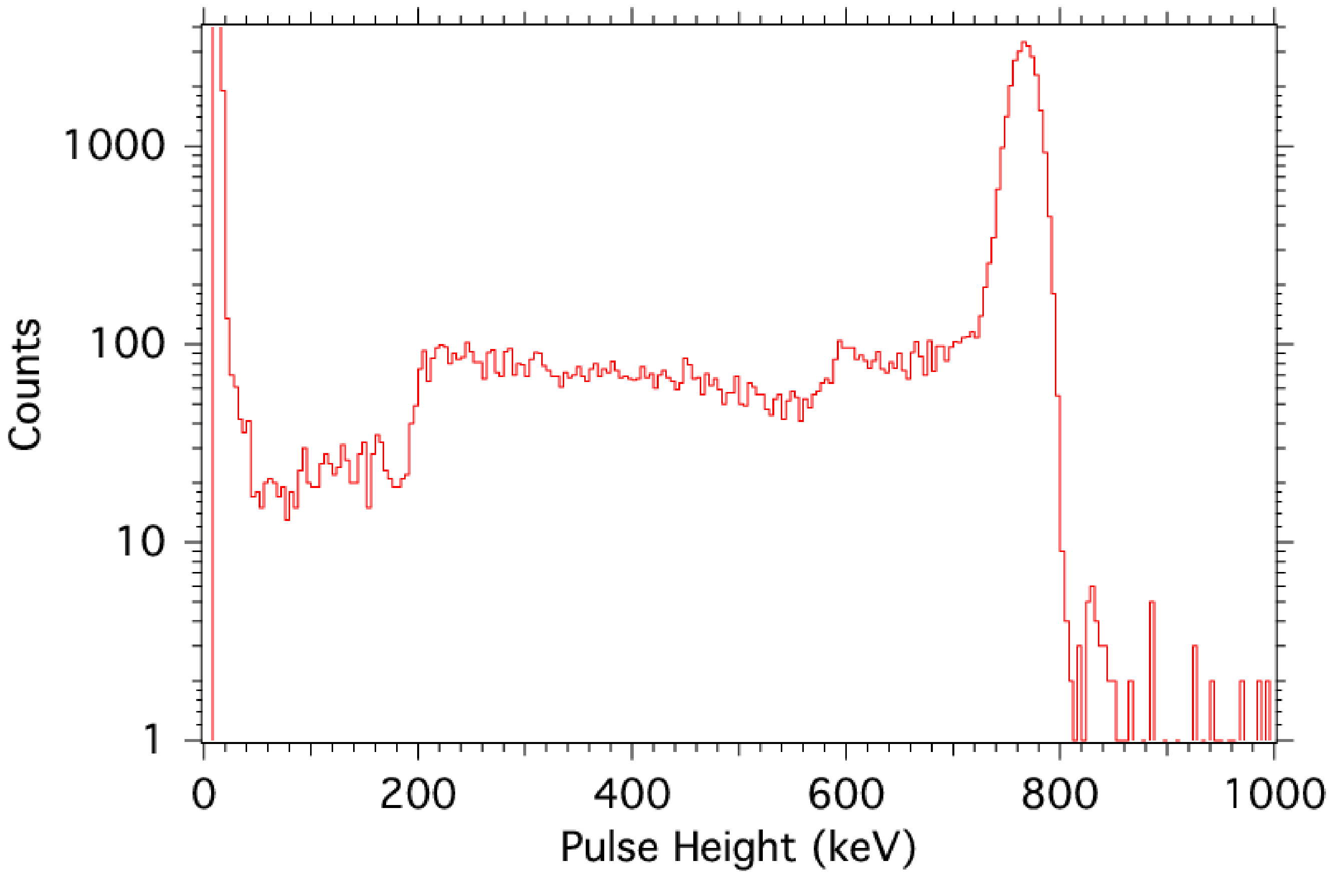

Langford et al., “Event Identification in 3He Proportional Counters Using Risetime Discrimination” arXiv:1212.4724v1

Lithium Conversion

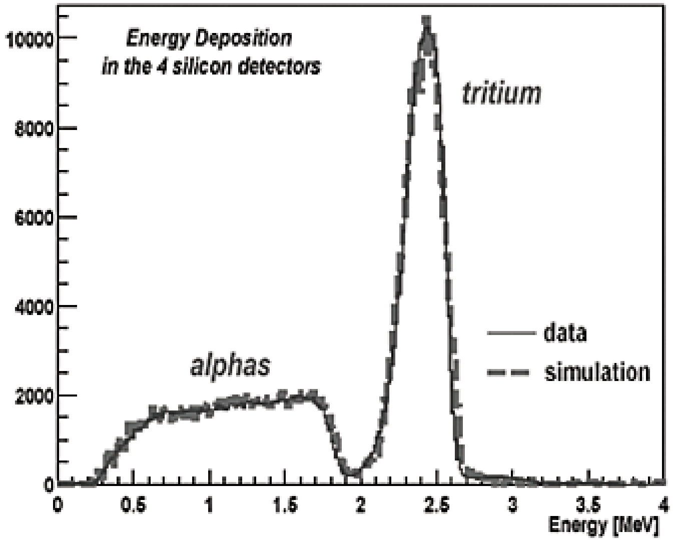

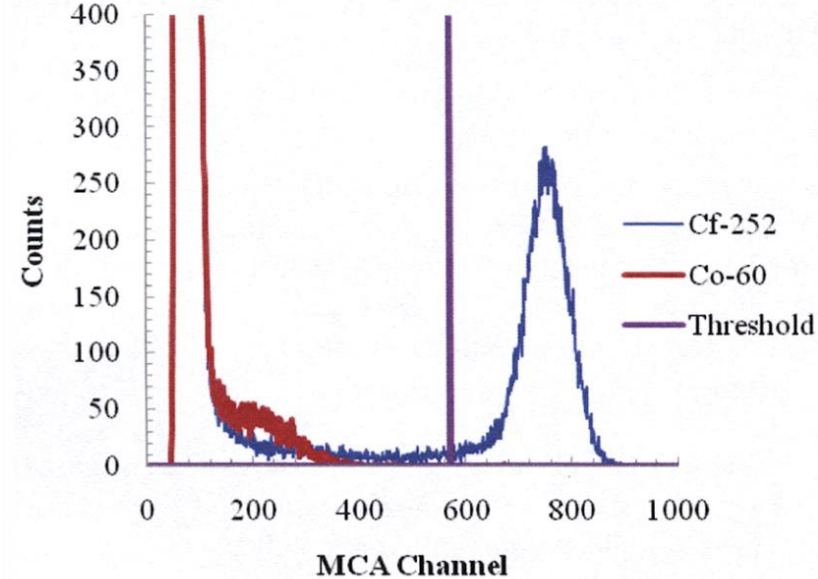

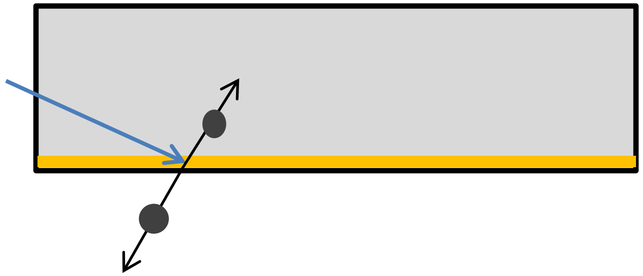

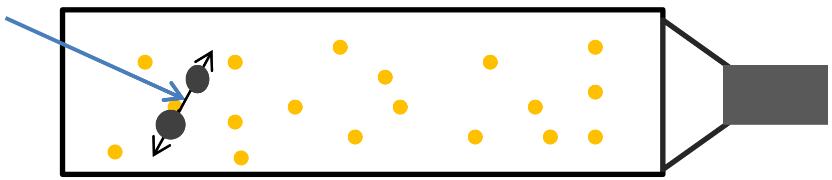

[1] P.F. Mastinu et al., “A low-mass neutron flux monitor for the n _TOF facility at CERN”, Braz. J. Phys. vol.34 no.3, 2004
[2] “A Compact Neutron Detector Based on the use of a SiPM Detector”, IEEE Nuc. Spring Symp., 2008

Boron Conversion

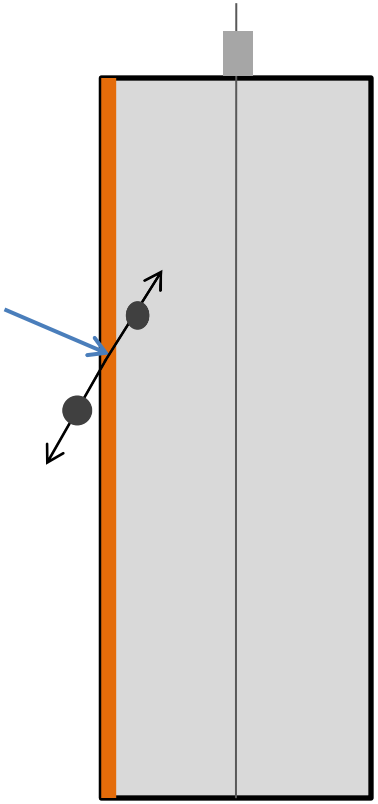

0.035 mm 10-B

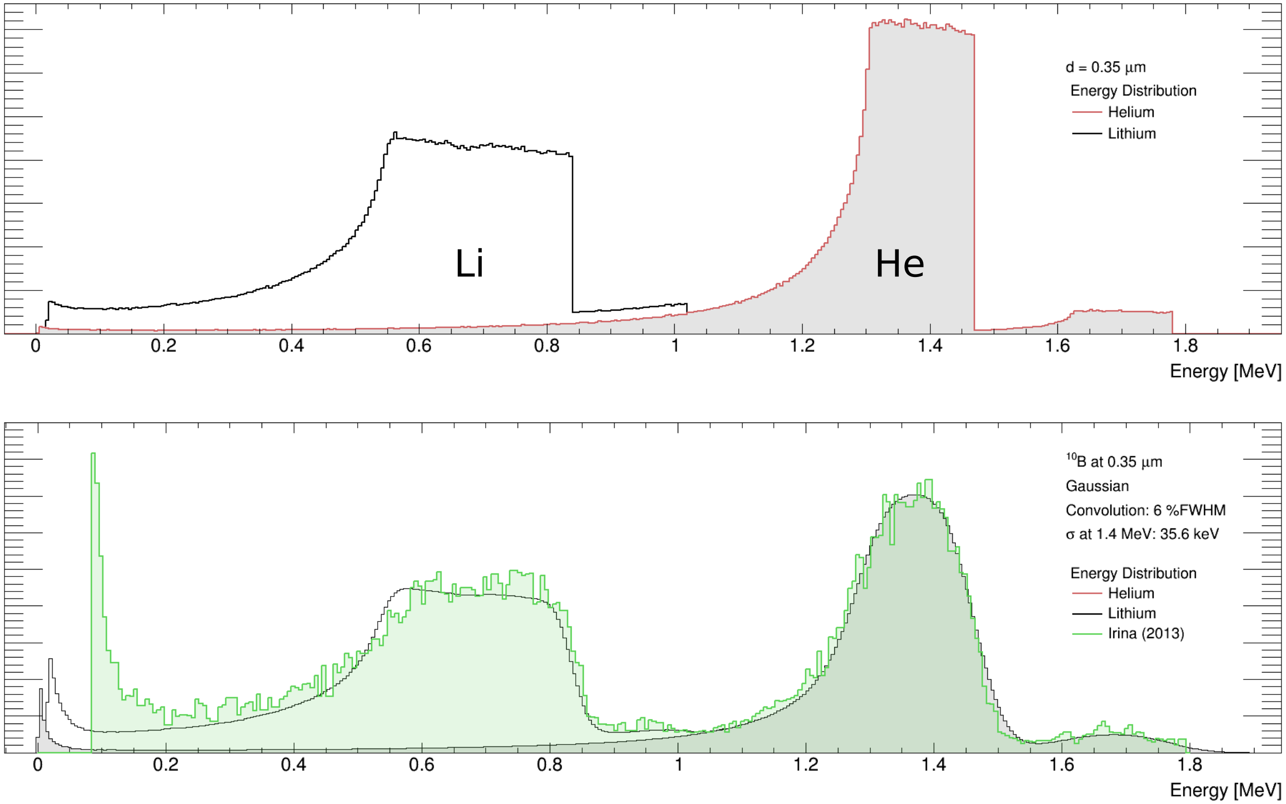

Boron Conversion

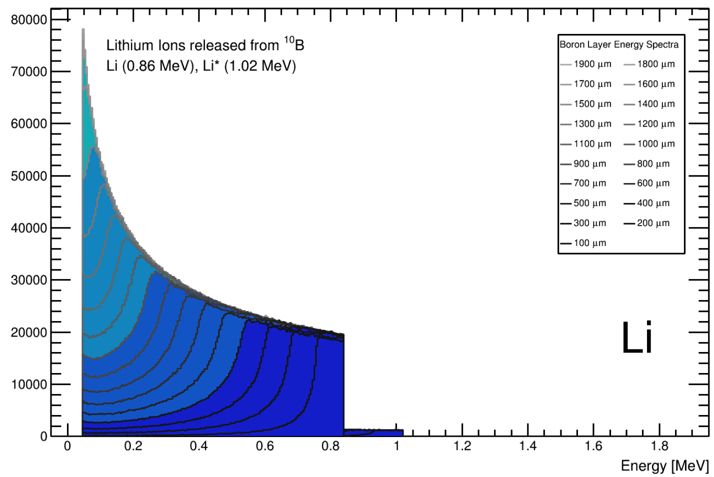

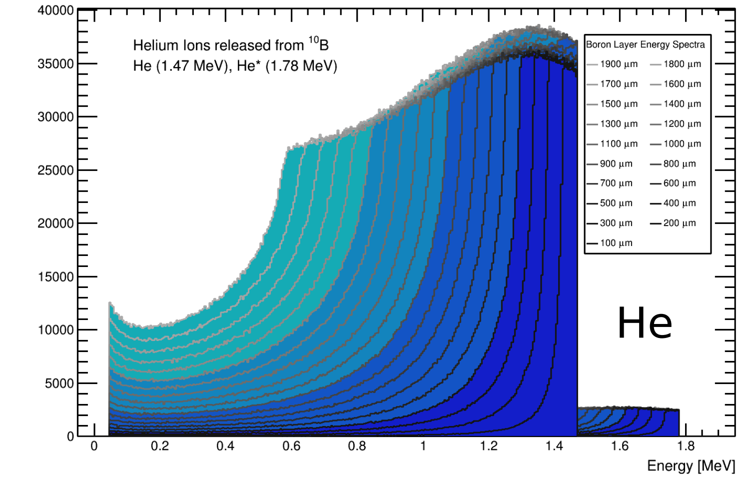

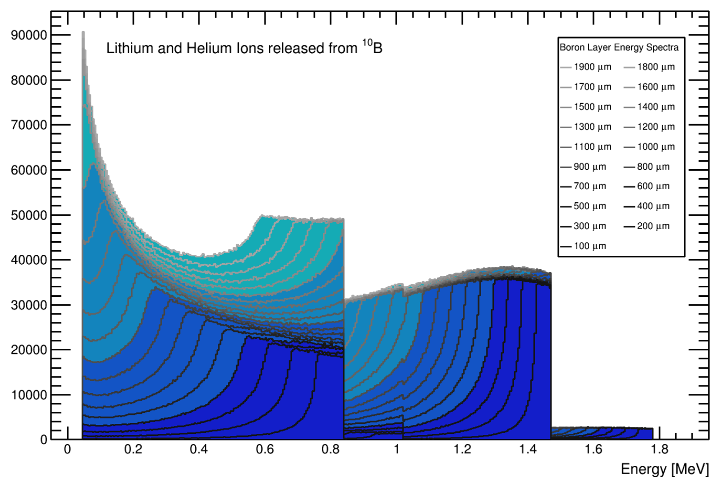

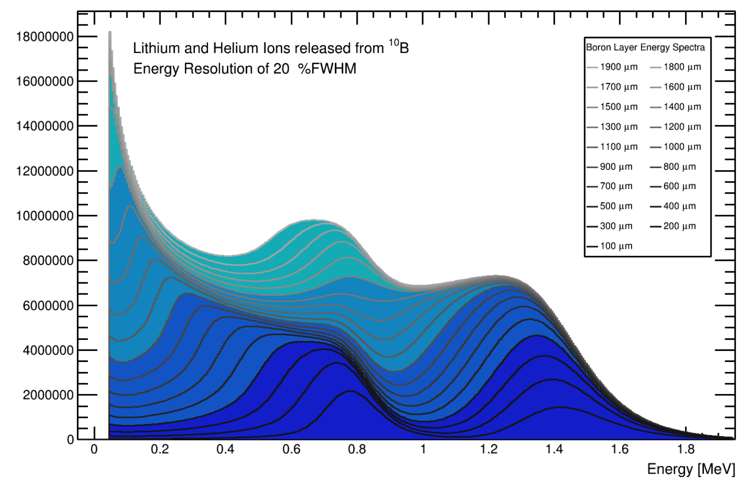

CNCS inelastic spectrometer, SNS

Titan II Rocket in Launch Silo, Arizona State Museum

The Helium-3 Crisis

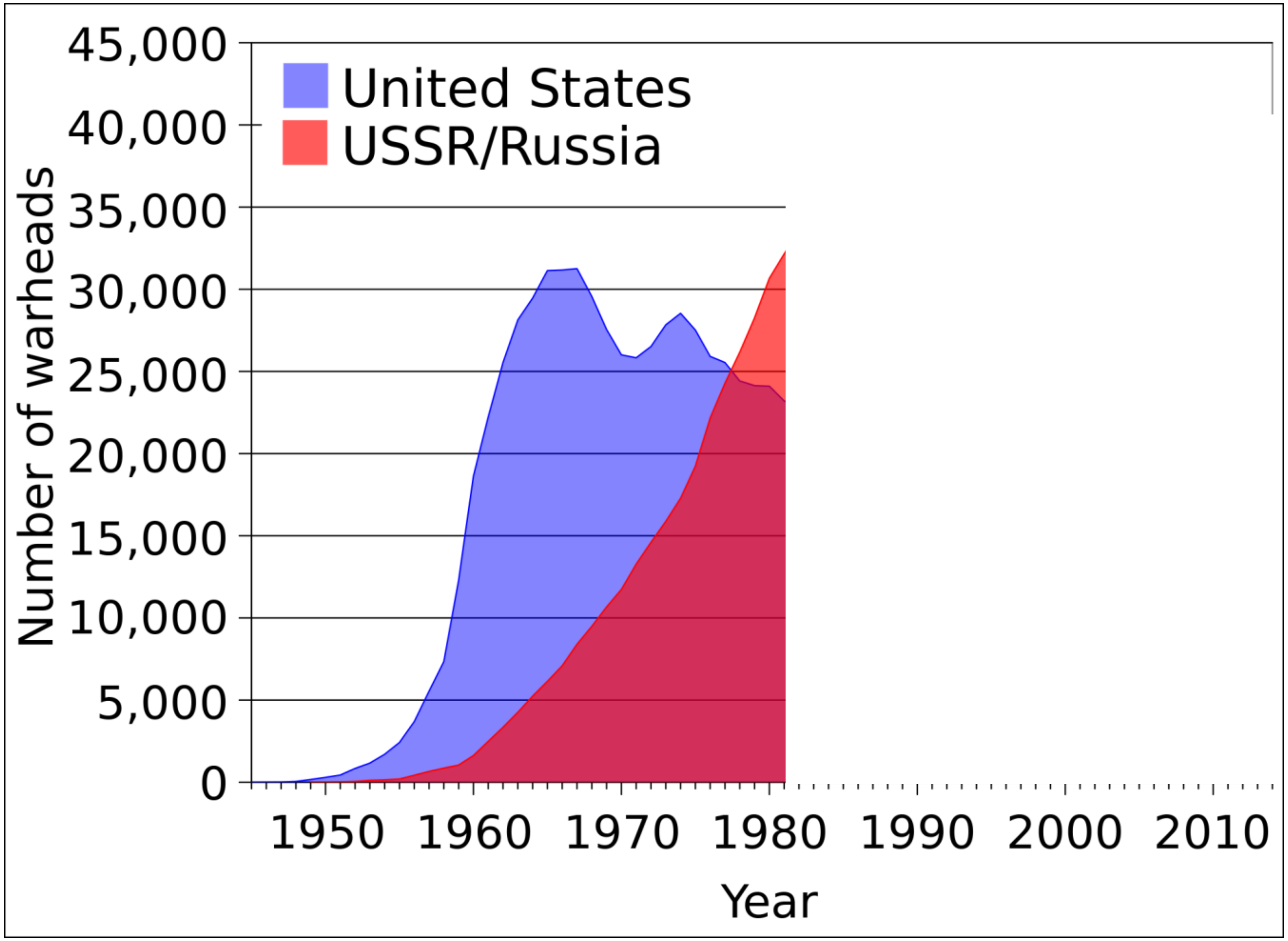

R. S. Norris and H. Kristensen, "Global nuclear stockpiles, 1945-2006," *Bulletin of the Atomic Scientists* 62, no. 4 (2006), 64-66

The Helium-3 Crisis

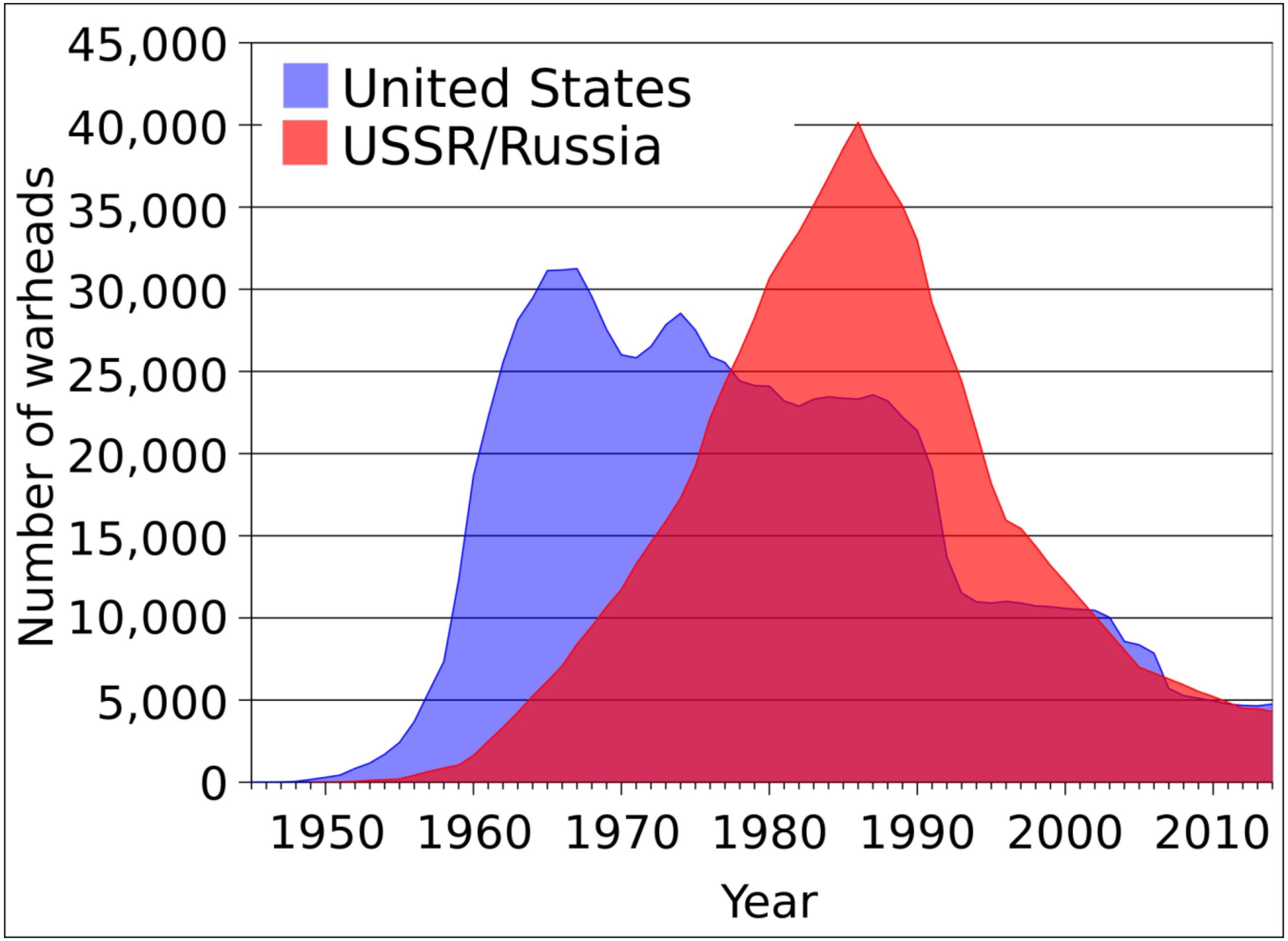

R. S. Norris and H. Kristensen, "Global nuclear stockpiles, 1945-2006," *Bulletin of the Atomic Scientists* 62, no. 4 (2006), 64-66

The Helium-3 Crisis

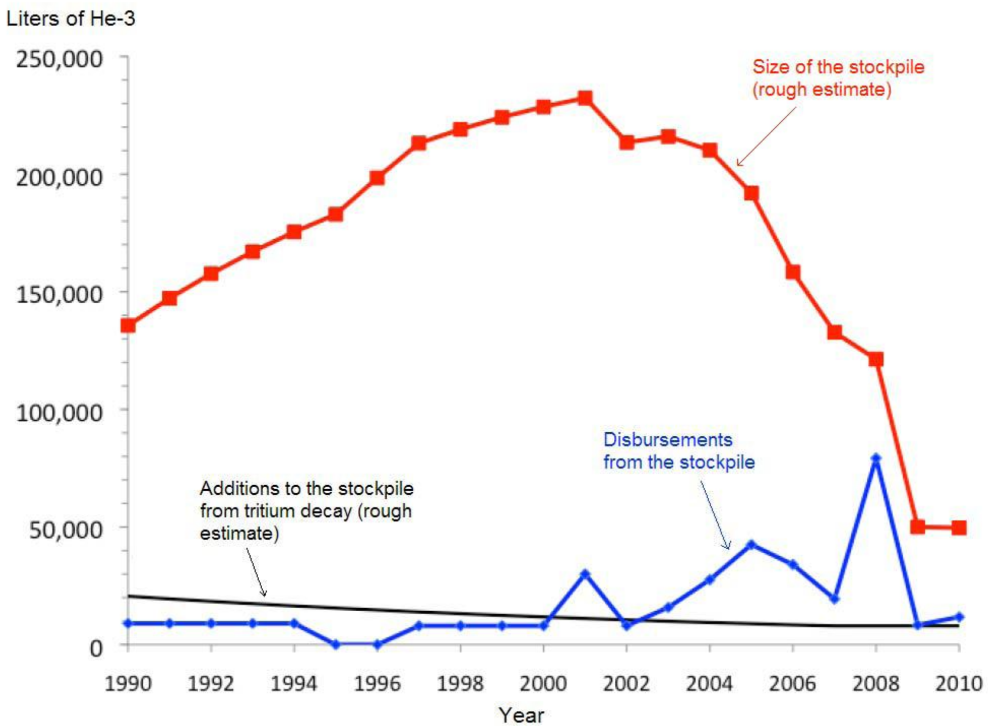

AAAS, Overview of Helium-3 Supply and Demand

[1] http://www.saphymo.com/photos/ecatalogue/116-2/access-control-clearance-monitors-rcp-radiological-control-for-pedestrian.jpg
[2] http://cits.uga.edu/uploads/1540compass/1540images/_compass750/RPM1.jpg

The Helium-3 Crisis

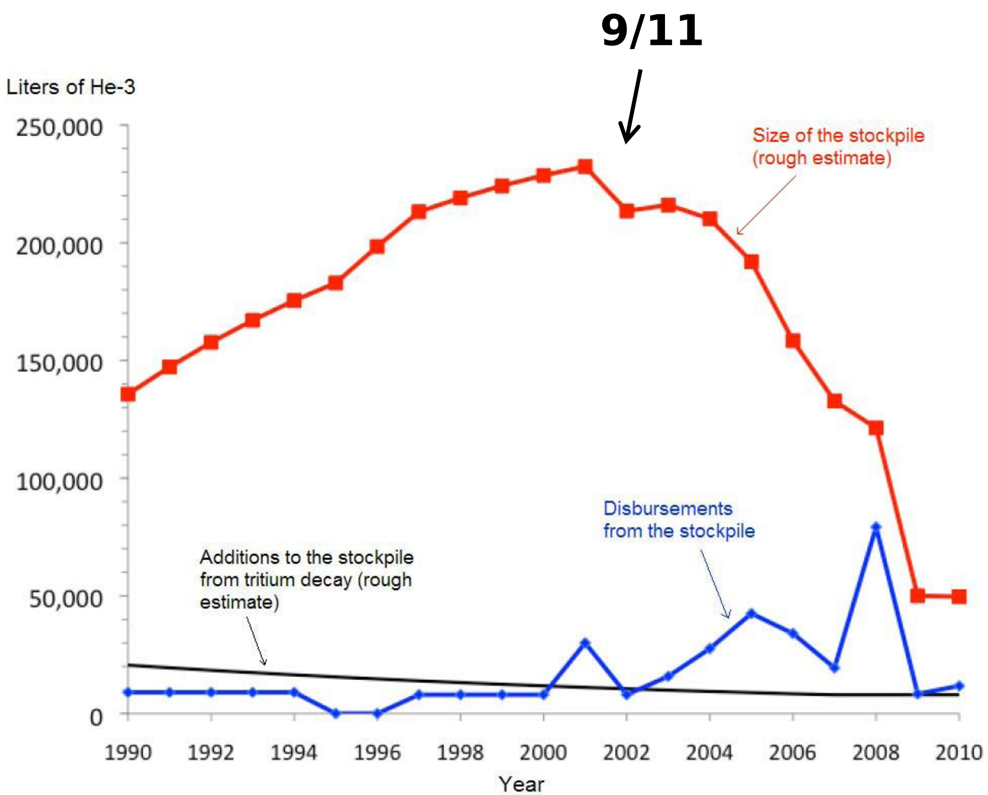

AAAS, Overview of Helium-3 Supply and Demand

[1]

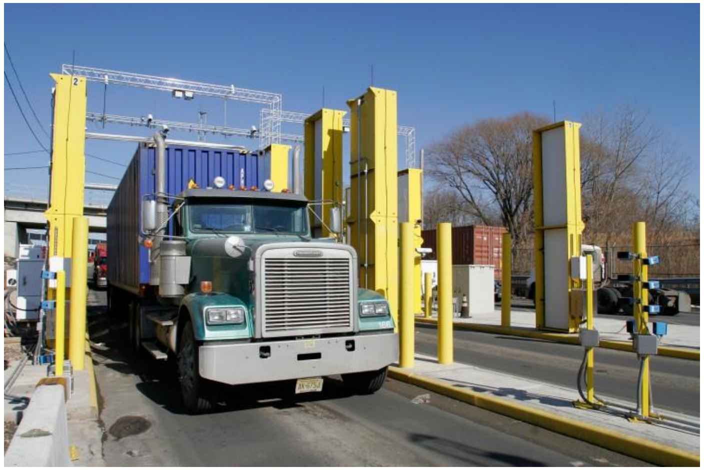

[2]

[1] http://www.saphymo.com/photos/ecatalogue/116-2/access-control-clearance-monitors-rcp-radiological-control-for-pedestrian.jpg
[2] http://cits.uga.edu/uploads/1540compass/1540images/_compass750/RPM1.jpg

The Helium-3 Crisis

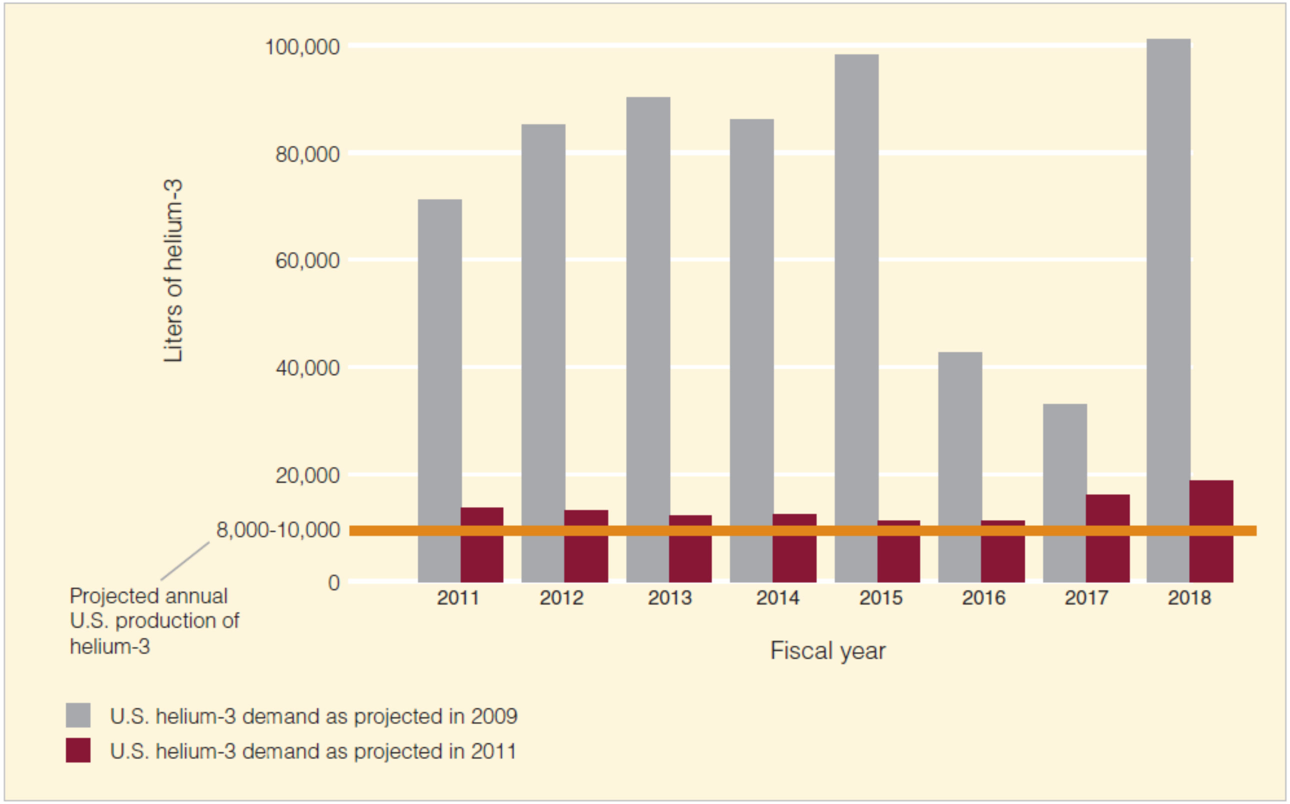

Figure 2.5 Helium-3 demand and annual U.S. production, 2011–18, as projected in 2009 and 2011.
Source: GAO analysis of information from the interagency policy committee.

„Neutron detectors - Alternatives to using helium-3“, GAO, 2011

ESS Instrumentation

Instrument	Detector area [m^2]	Wavelength range [Å]	Time resolution [μs]	Spatial resolution [mm]
Multi-purpose imaging	0.5	1 - 20	1	0.001 - 0.5
General purpose polarised SANS	5	4 - 20	100	10
Broad-band small sample SANS	14	2 - 20	100	1
Surface scattering	5	4 - 20	100	10
Horizontal reflectometer	0.5	5 - 30	100	1
Vertical reflectometer	0.5	5 - 30	100	1
Thermal powder diffractometer	20	0.6 - 6	< 10	2×2
Bi-spectral powder diffractometer	20	0.8 - 10	< 10	2.5×2.5
Pulsed monochromatic powder diffractom.	4	0.6 - 5	< 100	2×5
Material science & engineering diffractom.	10	0.5 - 5	10	2
Extreme conditions instrument	10	1 - 10	< 10	3×5
Single crystal magnetism diffractometer	6	0.8 - 10	100	2.5×2.5
Macromolecular diffractometer	1	1.5 - 3.3	1000	0.2
Cold chopper spectrometer	80	1 - 20	10	10
Bi-spectral chopper spectrometer	50	0.8 - 20	10	10
Thermal chopper spectrometer	50	0.6 - 4	10	10
Cold crystal-analyser spectrometer	1	2 - 8	< 10	5 - 10
Vibrational spectroscopy	1	0.4 - 5	< 10	10
Backscattering spectrometer	0.3	2 - 8	< 10	10
High-resolution spin echo	0.3	4 - 25	100	10
Wide-angle spin echo	3	2 - 15	100	10
Fundamental & particle physics	0.5	5 - 30	1	0.1
Total	**282.6**			

ESS TDR 2013

ESS Instrumentation

Instrument	Detector technology						
	^{10}B thin films		Scintillators		^{3}He	Micropattern	
	⊥	‖	WSF	Anger		Rate	Resolution
Multi-purpose imaging	-	-	-	-	-	o	+
General purpose polarised SANS	o	+	-	+	o	+	-
Broad-band small-sample SANS	o	+	-	+	-	+	-
Surface scattering	o	+	-	+	o	+	-
Horizontal reflectometer	-	o	-	+	+	o	-
Vertical reflectometer	-	o	-	+	+	o	-
Thermal powder diffractometer	o	+	+	-	-	o	-
Bi-spectral powder diffractometer	o	+	+	-	-	o	-
P-M powder diffractometer	o	+	+	-	-	o	-
MS engineering diffractometer	o	+	+	-	-	o	-
Extreme conditions diffractometer	o	+	+	-	-	o	-
Single crystal diffractometer	o	+	+	-	-	o	-
Macromolecular diffractometer	-	o	o	o	-	+	+
Cold chopper spectrometer	+	o	o	-	-	-	-
Bi-spectral chopper spectrometer	+	+	o	-	-	-	-
Thermal chopper spectrometer	+	+	+	-	-	-	-
Cold crystal analyser spectrometer	-	o	-	+	+	-	-
Vibrational spectrometer	-	o	-	o	+	-	-
Backscattering spectrometer	-	o	-	+	+	-	-
High-resolution spin echo	-	o	-	o	+	+	-
Wide-angle spin echo	-	o	-	o	+	+	-
Fundamental & particle physics	-	-	-	-	+	+	+

ESS TDR 2013

New Detectors – Tube Replacement

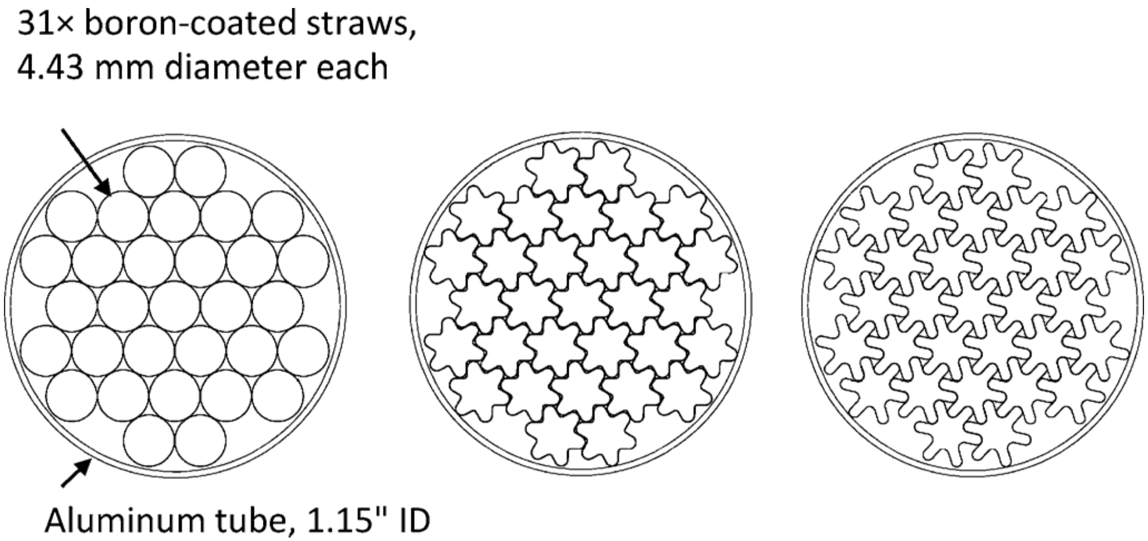

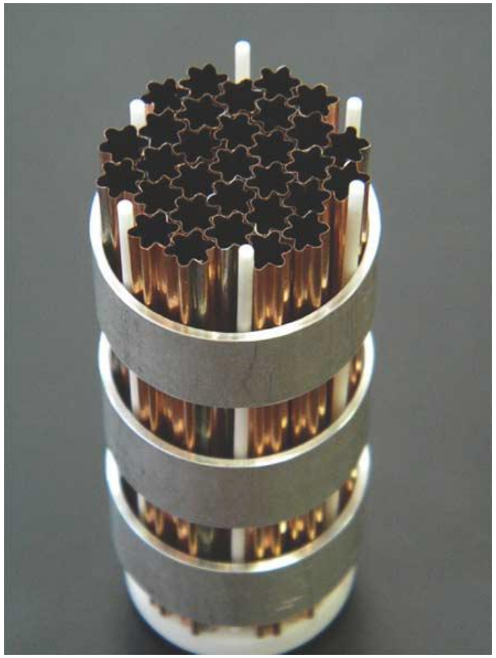

J. L. Lacy et al., "The Evolution of Neutron Straw Detector -Applications in Homeland Security",
IEEE Transactions on Nucl. Science, 60,2,2013

New Detectors – He-3 Replacements

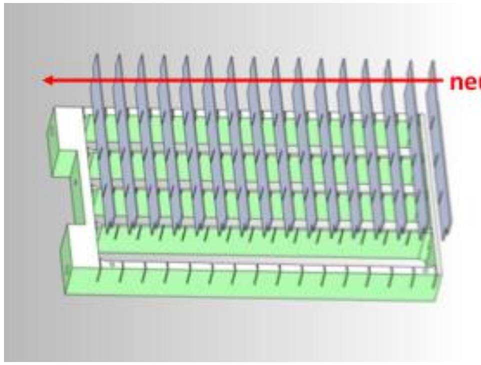

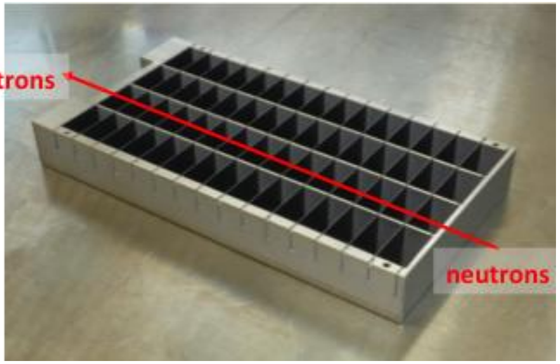

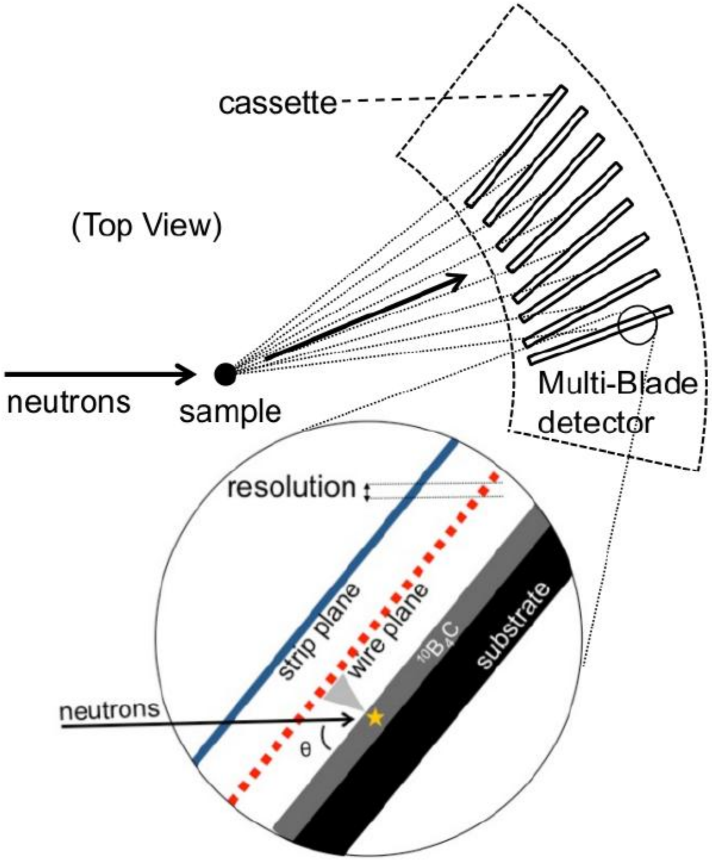

F. Piscitelli et al., “Novel Boron-10-based detectors for Neutron Scattering Science” arXiv:1501.05201v1

New Detectors – He-3 Replacements

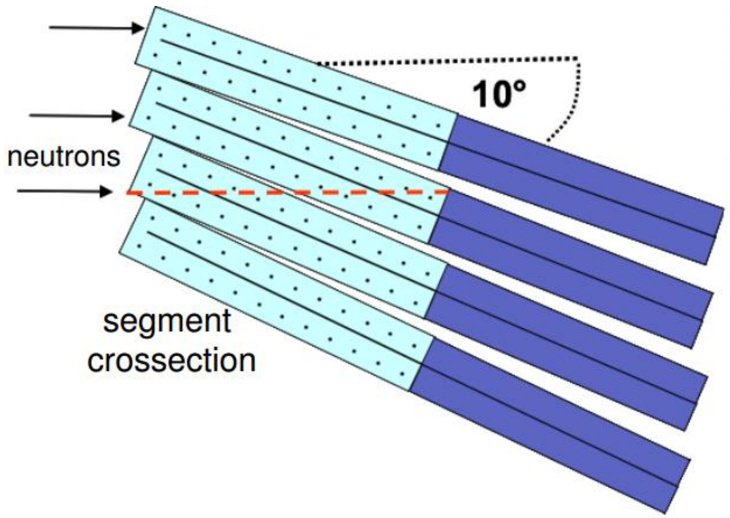

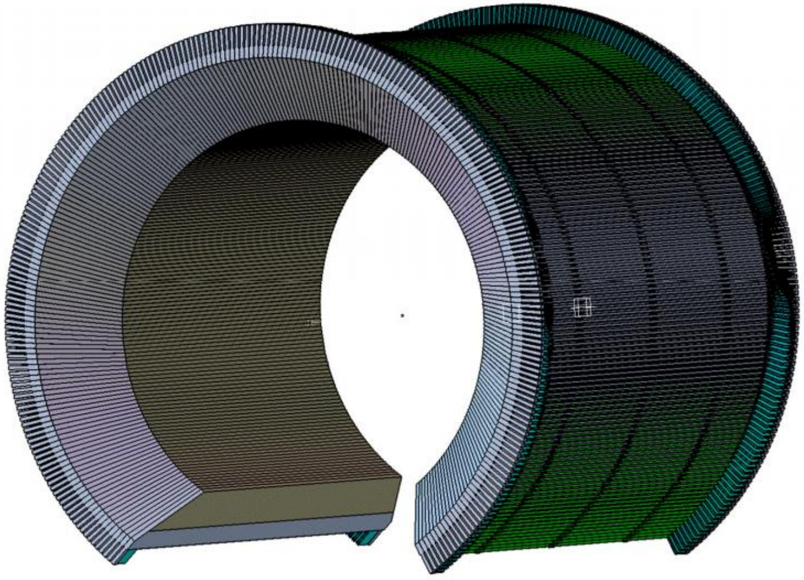

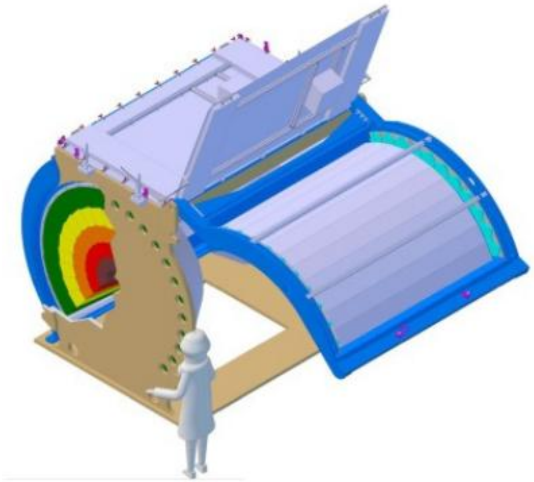

Ch. J. Schmidt, “The 10B-based Jalousie Neutron Detector”, DENIM 2015

New Detectors – Cathode Structures

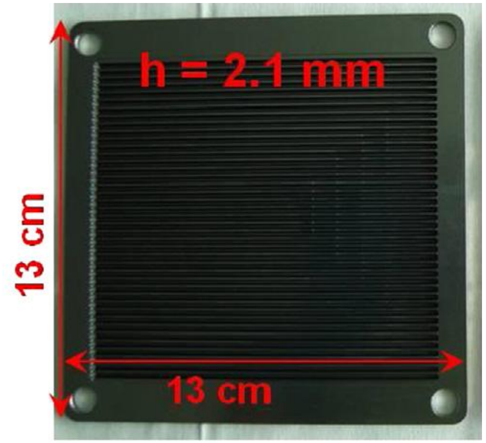

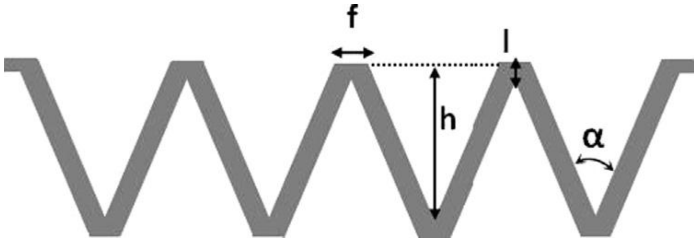

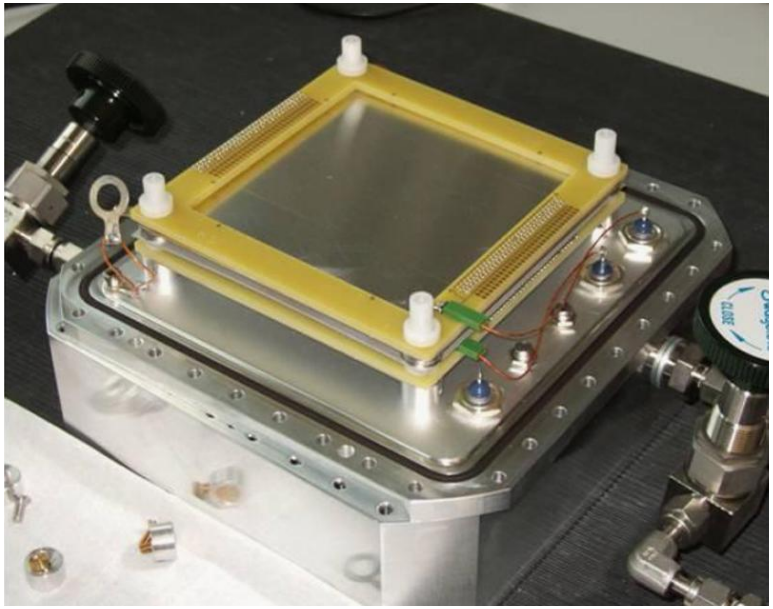

I. Stefanescu et al., „Development of a novel macrostructured cathode for large-area neutron detectors based on the 10B-containing solid converter“, NIMA 727, 2013

New Detectors – Time Projection

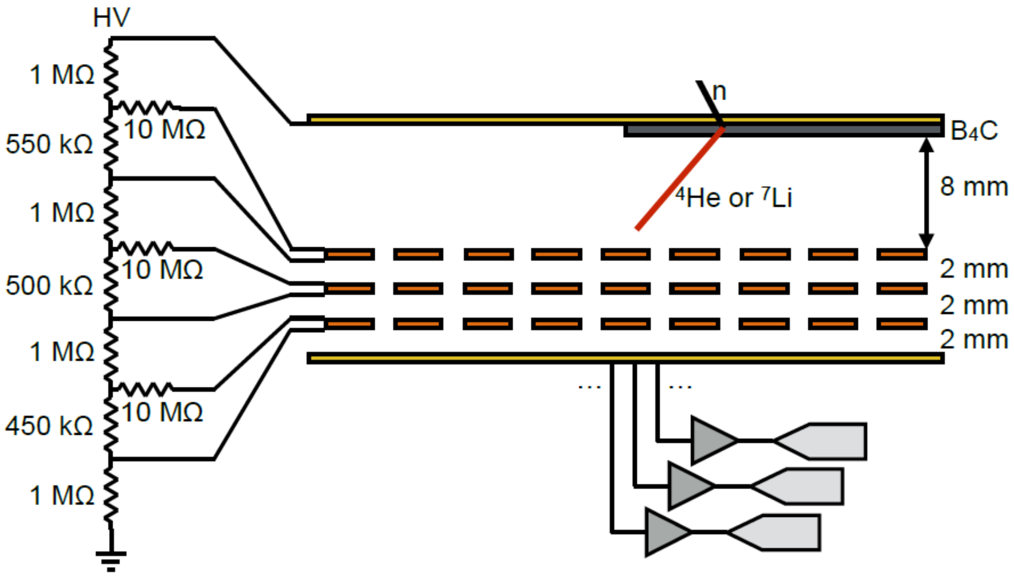

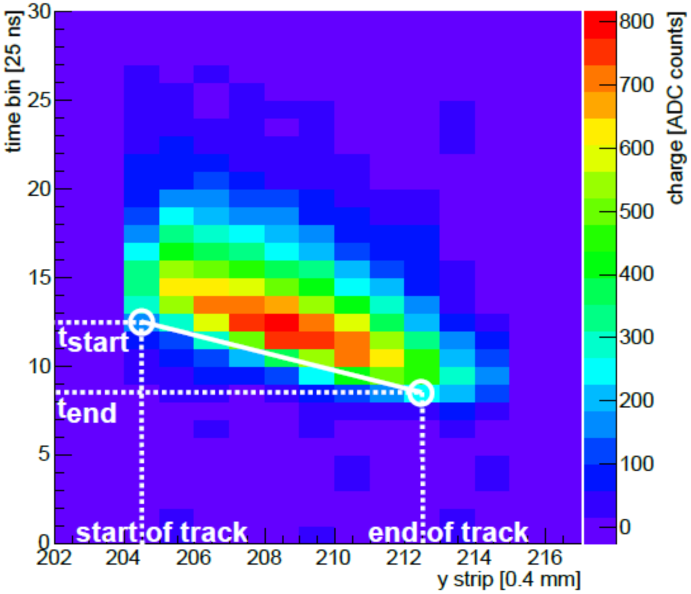

D. Pfeiffer et al., "The mTPC Method: Improving the Position Resolution of Neutron Detectors Based on MPGDs", 2015 arXiv:1501.05022v1

New Detectors – Gd Imaging

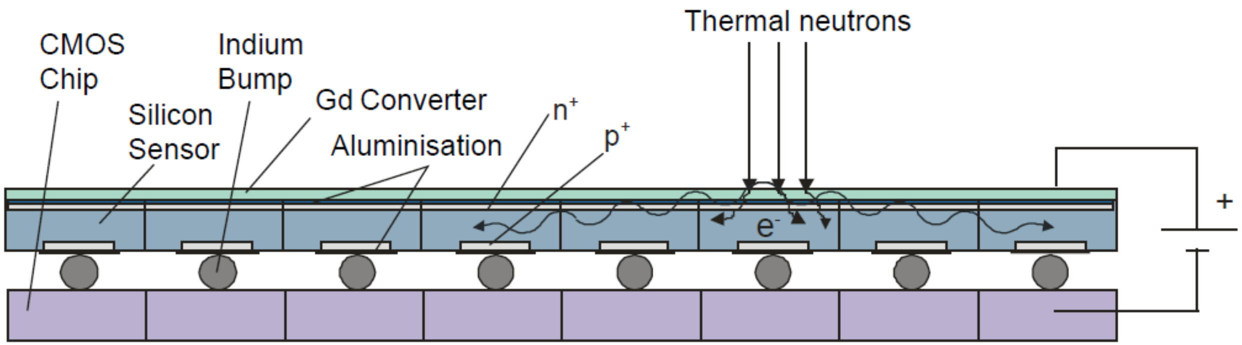

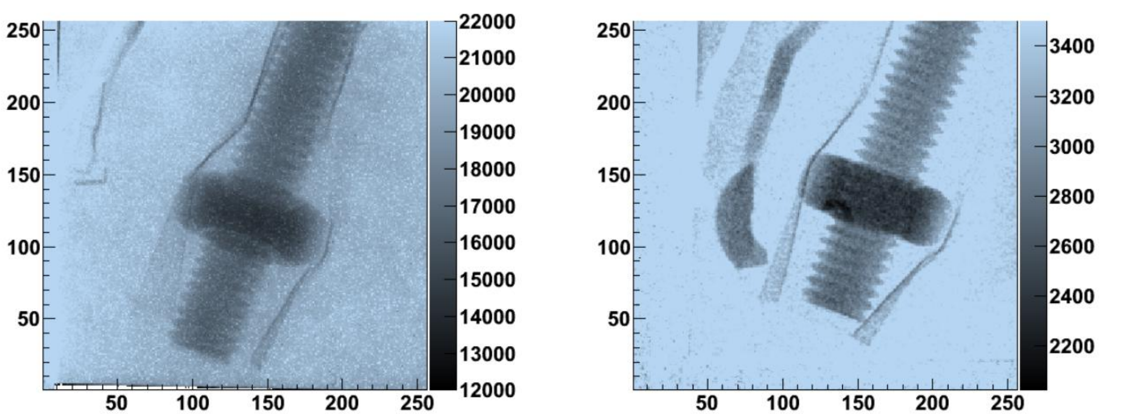

Figure 13. Neutron images of a screw and nut: left image a 240 sec. exposure with a Gd converter, rigl image a 120 sec. exposure with a 10-B converter.

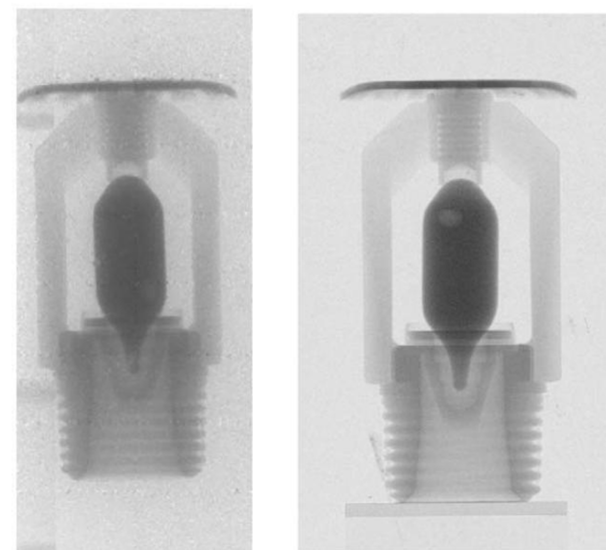

Fig. 7. Radiography image of a sprinkler nozzle made with different imaging systems, PILATUS (left), imaging plate (right).

E. Lehmann et al., "Neutron imaging—detector options and practical results", NIM A 531, 2004
E. Lehmann et al., "Neutron imaging — Detector options in progress ", JINST, 2011

New Detectors – 3D Silicon

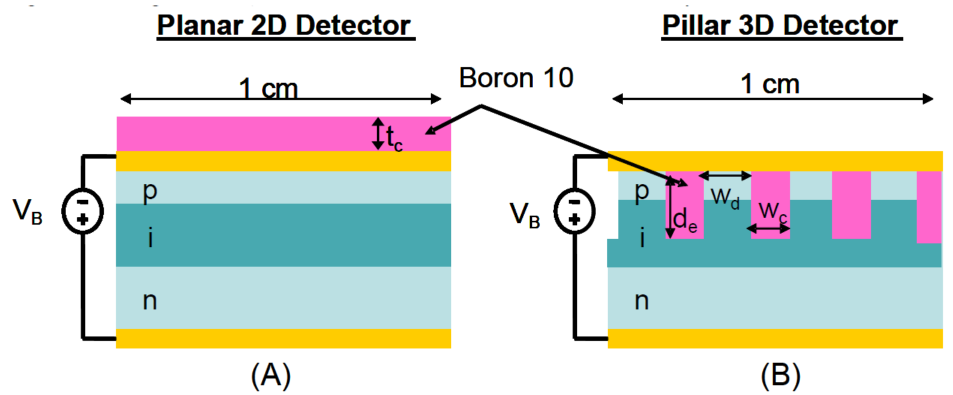

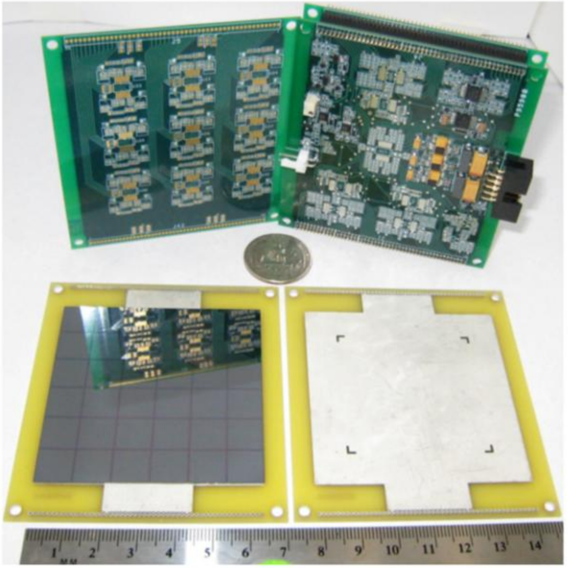

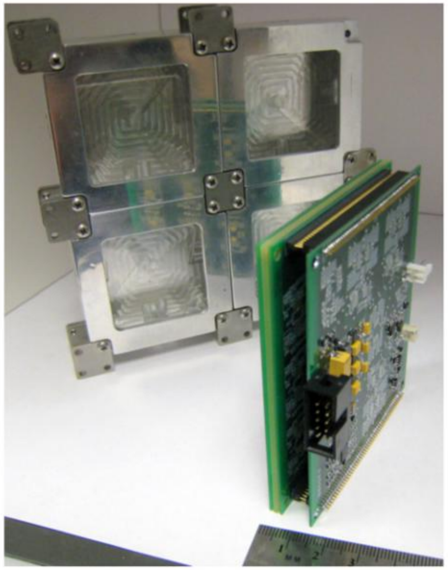

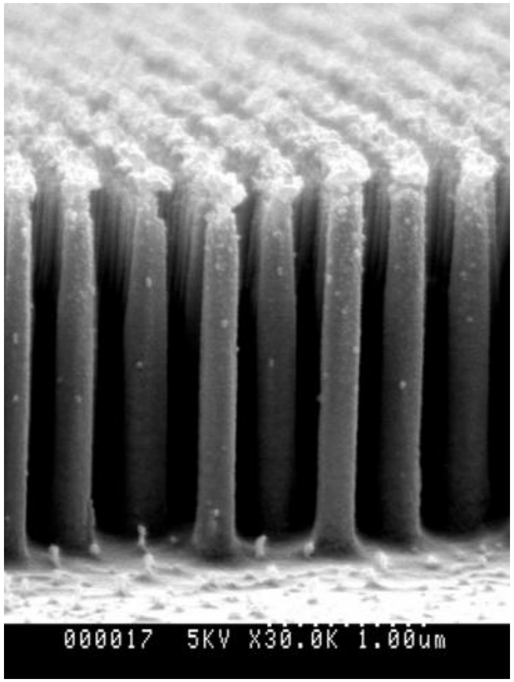

R.J. Nikolic et al. "Roadmap for High Efficiency Solid-State Neutron Detectors", Barry Chin Li Cheung Publications, 15

D.S. McGregor et al., „High-efficiency microstructured semiconductor neutron detectors that are arrayed, dual-integrated, and stacked ", Applied Radiation and Isotopes 70, 2012

New Detectors – MediPix/TimePix

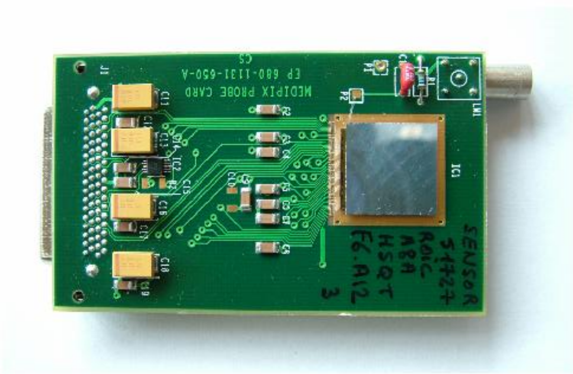

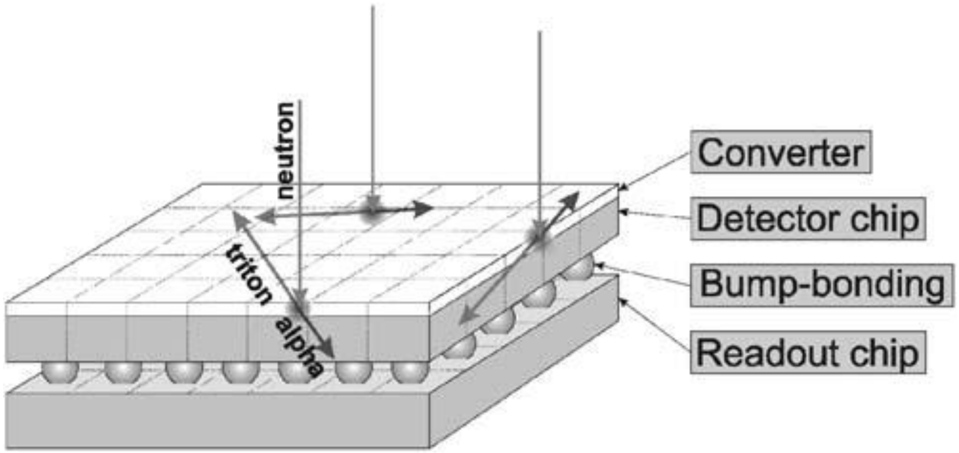

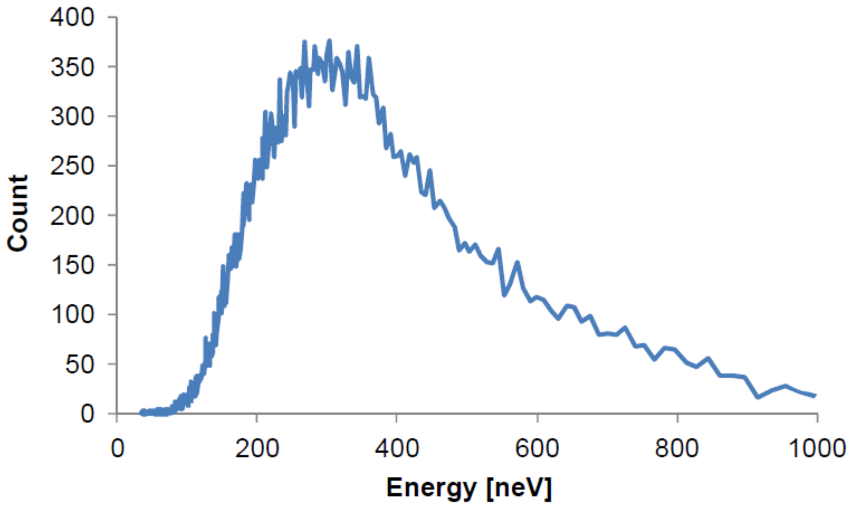

Fig. 2. Energy spectrum of UCN beam.

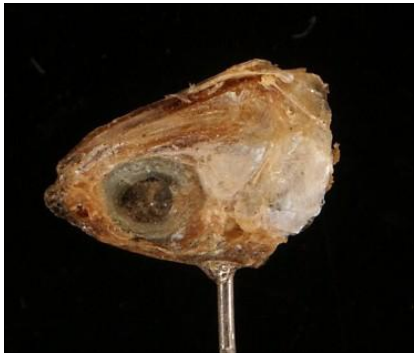

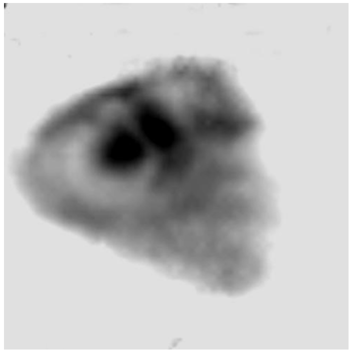

J. Uhrt et al., "Single Neutron Pixel Detector Based on Medipix-1 Device", 2004 „Performance of a pixel detector suited for slow neutrons", 2005 „3D Neutron Detectors", 2007, „ Position-sensitive spectroscopy of ultra-cold neutrons with Timepix pixel detector ", 2009

New Detectors - MCP

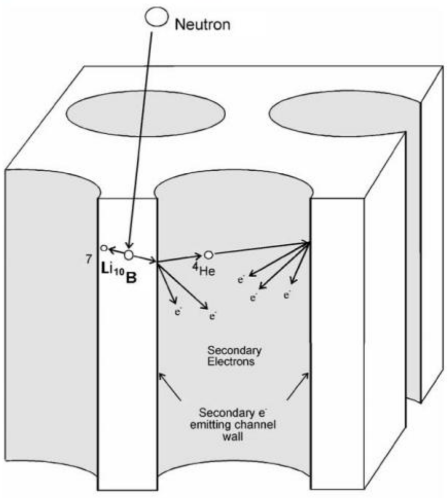

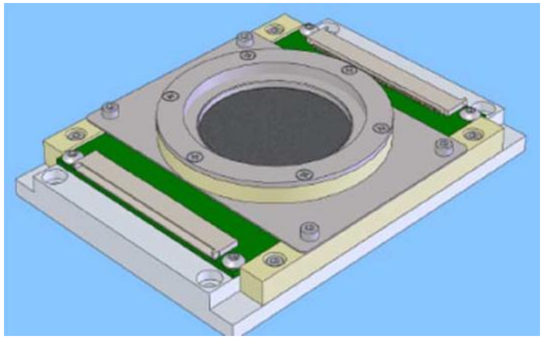

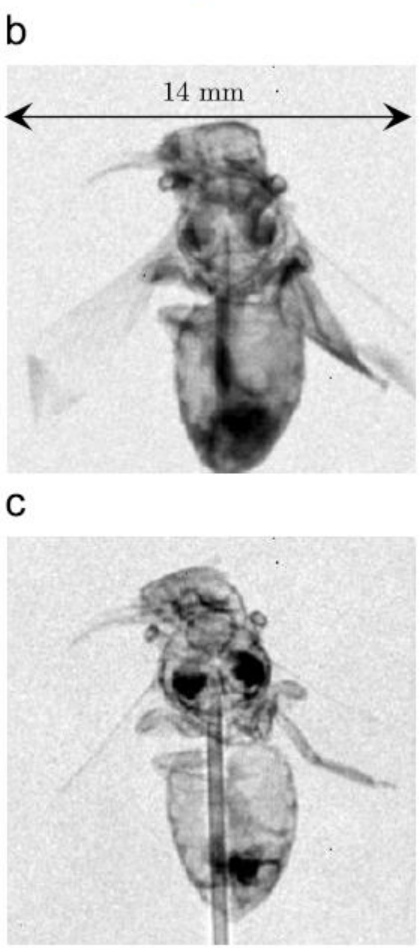

A. Tremsin et al., “High-resolution neutron radiography with microchannel plates: Proof-of-principle experiments at PSI”, NIM A, 605, 2009
A. Tremsin et al., „Efficiency optimization of microchannel plate (MCP) neutron imaging detectors. I. Square channels with 10B doping“, NIM A, 539, 2005

Fig. 3. Photograph (a) and neutron radiographic images of a bee; (b) thermal neutron beamline NEUTRA, acquisition time 15 min; (c) cold neutorn beamline ICON, acquisition time 3 min. The edges of the hypodermic needle show some diffraction enhancement.

New Detectors – GEM + Scintillation

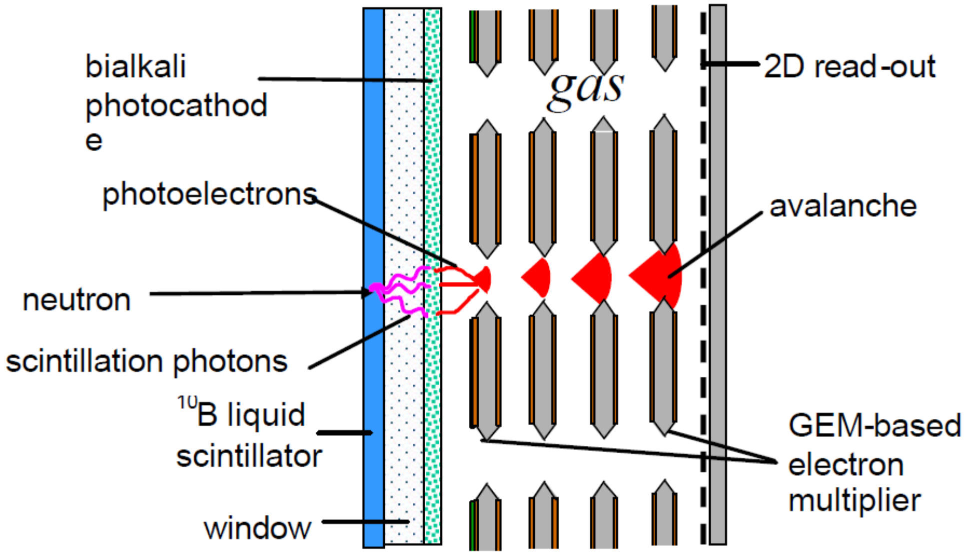

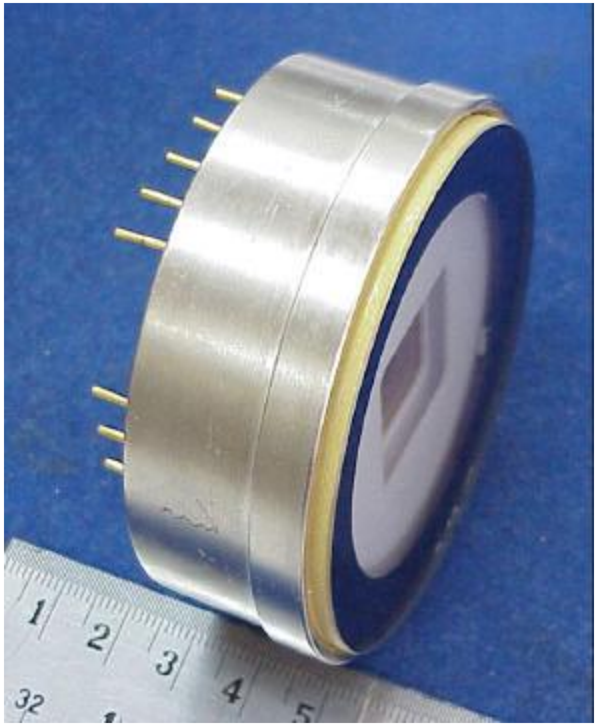

D. Vartsky et al., “Large Area Imaging Detector for Neutron Scattering Based on Boron-Rich Liquid Scintillator”, NIMA 504, 2003

New Detectors – GEM + Scintillation

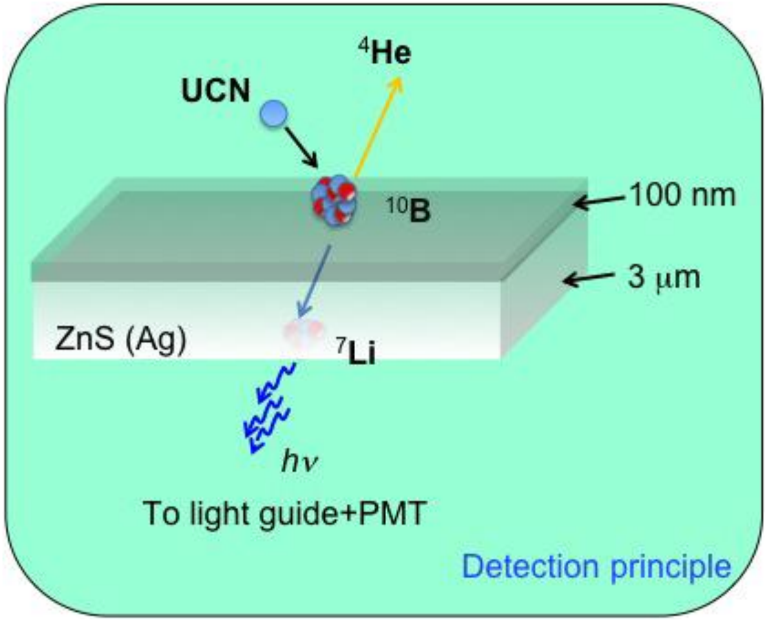

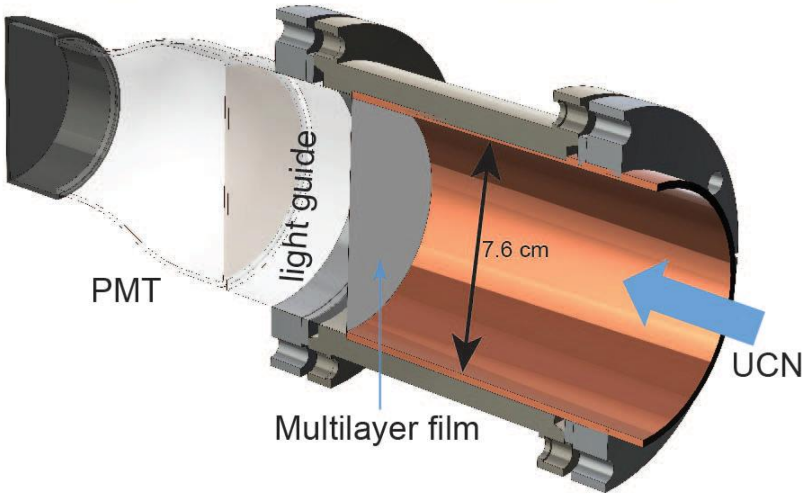

^{10}B-Coated ZnS screen

Z. Wang et al., "A multilayer surface detector for ultracold neutrons", arXiv:1503.03424v3

New Detectors - WLSF

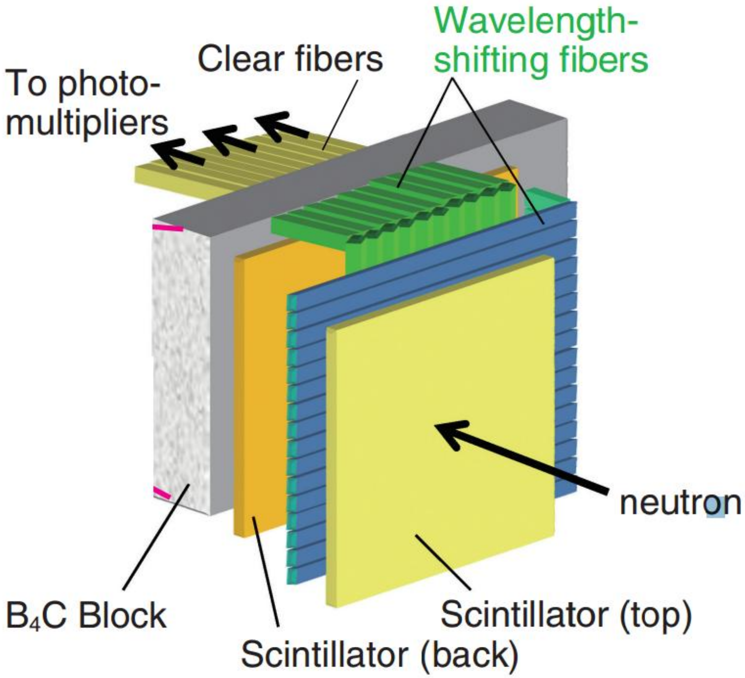

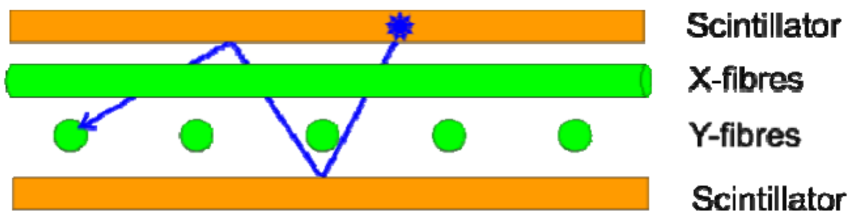

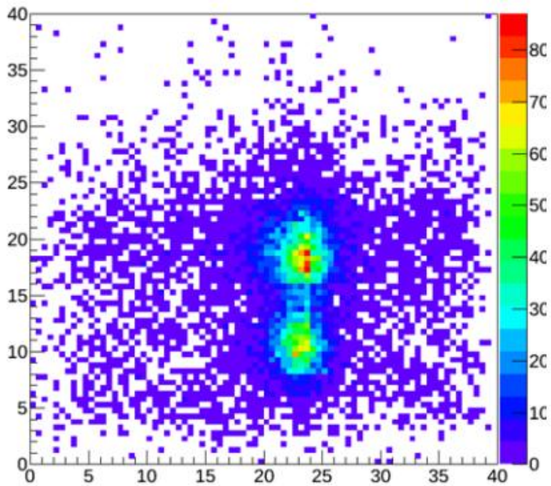

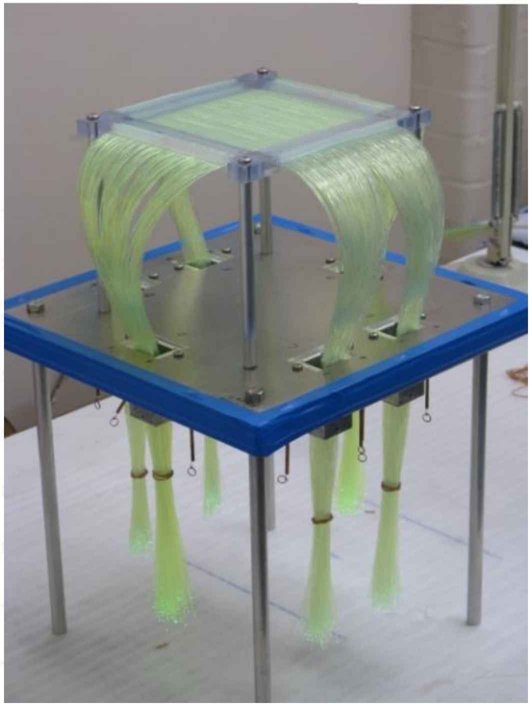

J. Sykora, "WLSF detector status and future plans at ISIS", 2013
R. Engels "Status WLSF Neutron Detector Prototype from FZJ", 2012
Nakamura, T. et al., "A Large-Area Two-Dimensional Scintillator Detector with a Wavelength-Shifting Fibre Readout for a Time-of-Flight Single-Crystal Neutron Diffractometer", NIM A, 686, issue 1, 2012.

New Detectors – Excited Dimer

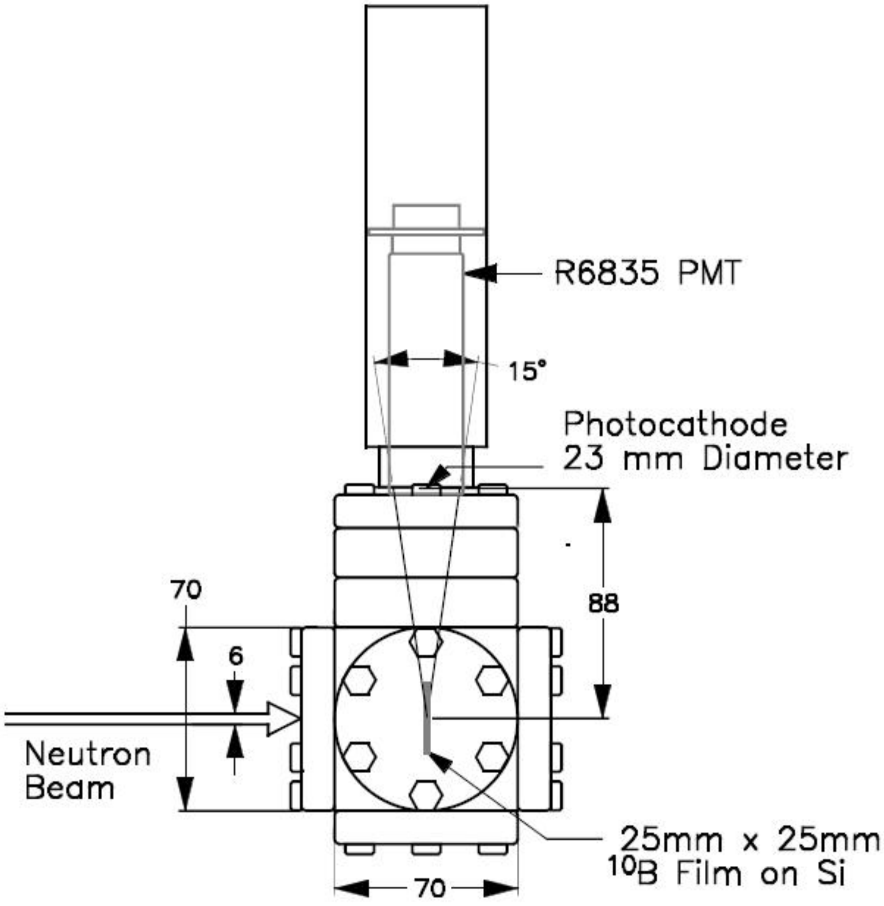

C.M. Lavelle et al., "Demonstration of neutron detection utilizing open cell foam and noble gas Scintillation", Apl. Phys. Let. 106, 2015

CASCADE

The Detector

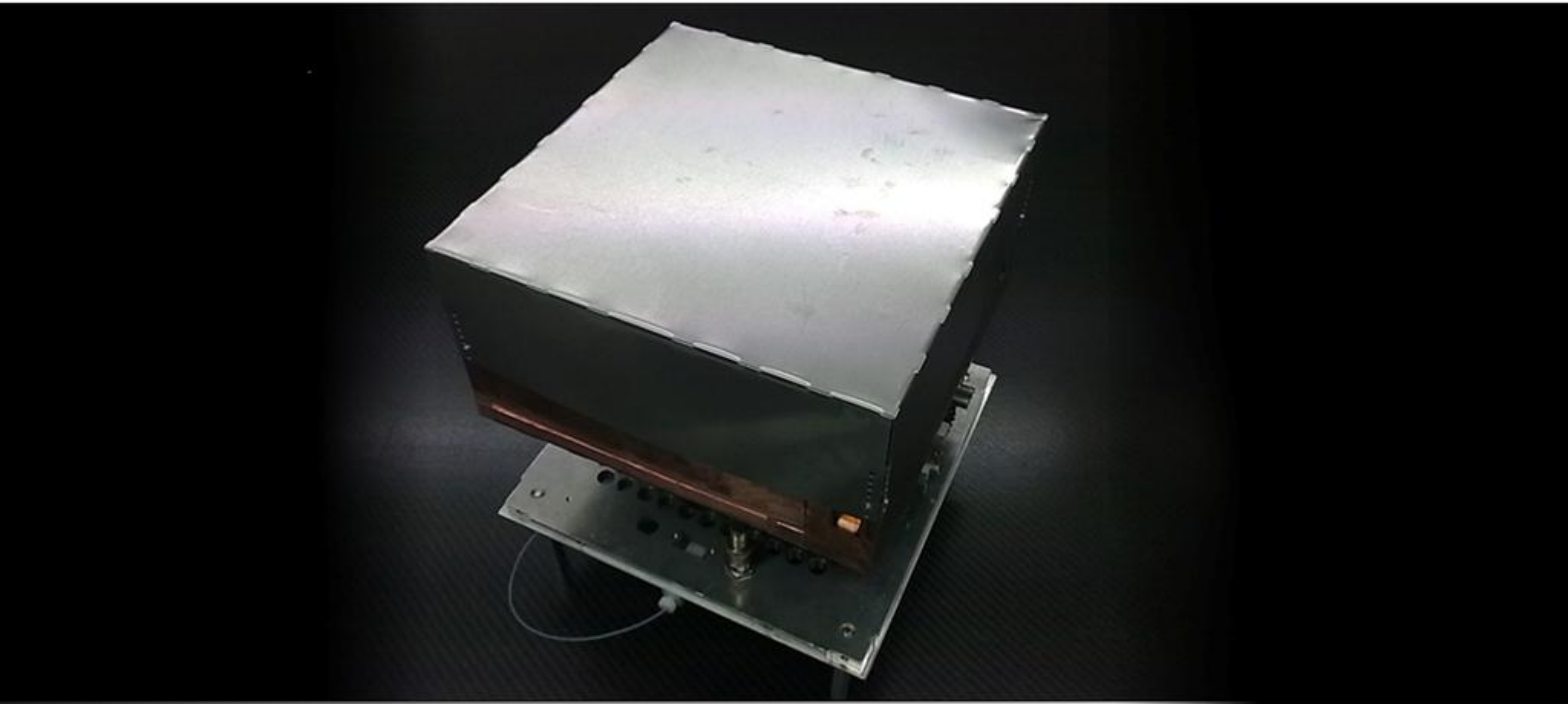

The CASCADE Detector

CASCADE detector without housing

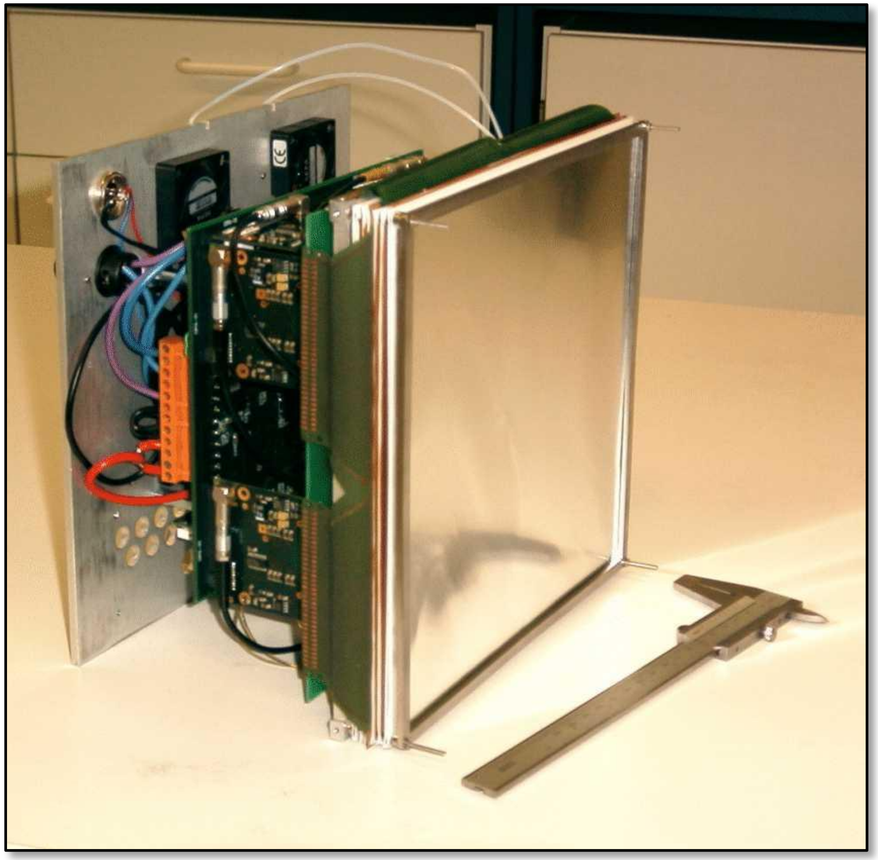

The CASCADE Detector

CASCADE detector without housing

Active Detection Volume

Readout

Electronics

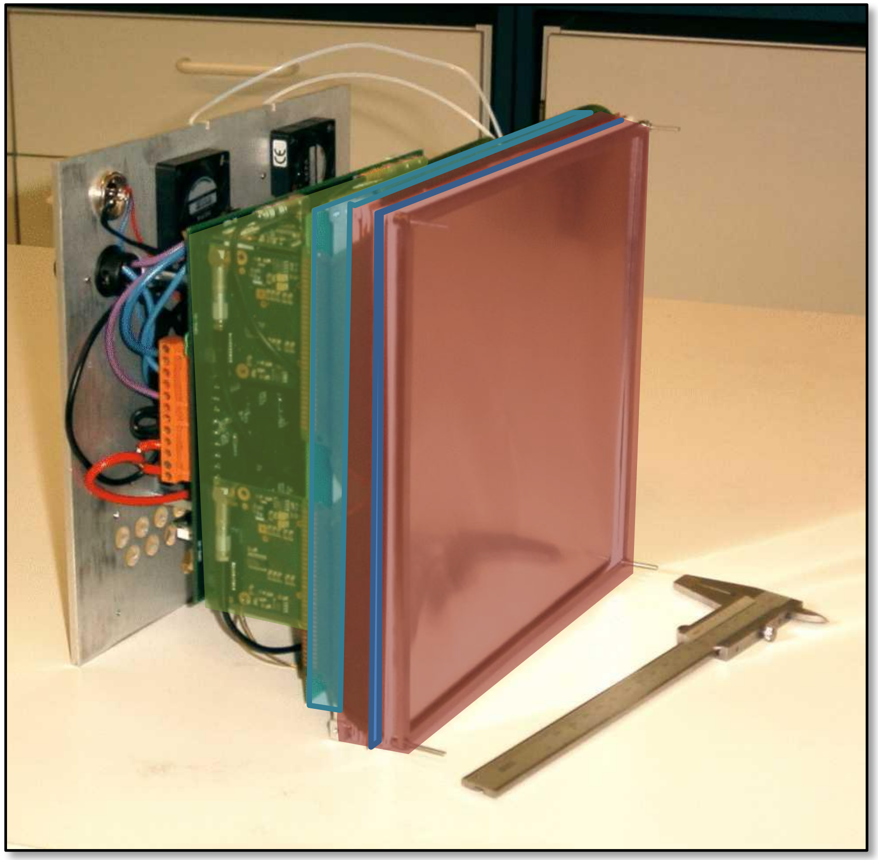

The CASCADE Concept

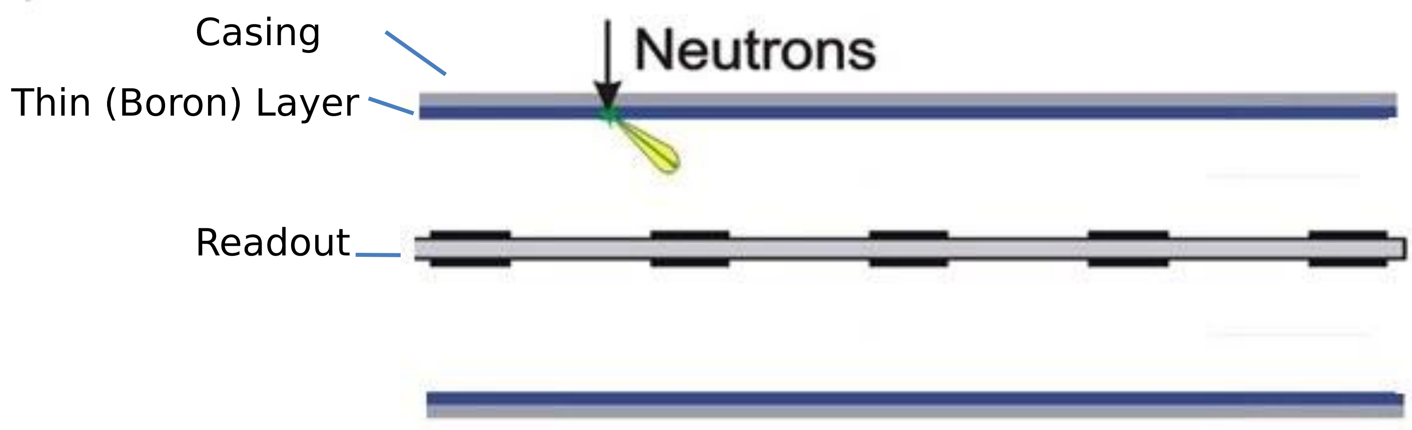

The CASCADE Concept

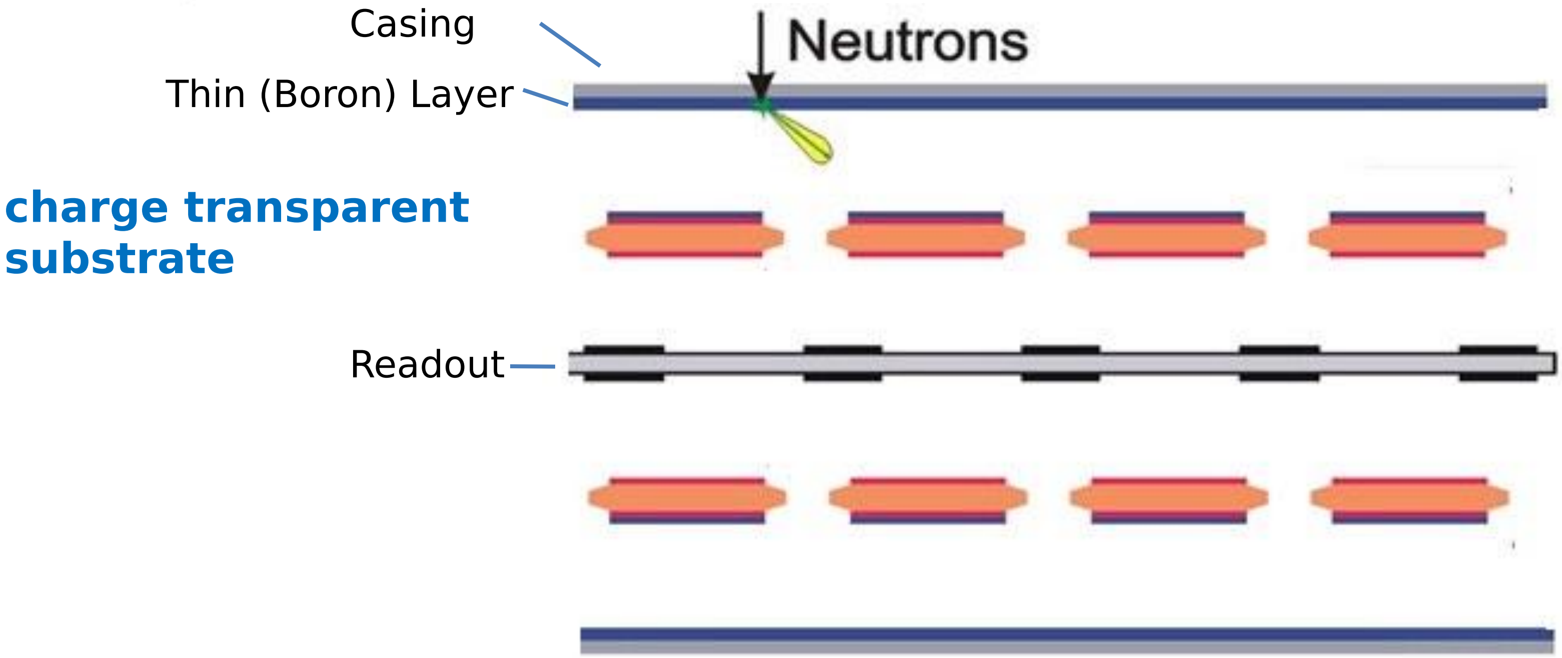

The CASCADE Concept

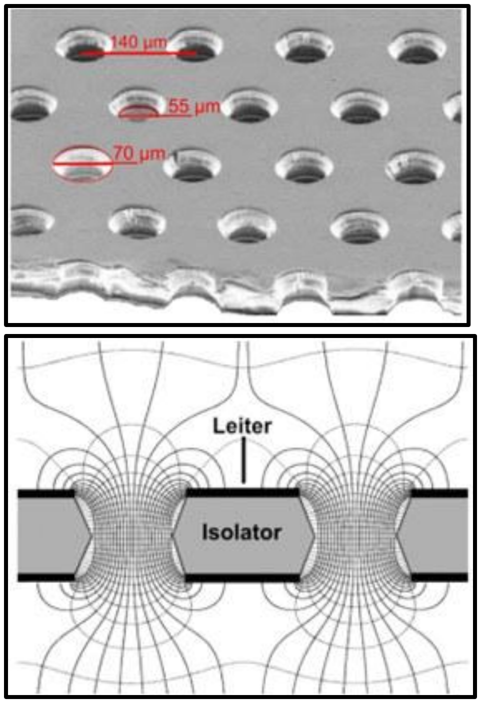

GEM
(Gas Electron Multiplier foil)

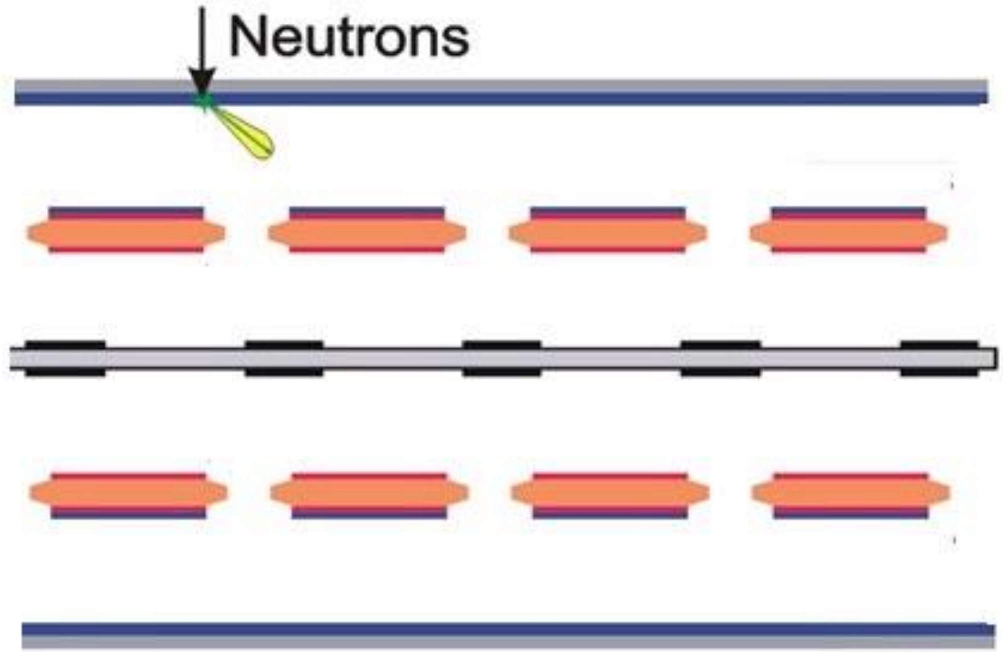

The CASCADE Concept

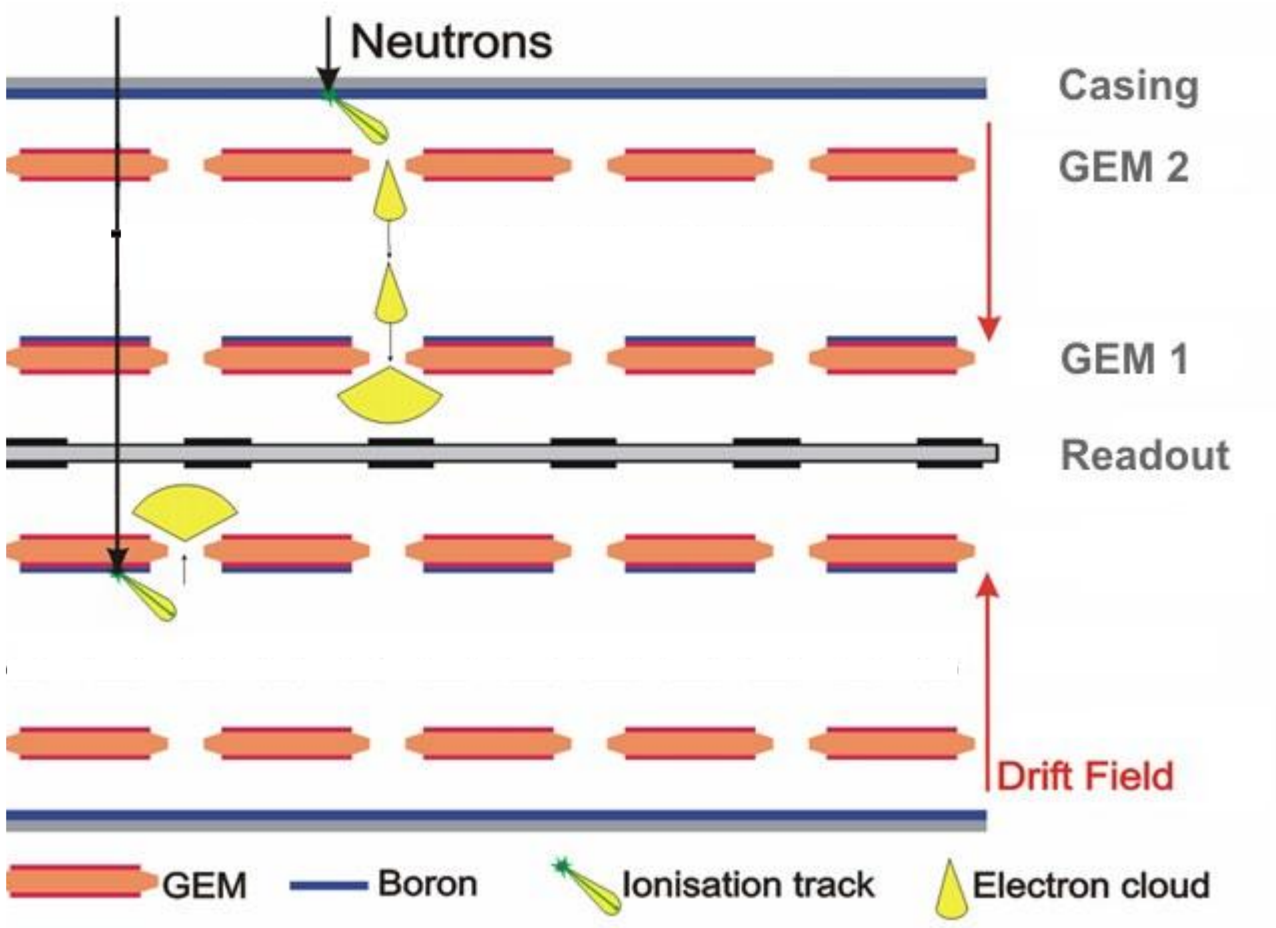

The CASCADE Concept

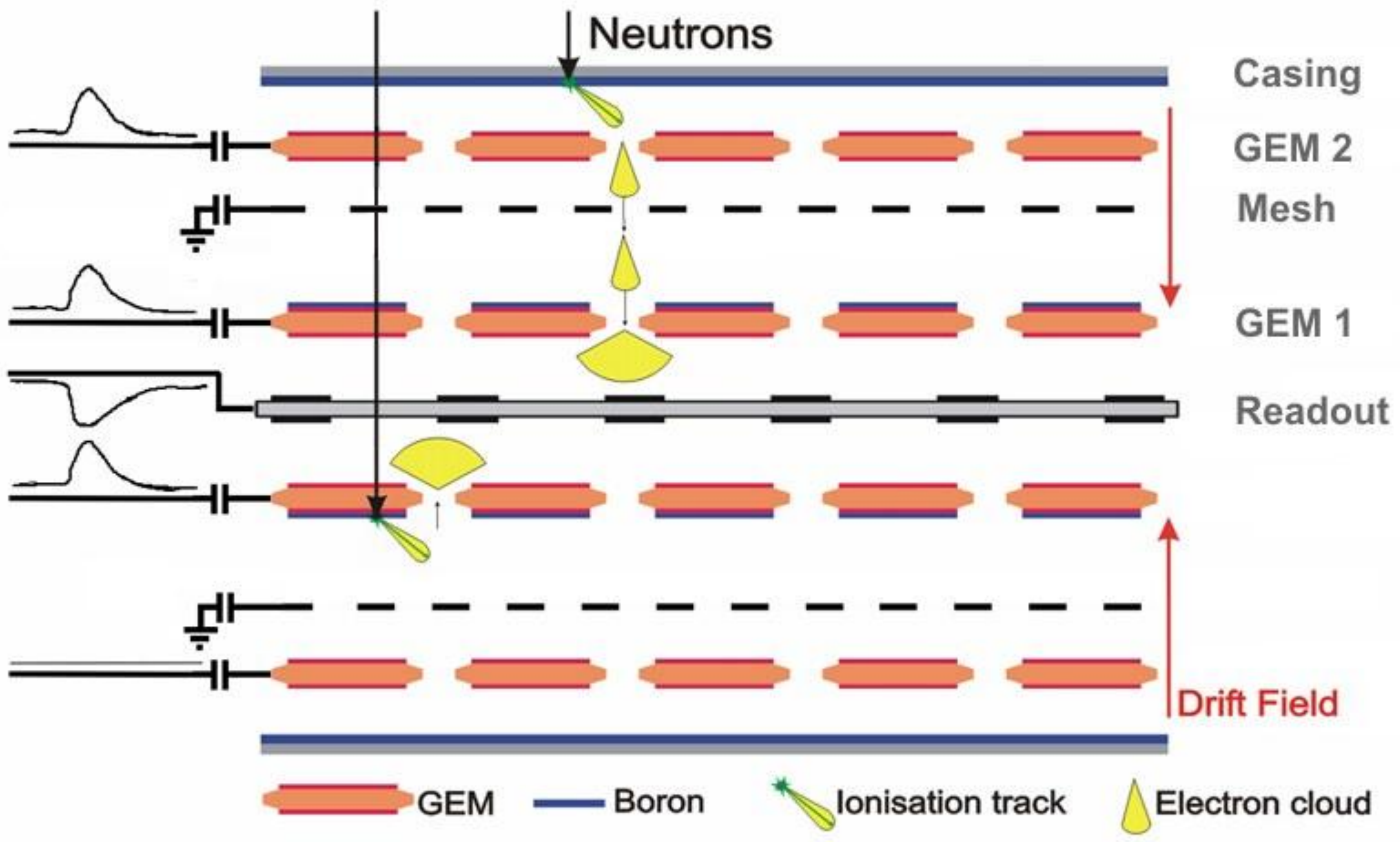

The CASCADE Concept

thin gap
measures dE/dx

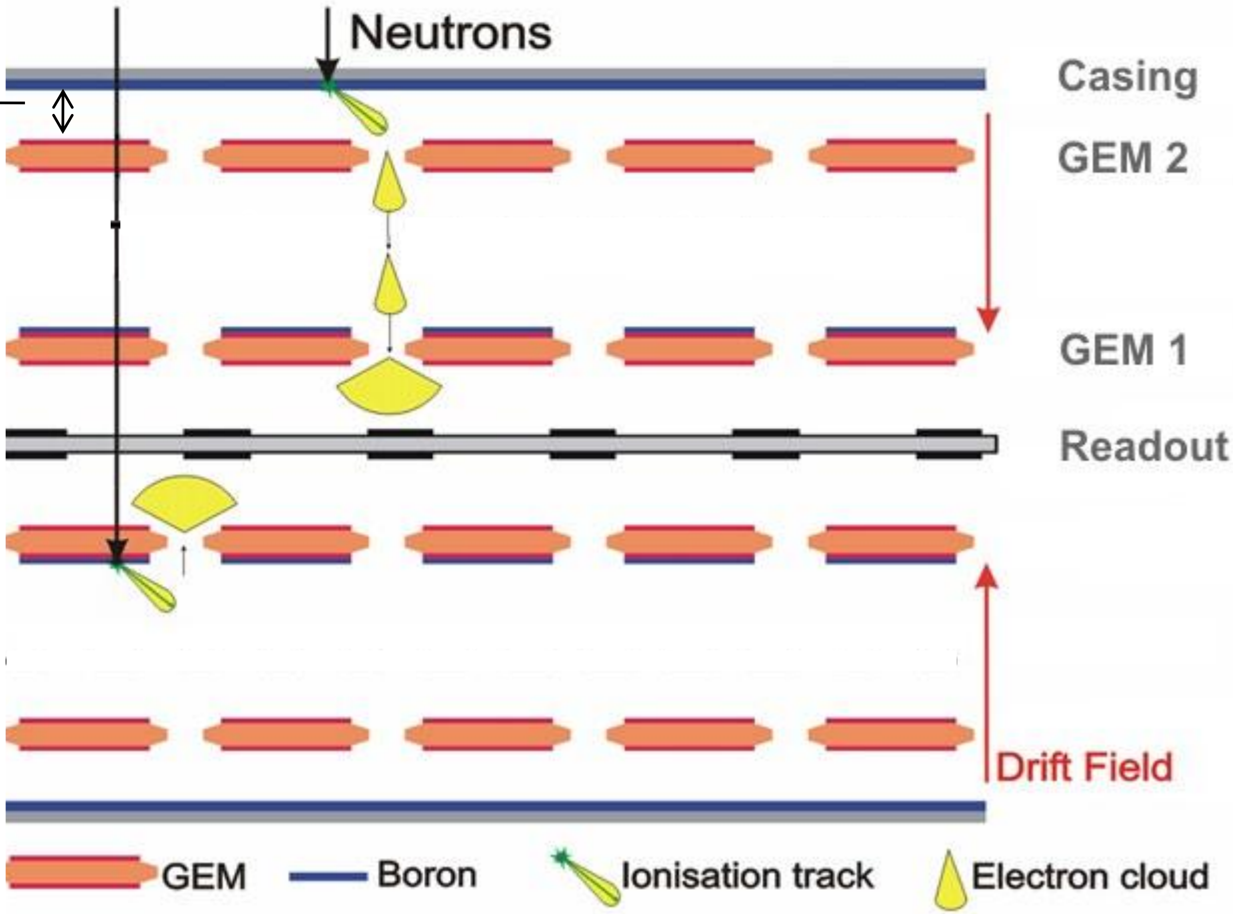

Signals in the Detector

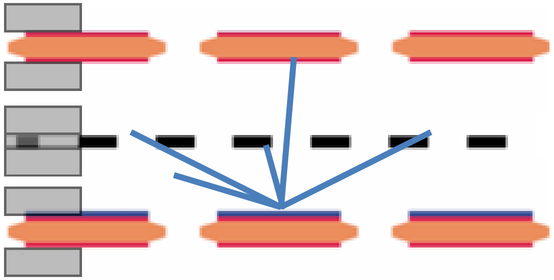

Signals in the Detector

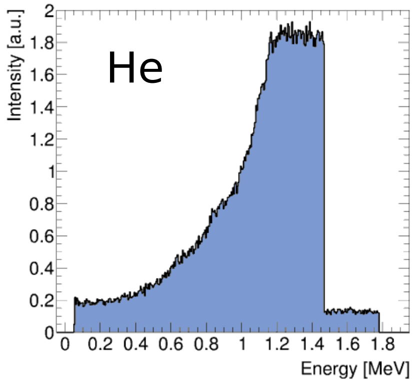

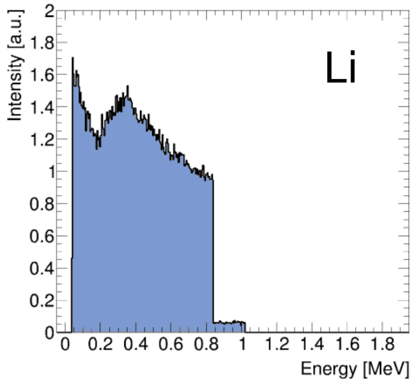

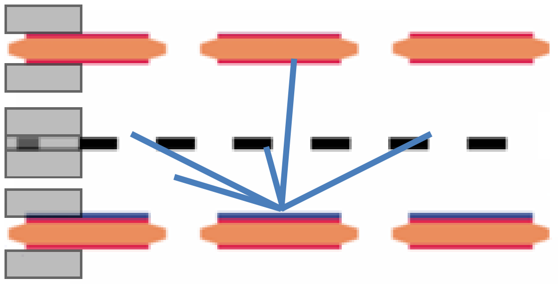

Signals in the Detector

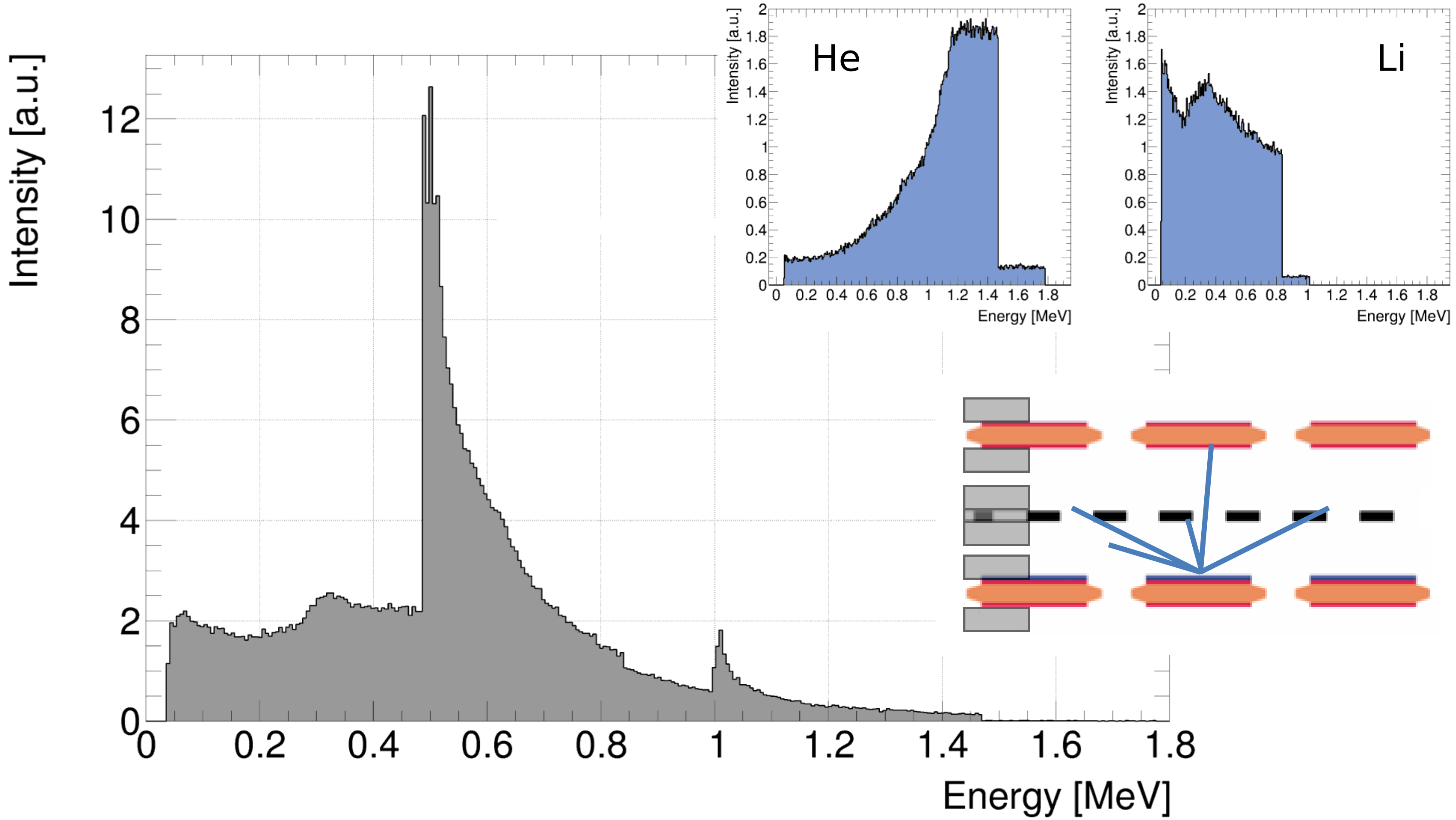

Signals in the Detector

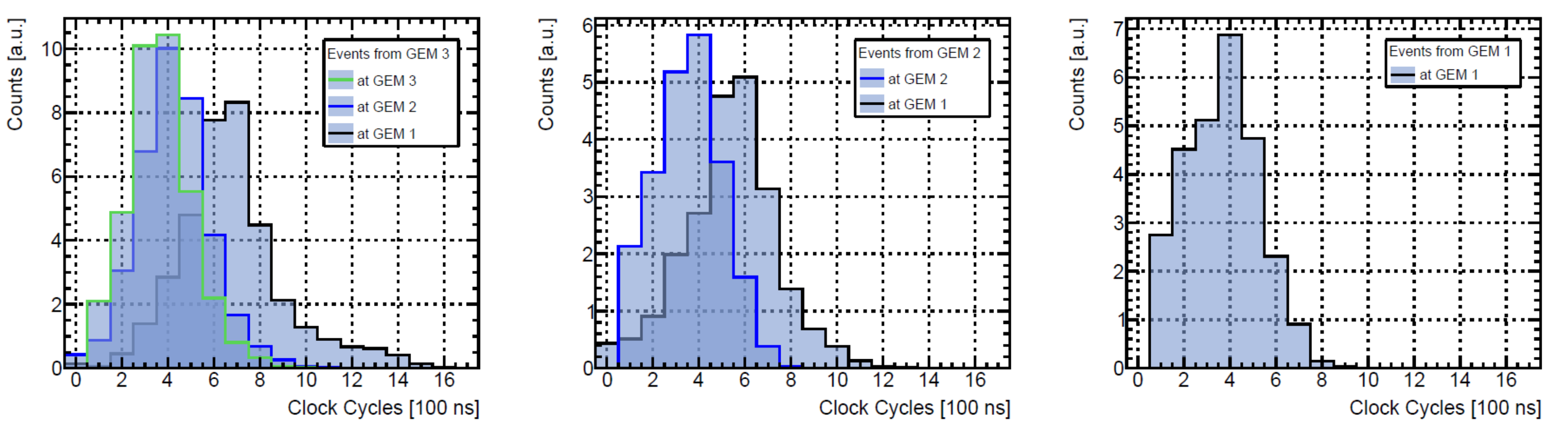

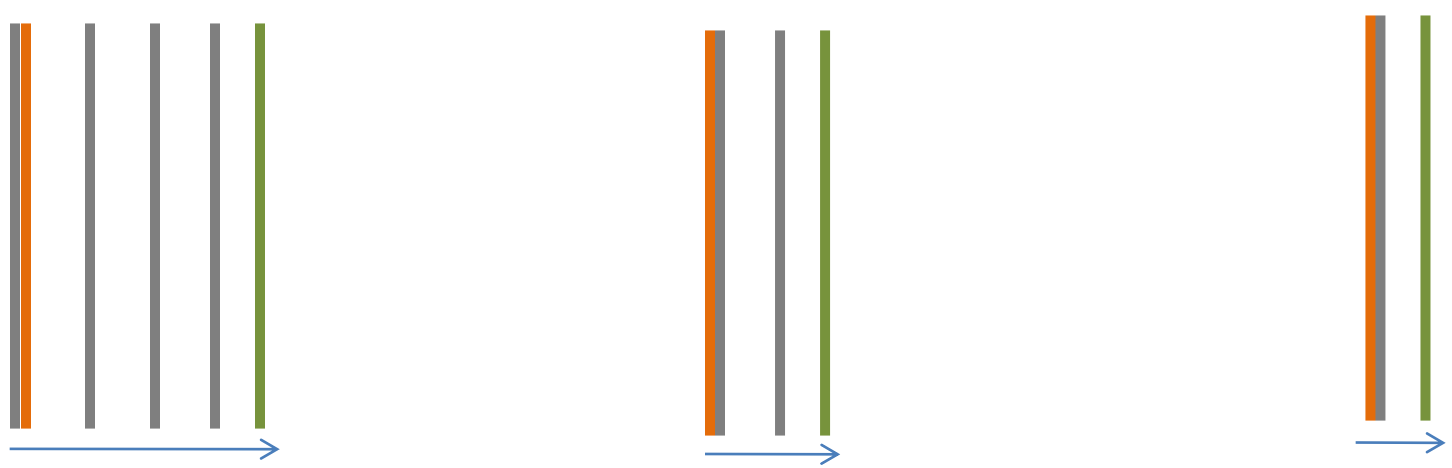

Conversion Products: Energy Spectra

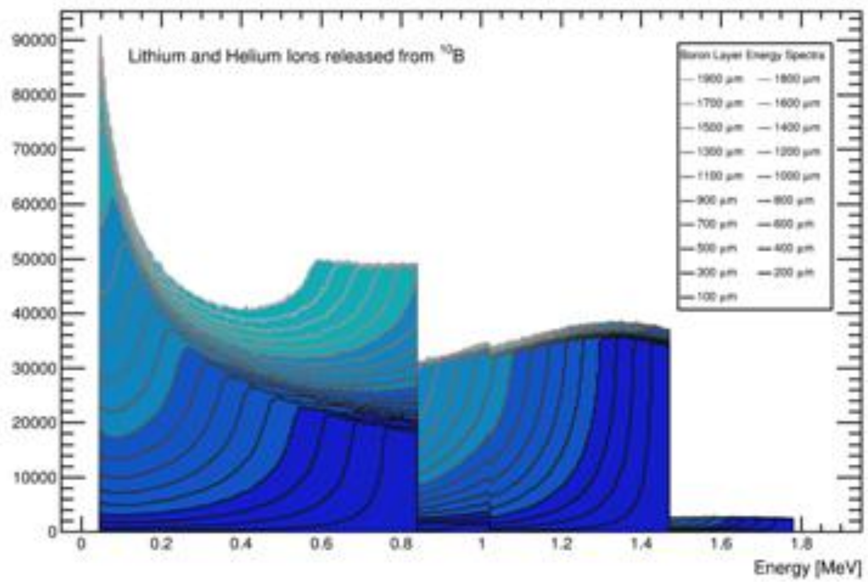

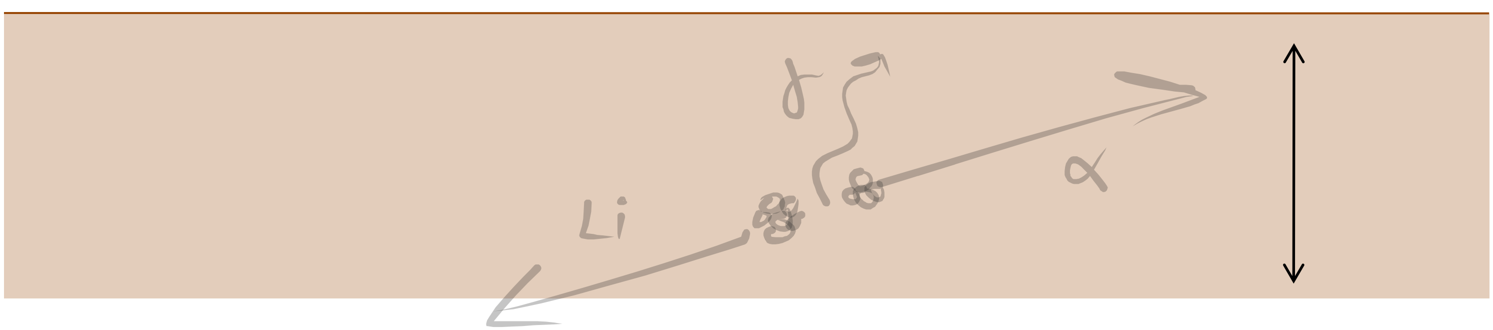

Conversion Products: Energy Spectra

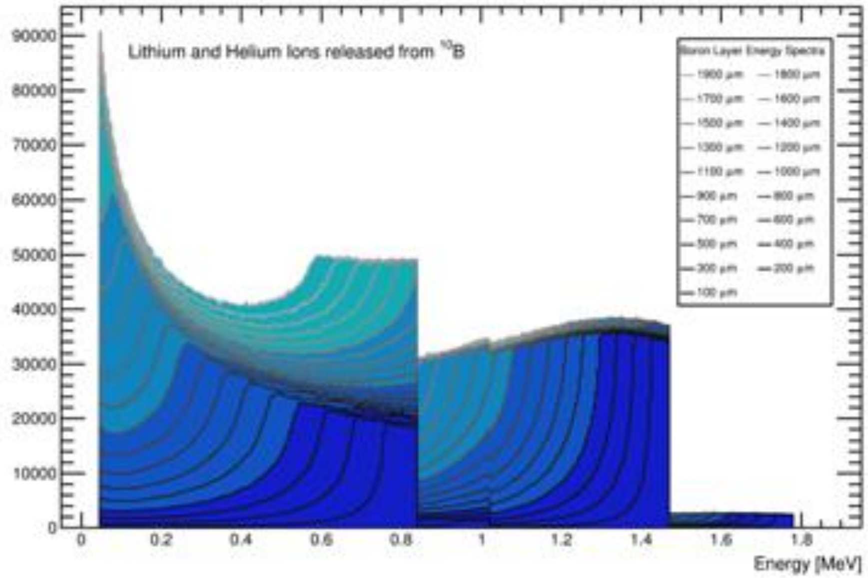

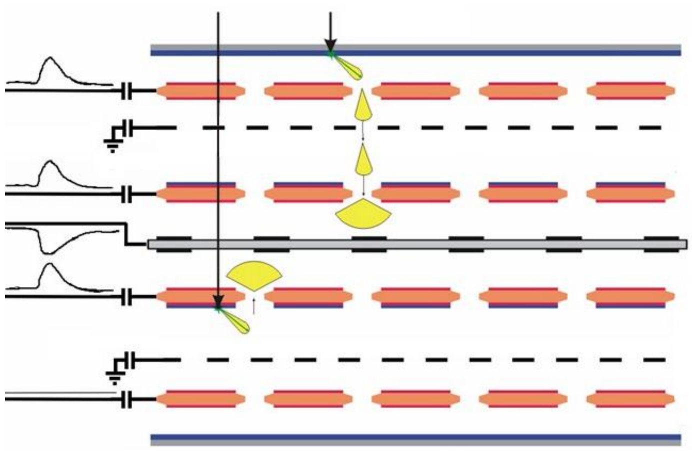

Conversion Products: Energy Spectra

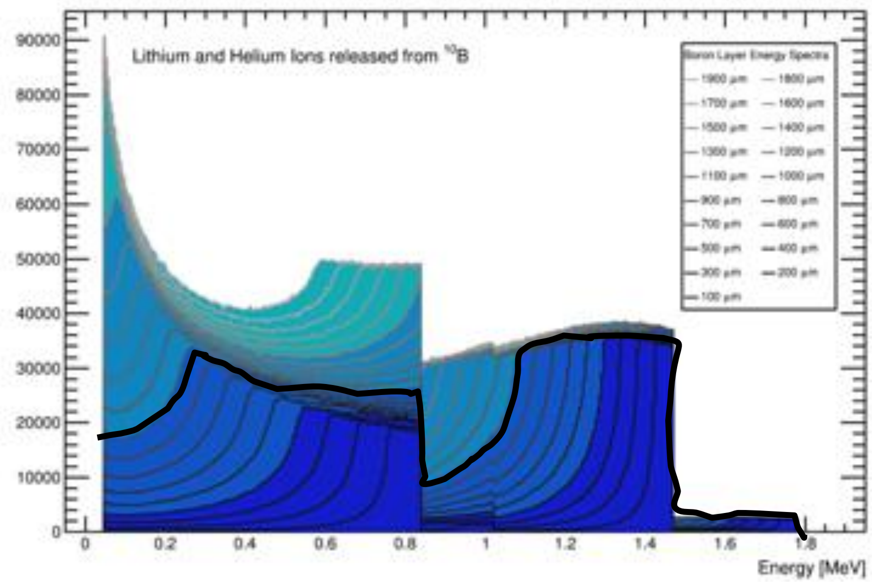

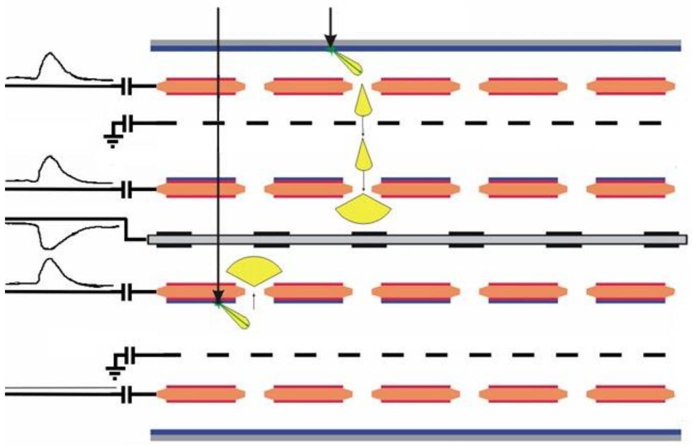

CASCADE

Characterization Measurements

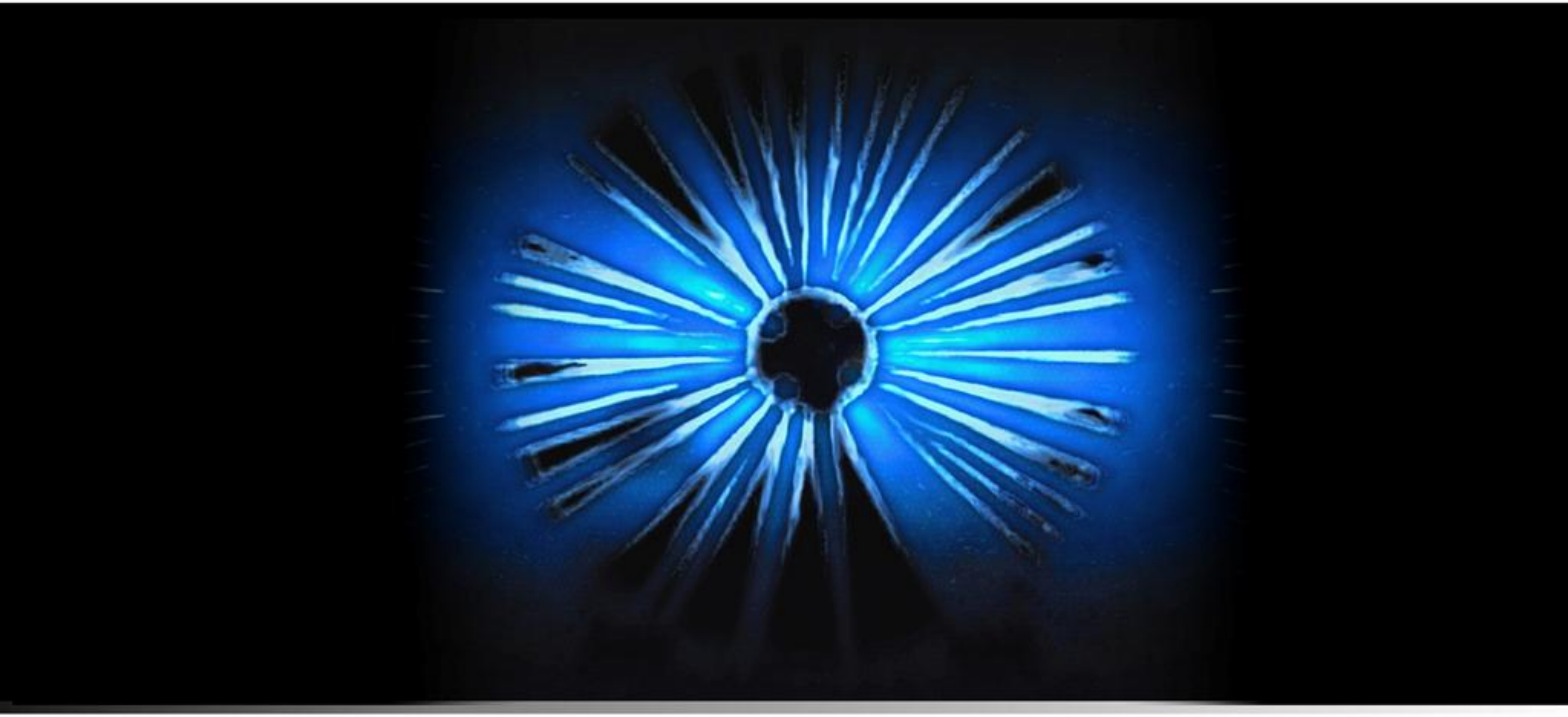

CASCADE

Characterization Measurements

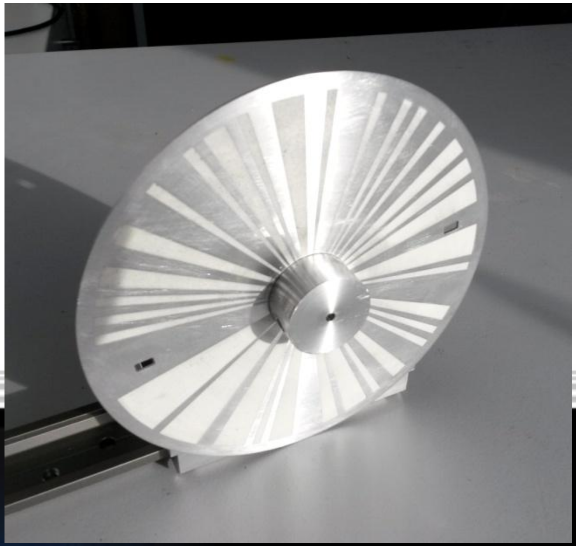

Spatial Resolution

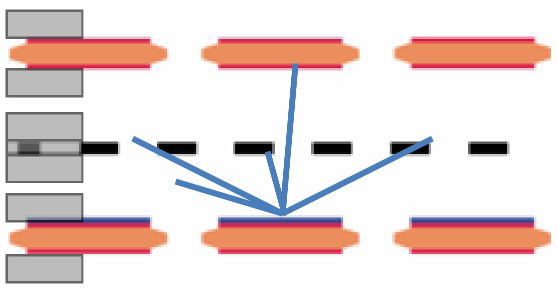

Spatial resolution: 2.4 mm FWHM

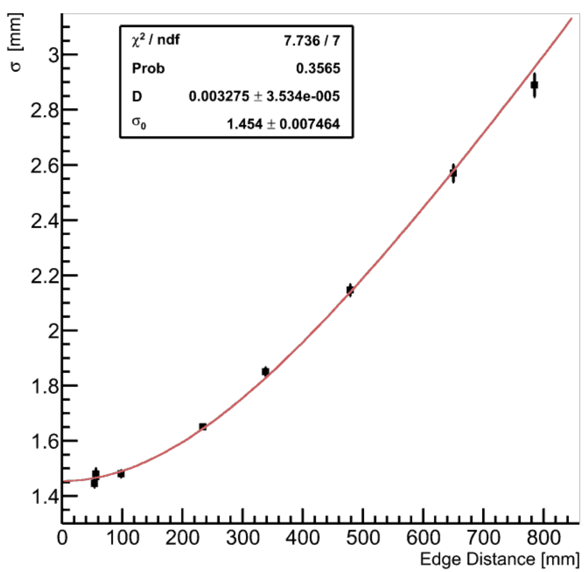

Image of a cold neutron beam (after guide)

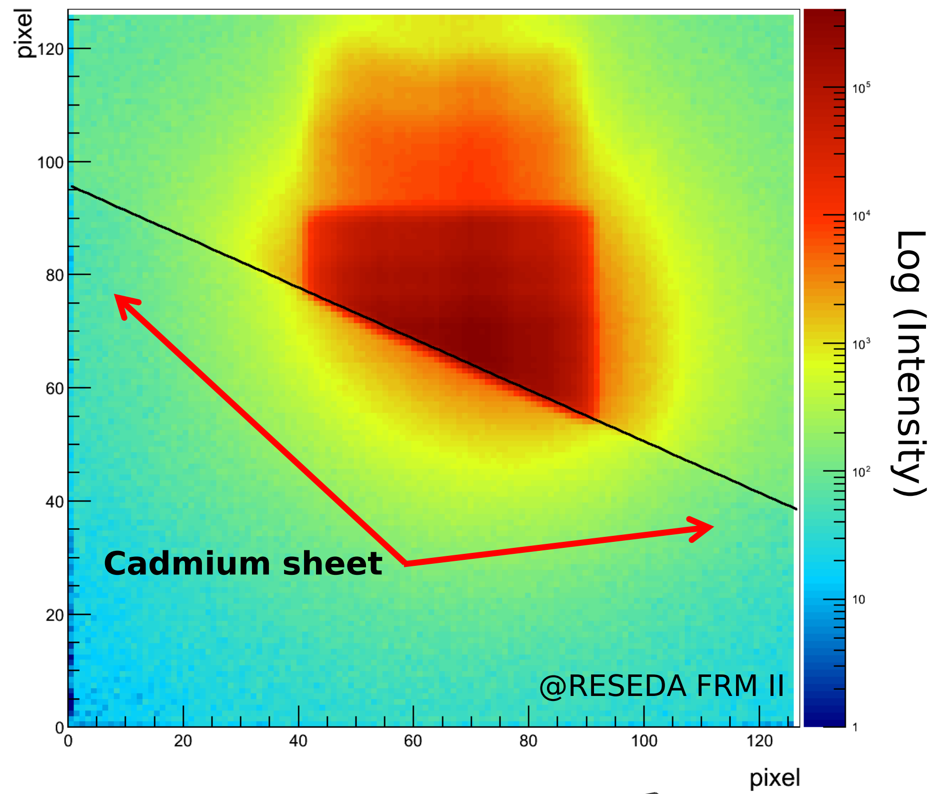

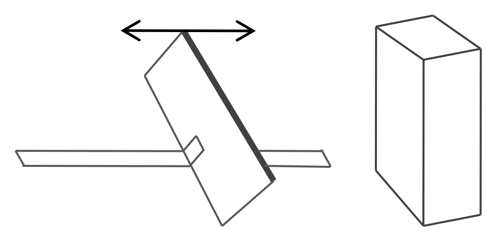

Spatial Resolution

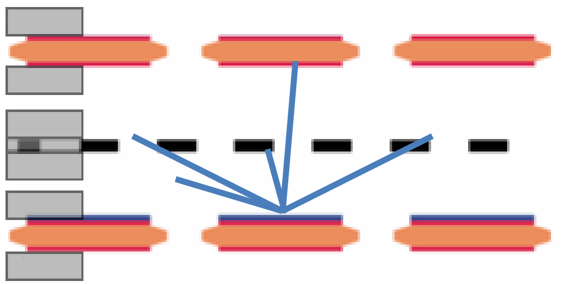

Spatial resolution: 2.4 mm FWHM

Cross section of a collimated n beam

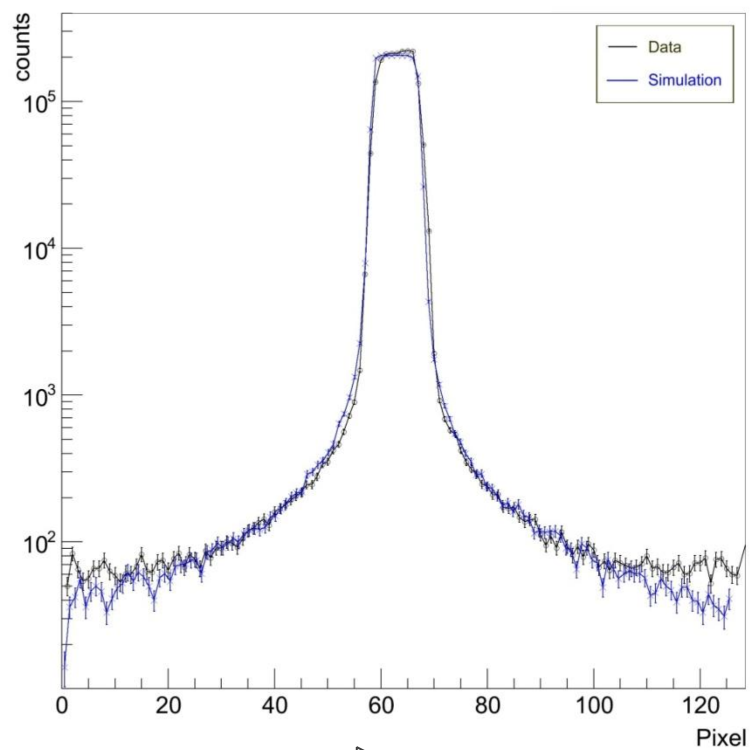

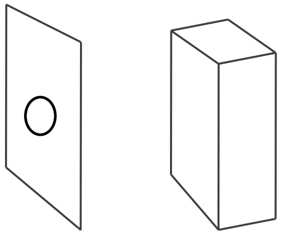

Imaging Mode

Rate Capability

count rate
2-3 MHz

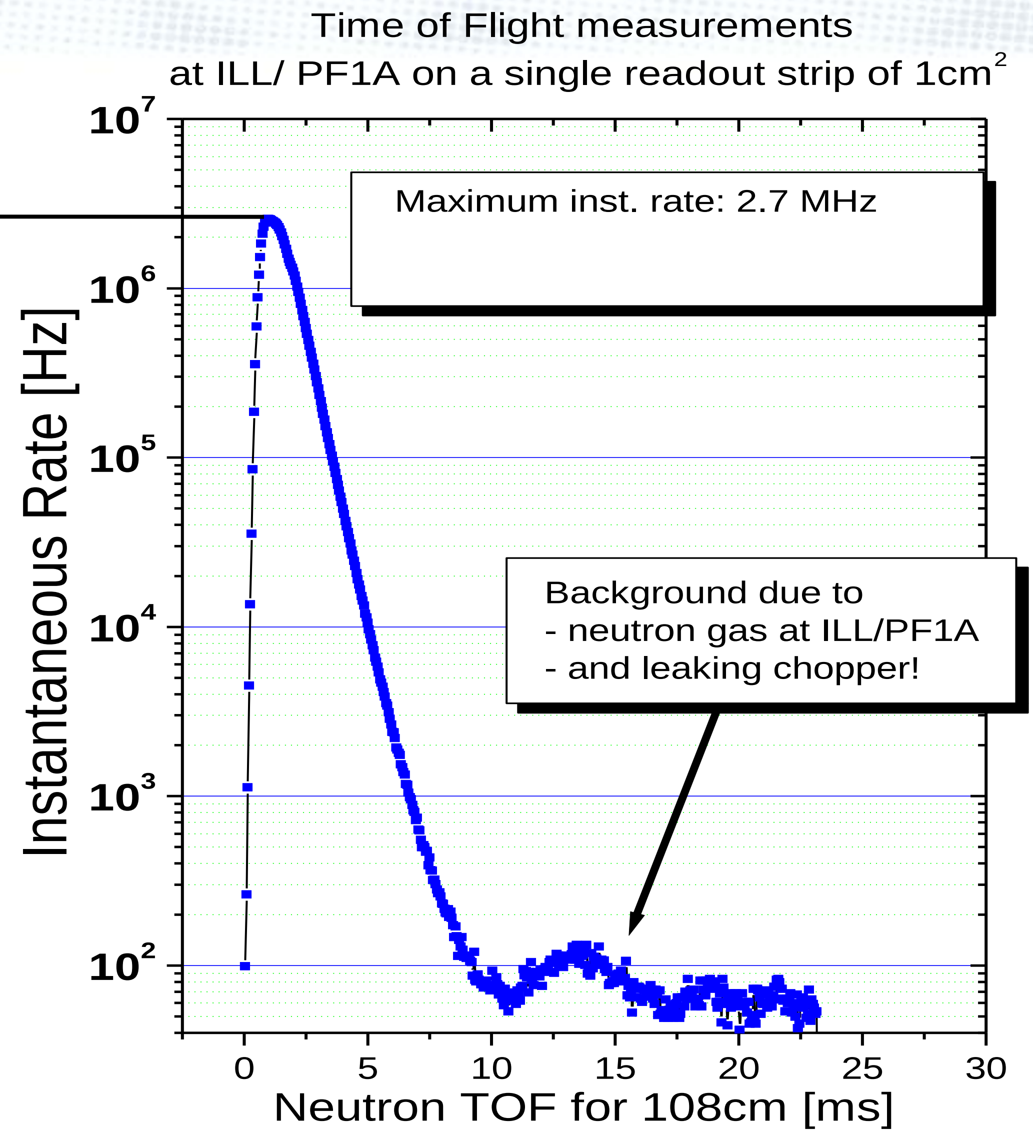

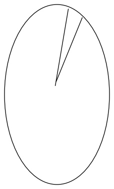

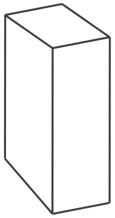

Detection Efficiency

1.5 – 0.8 – 1.0 – 1.0 – 0.8 – 2.5

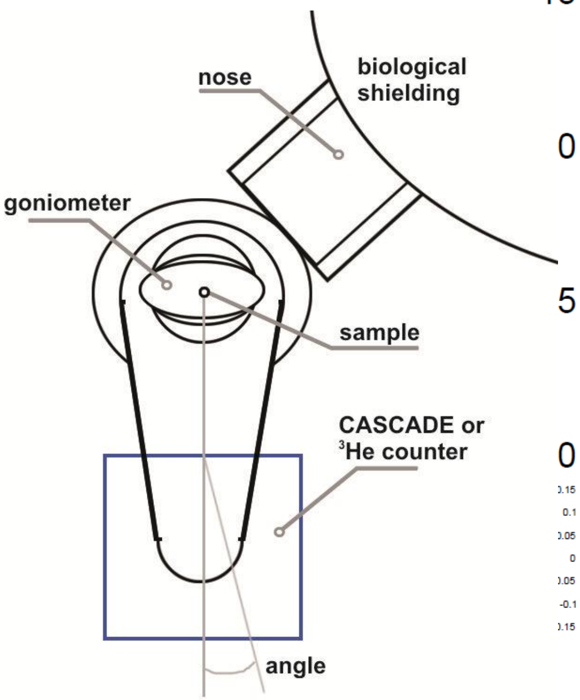

Efficiency at 0.6 Å, 0.8 Å and 1.2 Å in 2D and 3D

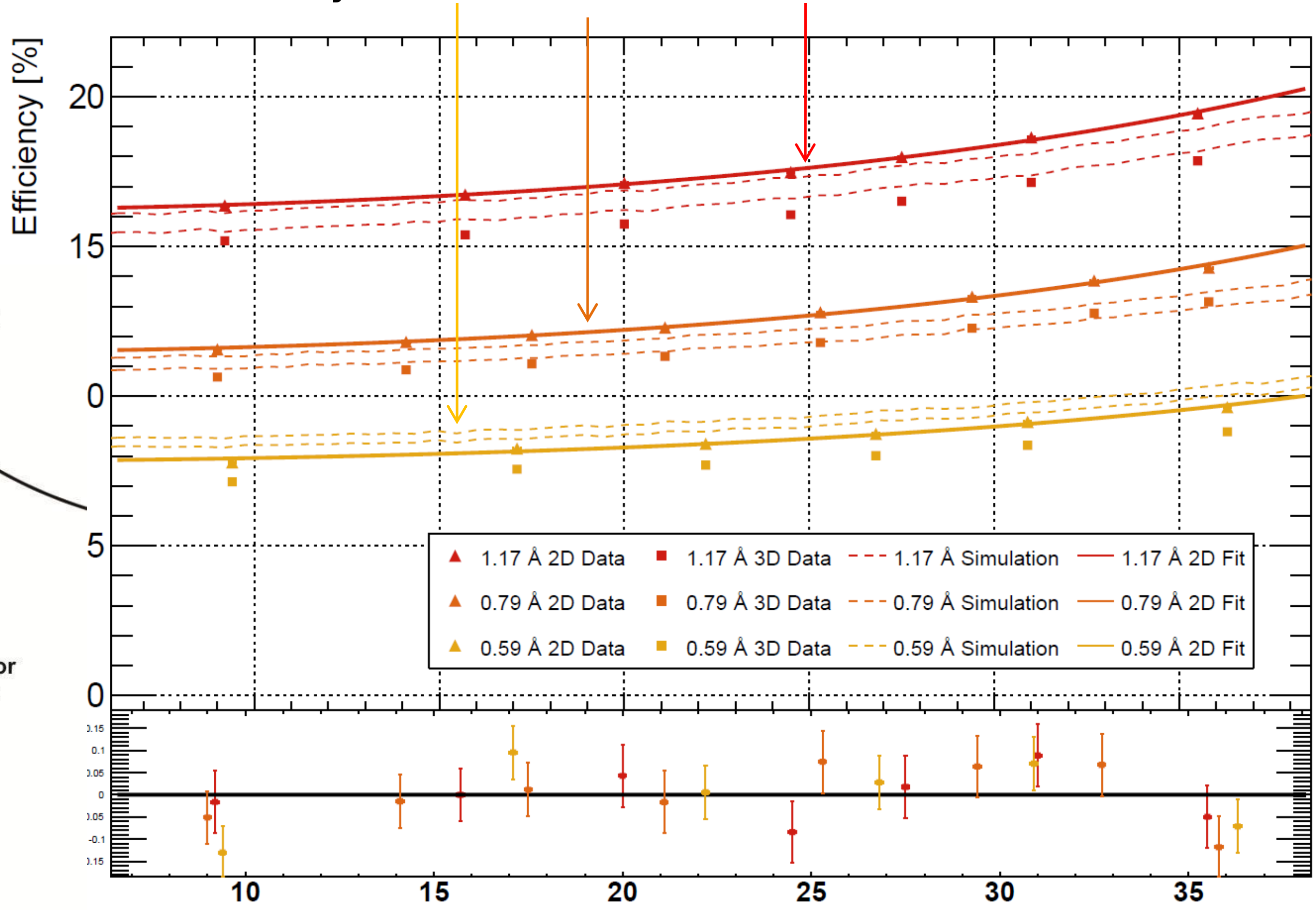

@HEIDI FRM II

Detection Efficiency

1.5 – 0.8 – 1.0 – 1.0 – 0.8 – x

Simulation of the 2D efficiency and data of 0.6 Å, 0.8 Å and 1.2 Å

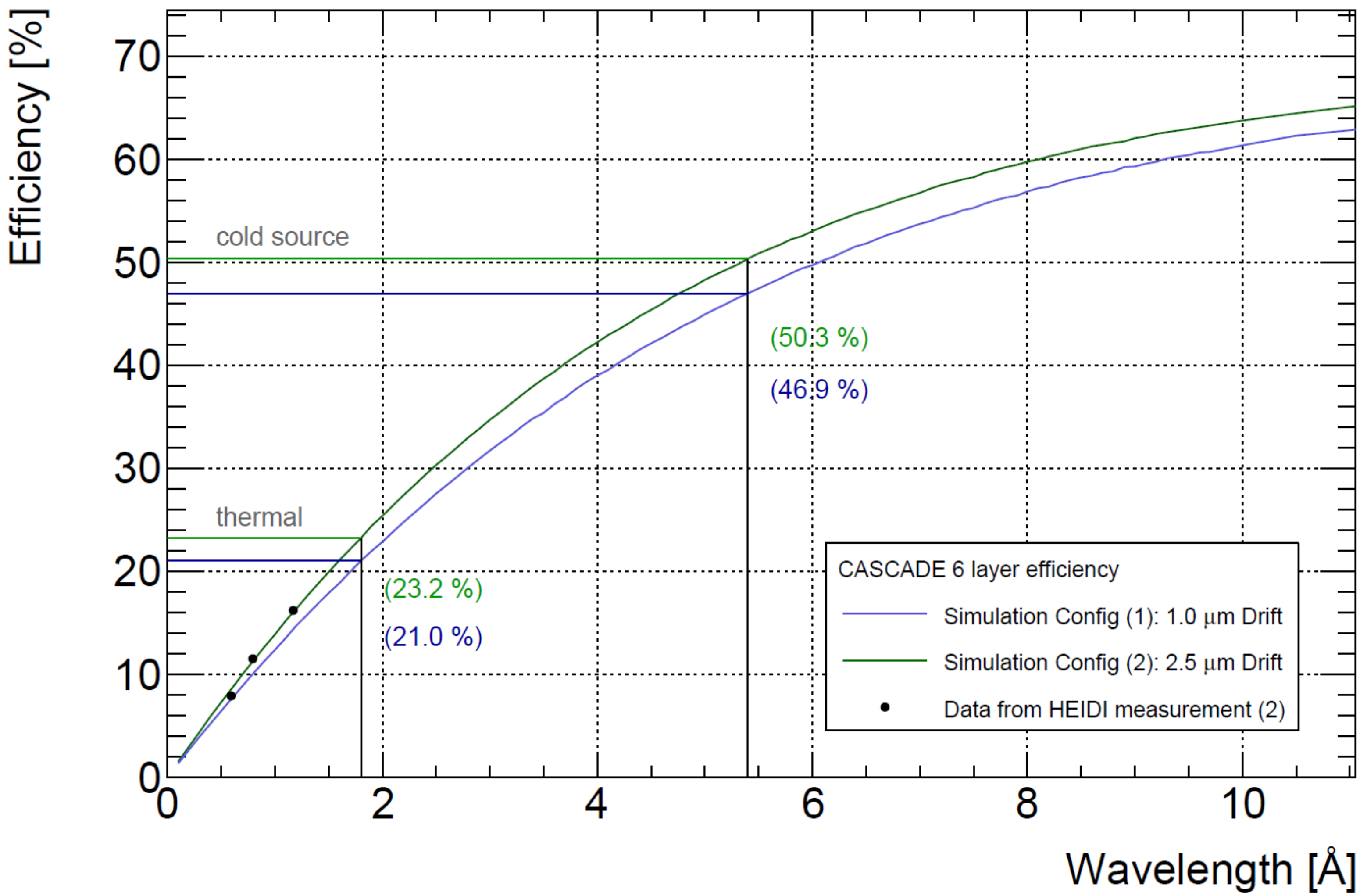

Detection Efficiency

Simulation of the 2D efficiency with different coating thicknesses

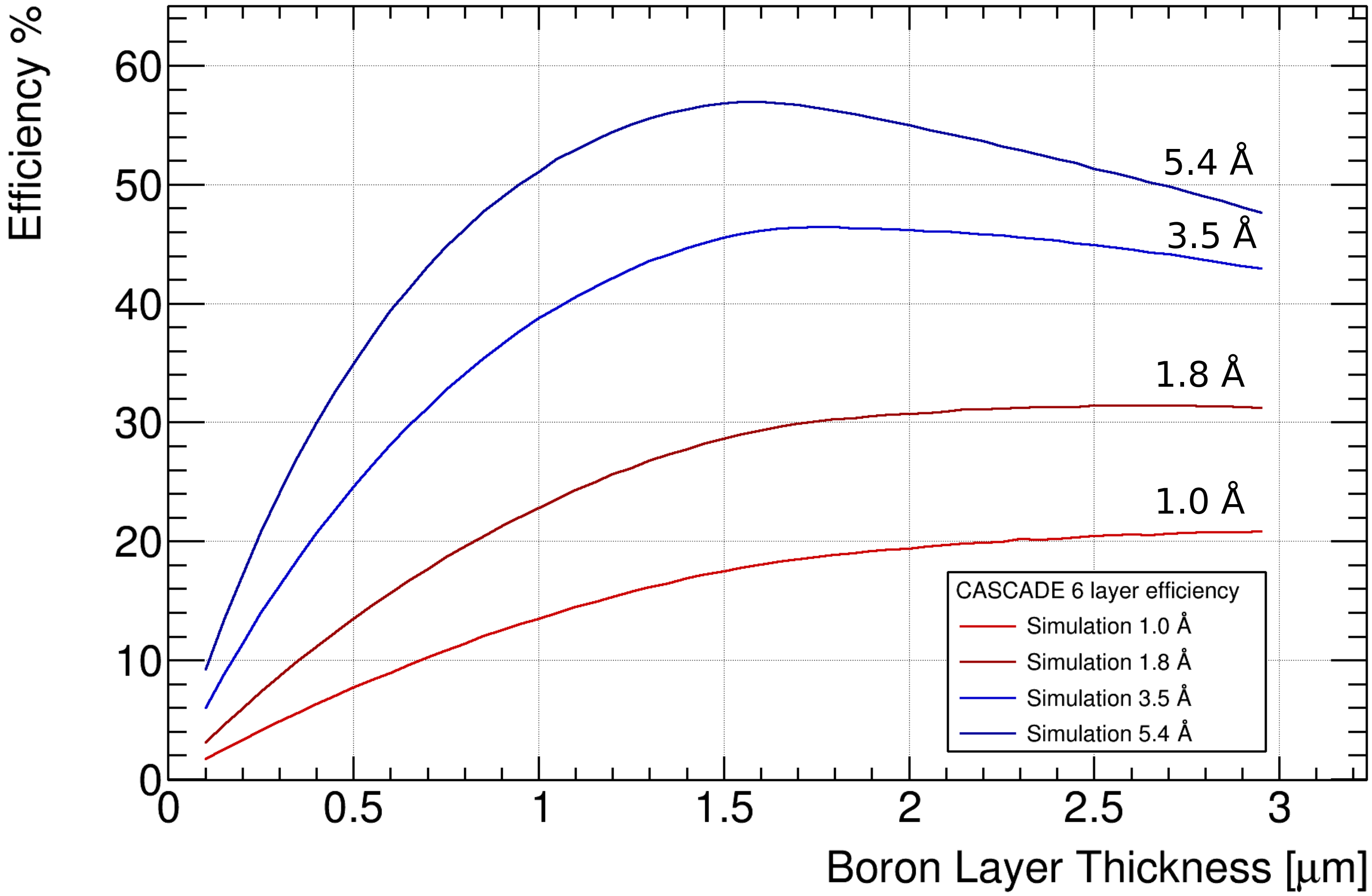

Detection Efficiency

Comparison of the efficiency to a Helium-3 tube

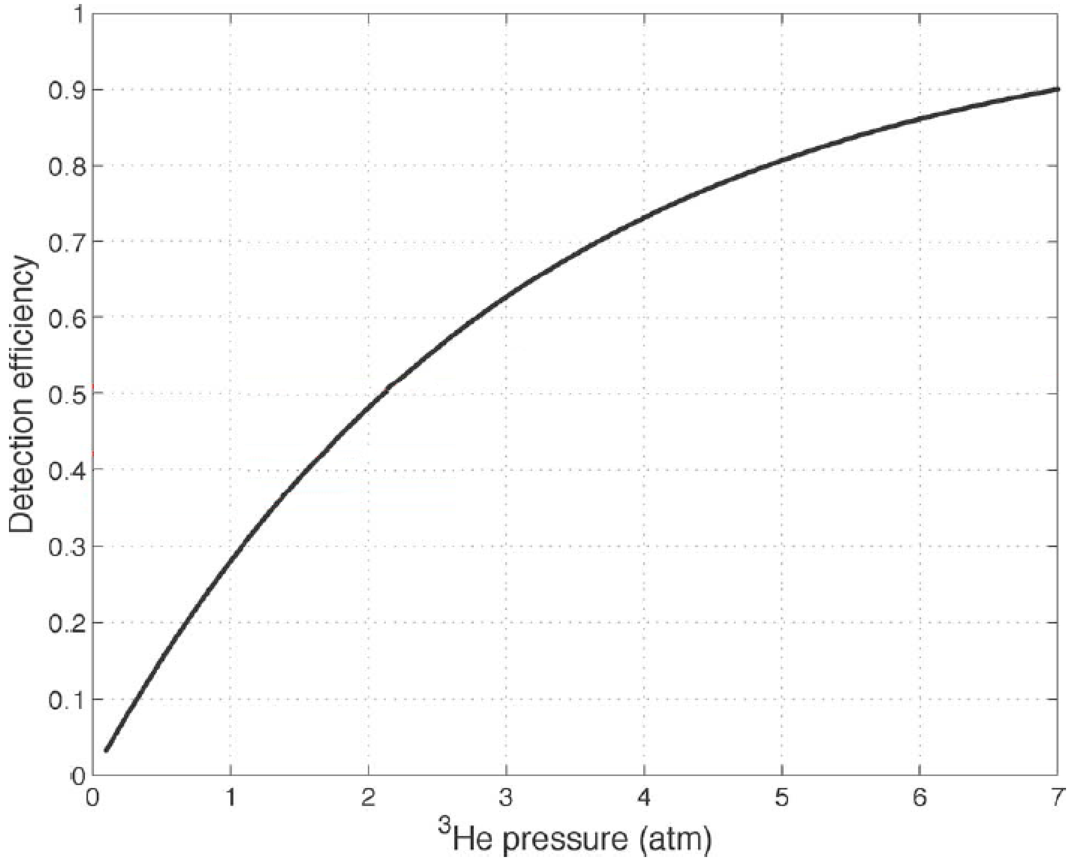

J. L. Lacy et al., "The Evolution of Neutron Straw Detector -Applications in Homeland Security", IEEE Transactions on Nucl. Science, 60,2,2013

Fig. 7. Intrinsic thermal neutron efficiency of a 2.92 cm (1.15in) ^{3}He tube as a function of gas pressure. The horizontal lines mark the efficiency calculated by (3).

CASCADE

Spin Echo

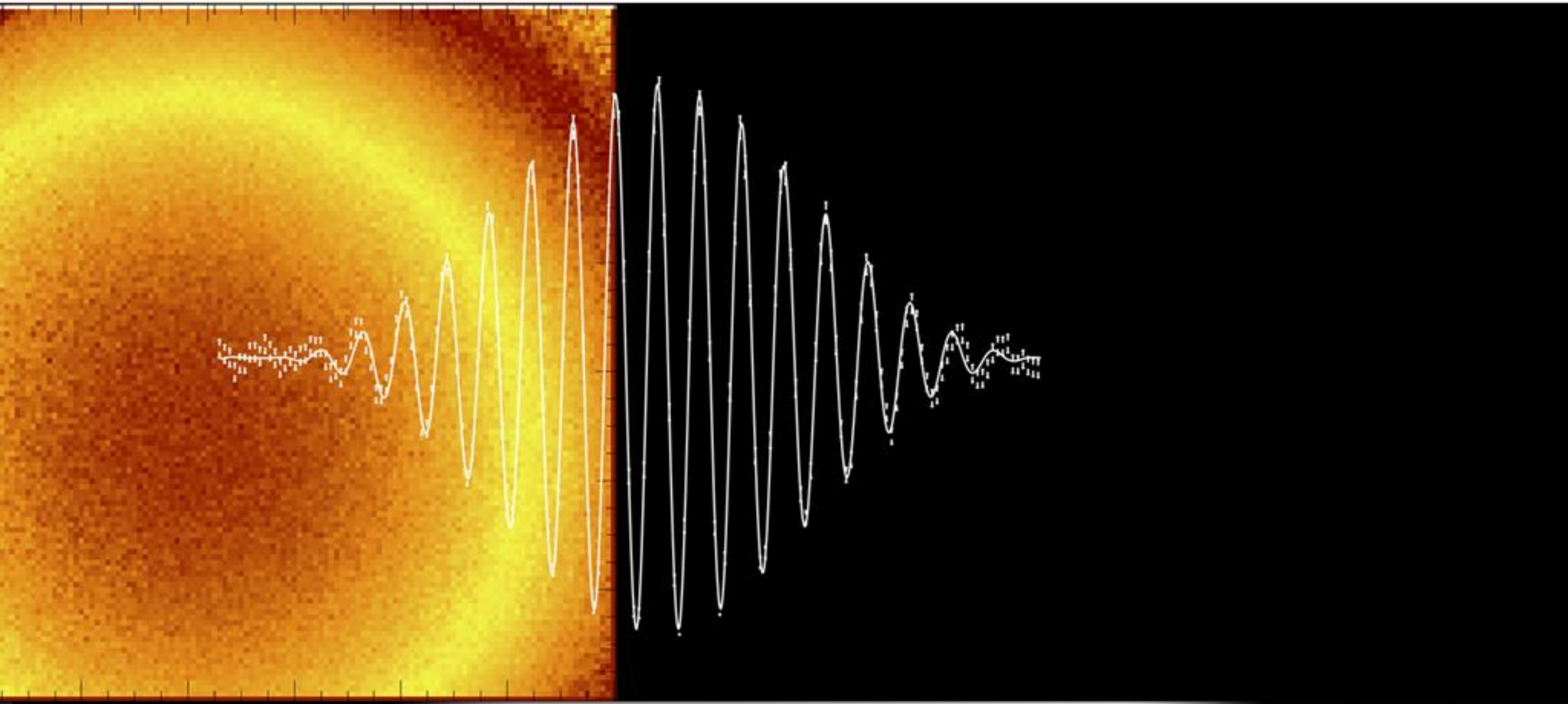

Spin Echo

1972, F. Mezei, ILL

Spin Echo

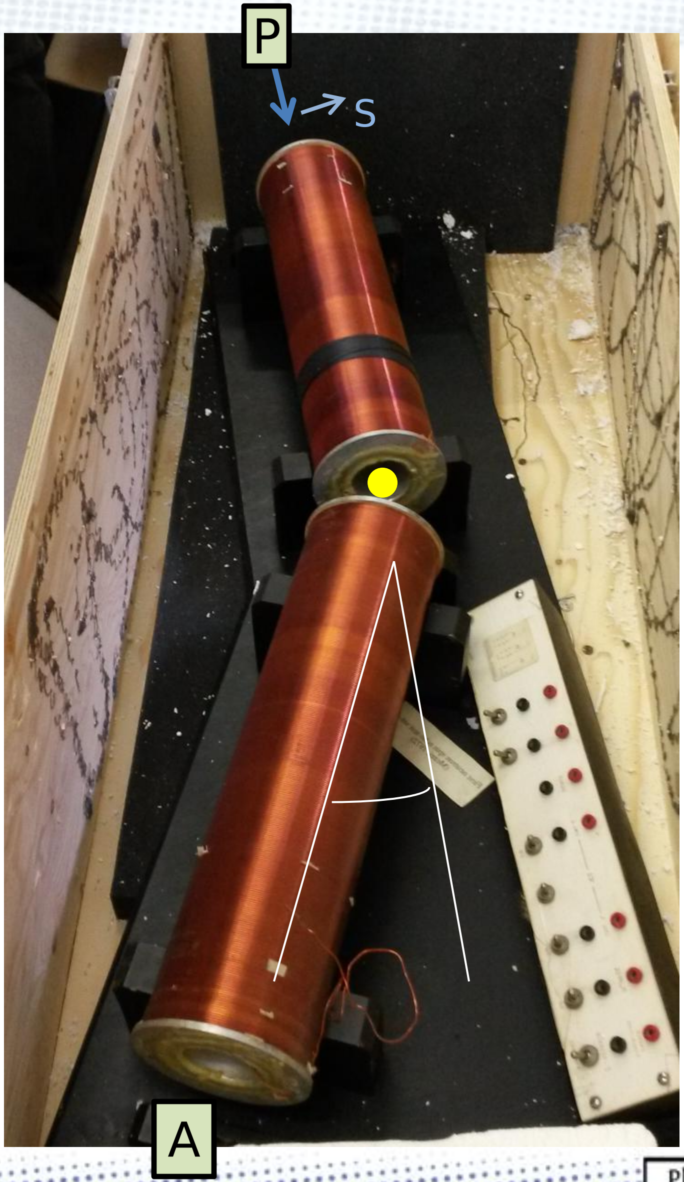

1972, F. Mezei, ILL

Spin Echo

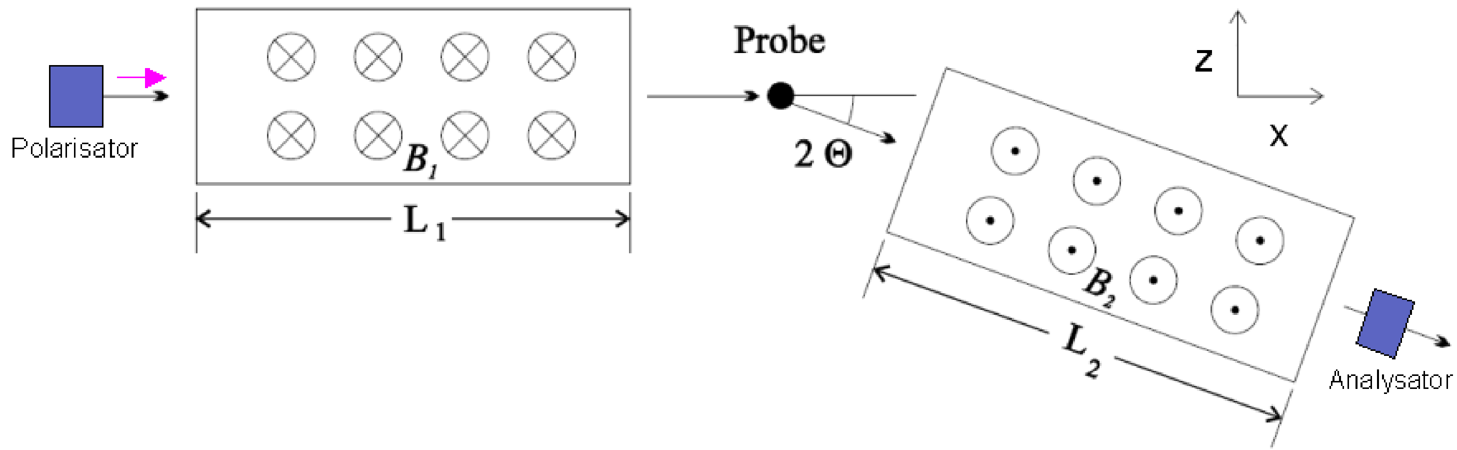

Polarisator
B_1
L_1
Probe
2Θ
z
x
B_2
L_2
Analysator

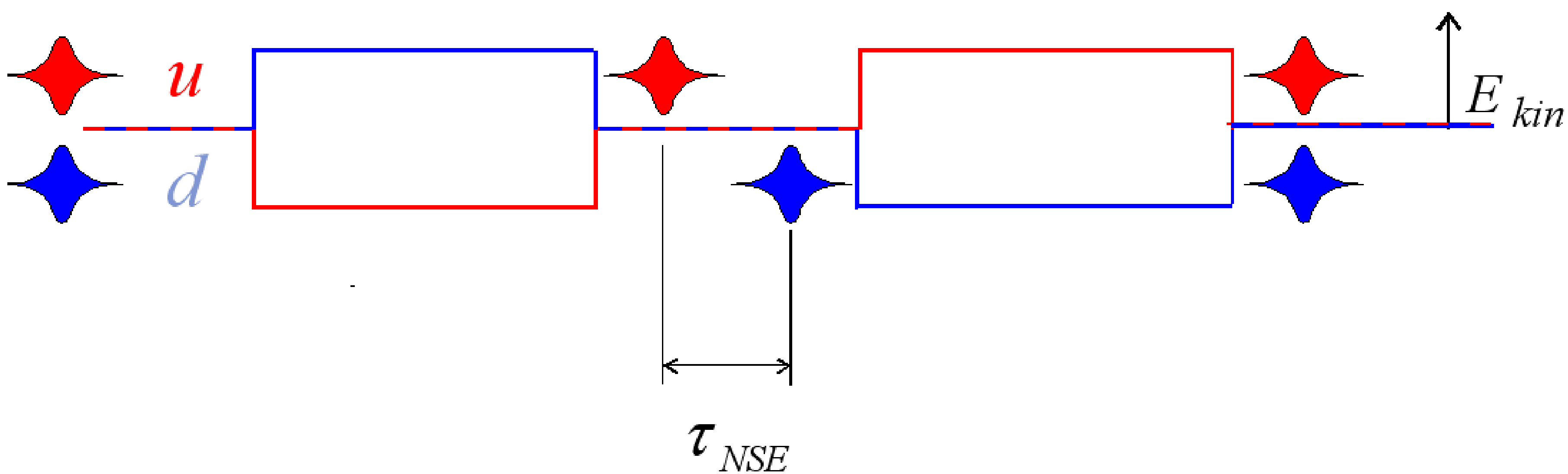

u
d
E_{kin}
τ_{NSE}

Spin Echo

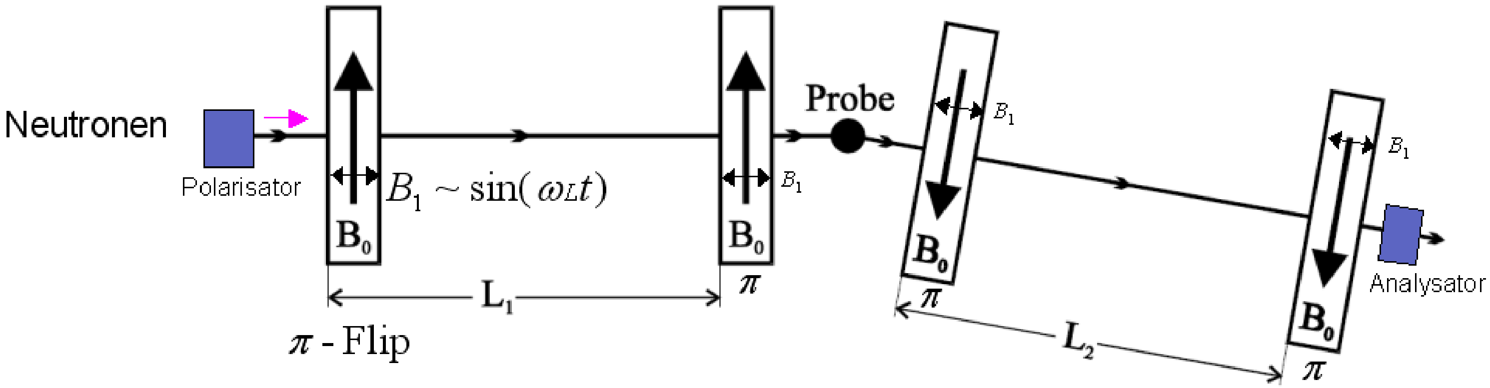

Neutronen
Polarisator
B_0
$B_1 \sim \sin(\omega_L t)$
B_1
B_0
π
Probe
B_1
B_0
π
B_1
B_0
π
Analysator
L_1
L_2
π - Flip

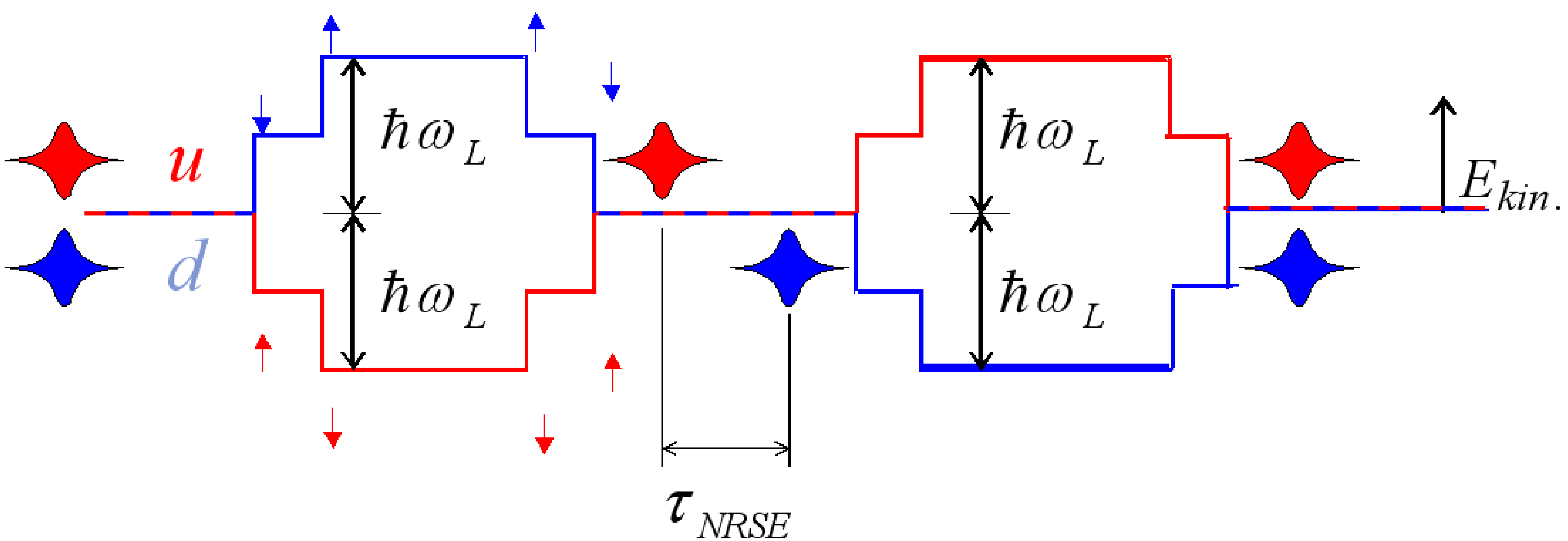

u
d
$\hbar\omega_L$
$\hbar\omega_L$
$\hbar\omega_L$
$\hbar\omega_L$
$E_{kin.}$
τ_{NRSE}

Spin Echo

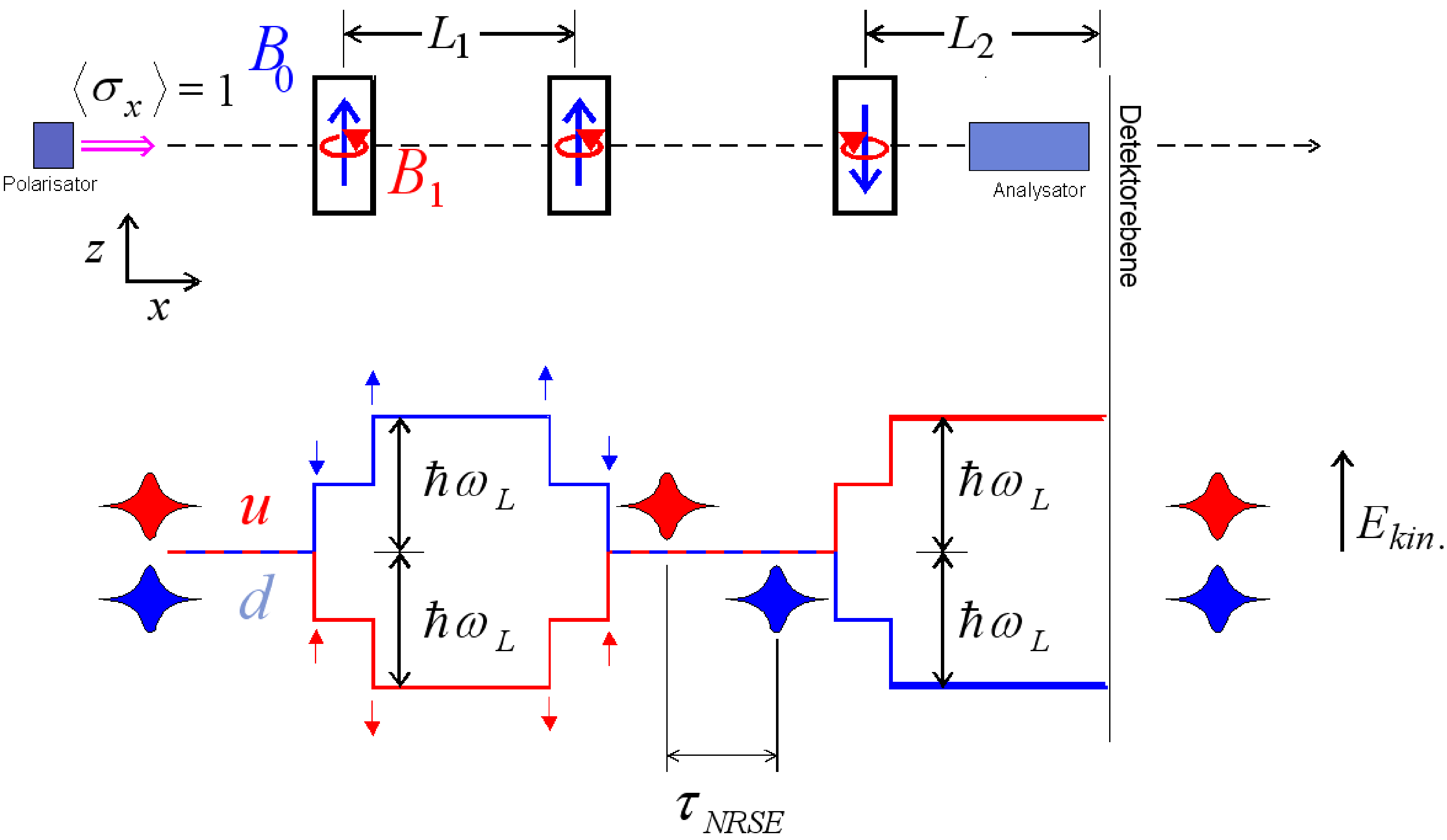

L_1
L_2
B_0
$\langle \sigma_x \rangle = 1$
Polarisator
B_1
Analysator
Detektorebene
z
x
u
d
$\hbar\omega_L$
$\hbar\omega_L$
$\hbar\omega_L$
$\hbar\omega_L$
$E_{kin.}$
τ_{NRSE}

Spin Echo - MIEZE

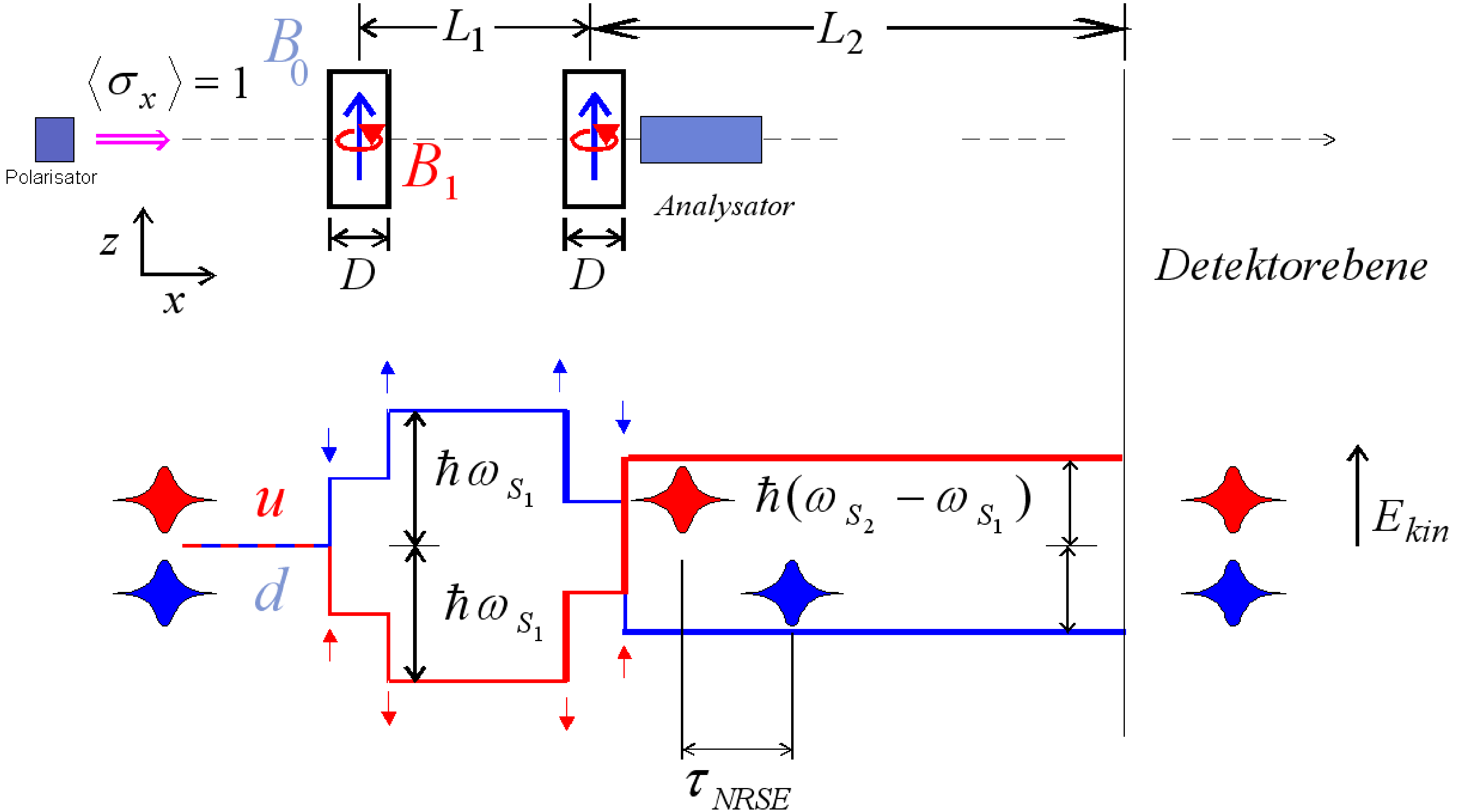

Spin Echo - MIEZE

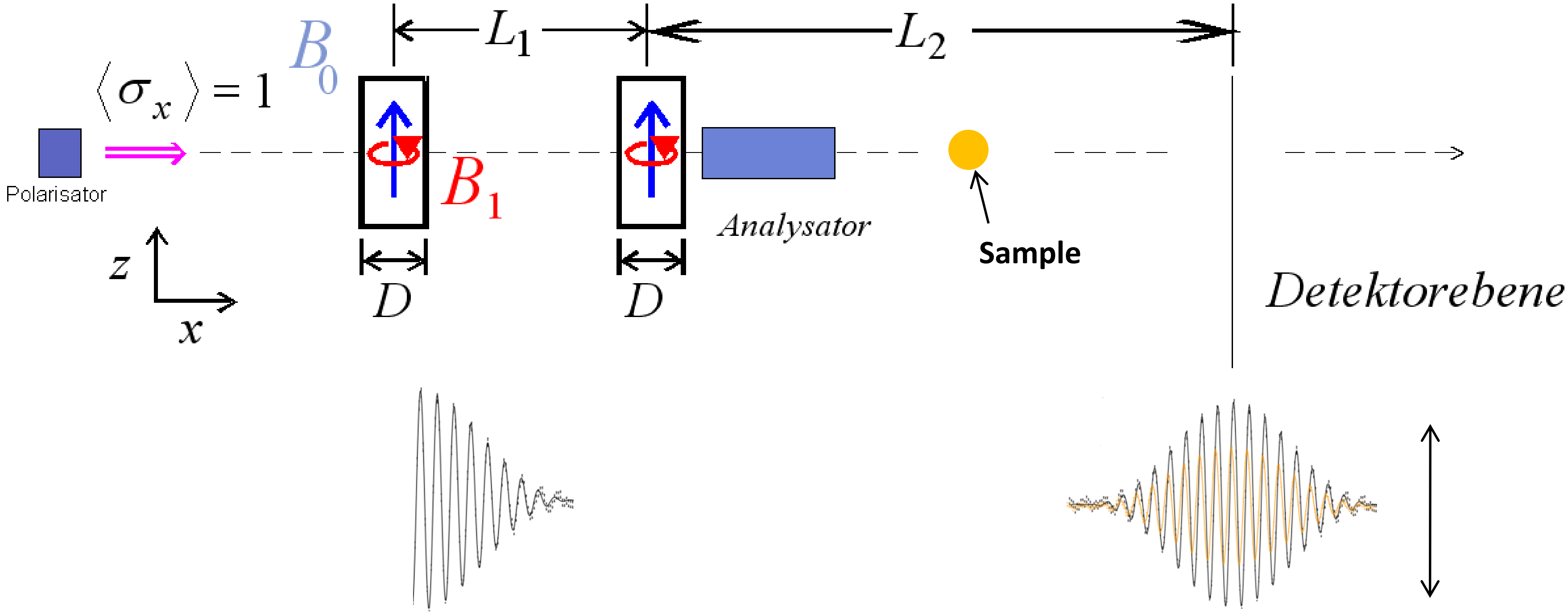

Spin Echo Example

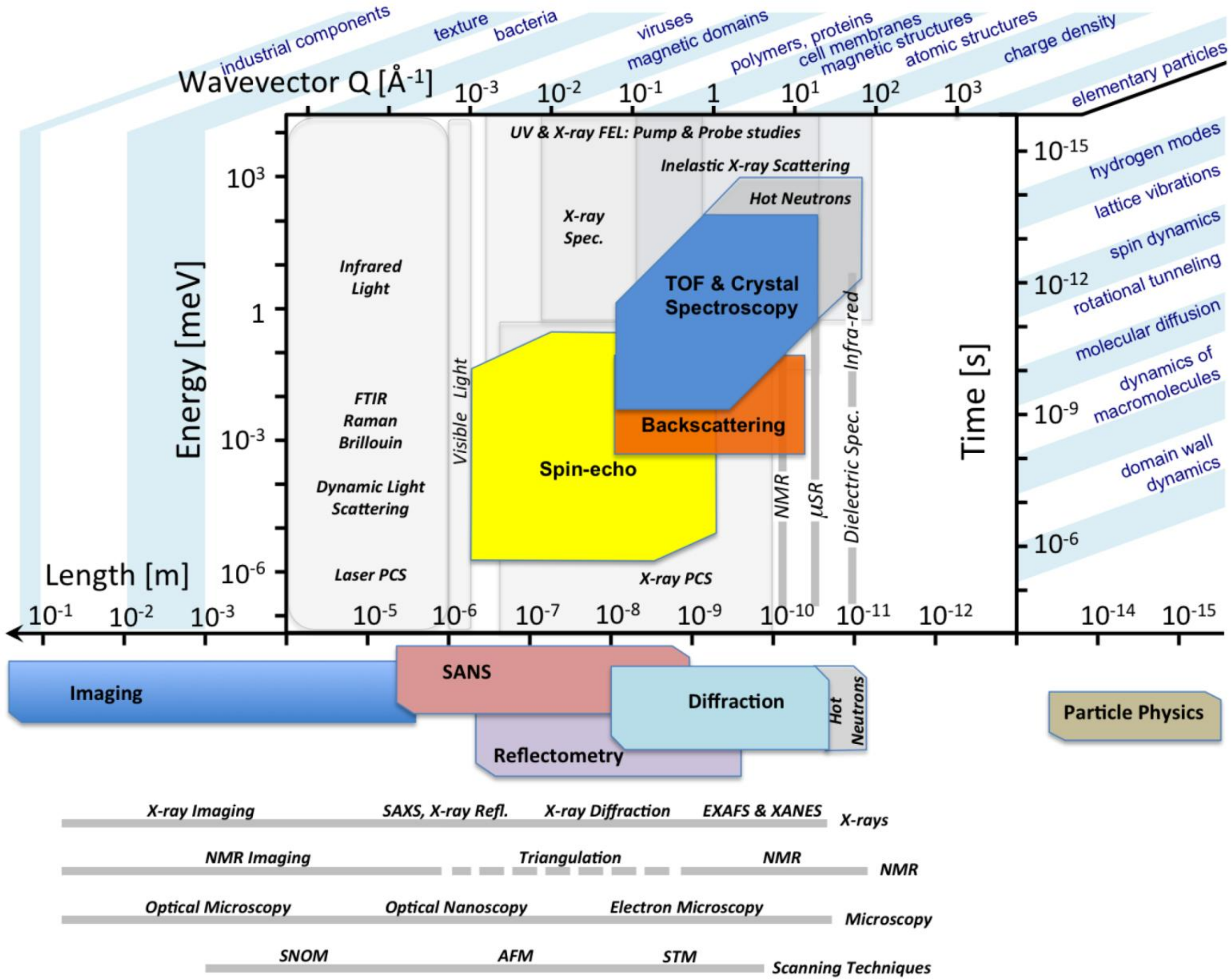

ESS TDR 2013

Spin Echo Example

Classical Diffusion of micelles

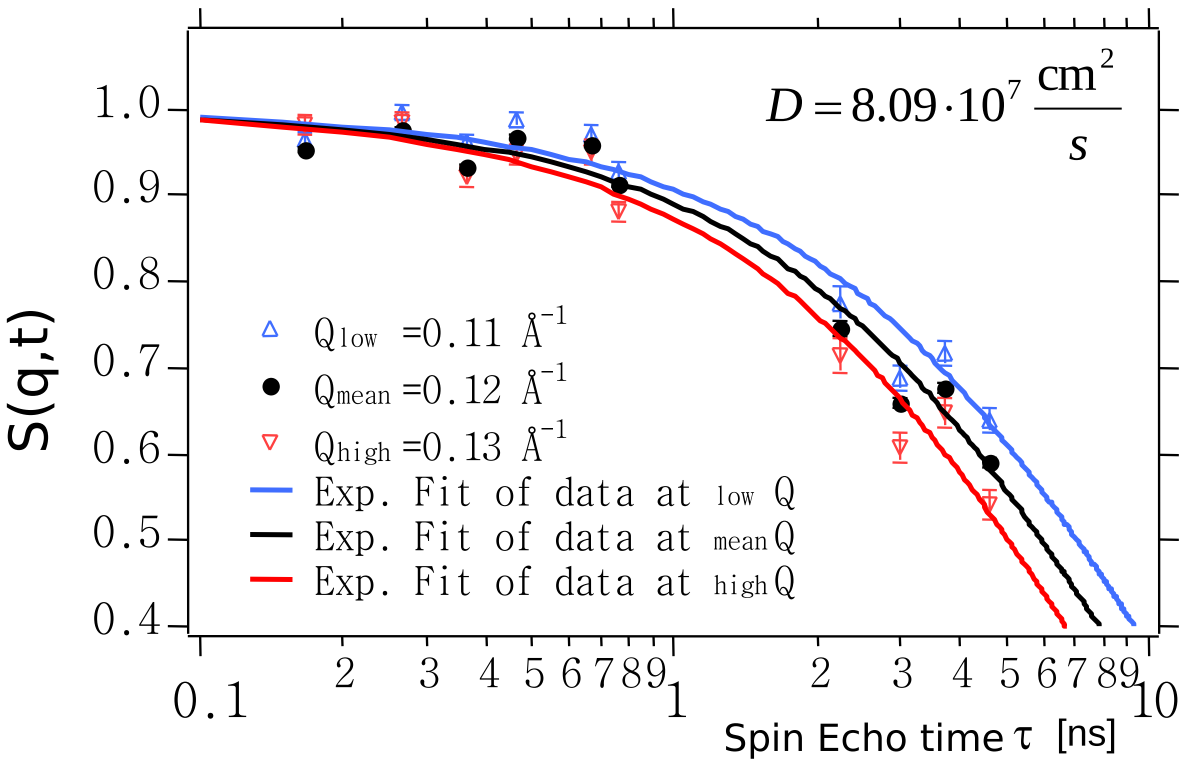

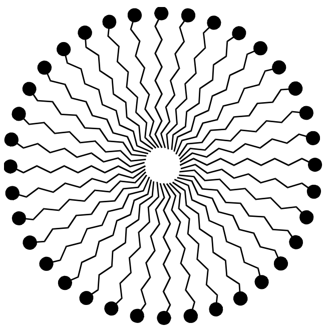

Natriumdodecylsulfat

in D_2O

for classical diffusion :

$$\tilde{S}_{inc}(\vec{q},t) \propto e^{-Dq^2 t}$$

Spin Echo Measurements

RESEDA, FRMII: spectrometer arms
3 – 15 Å @ 11% FWHM

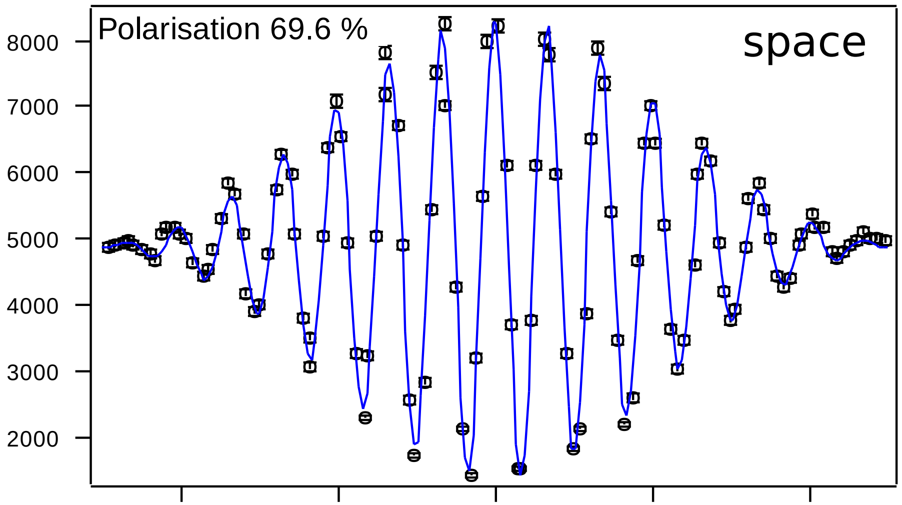

Spin Echo Measurements

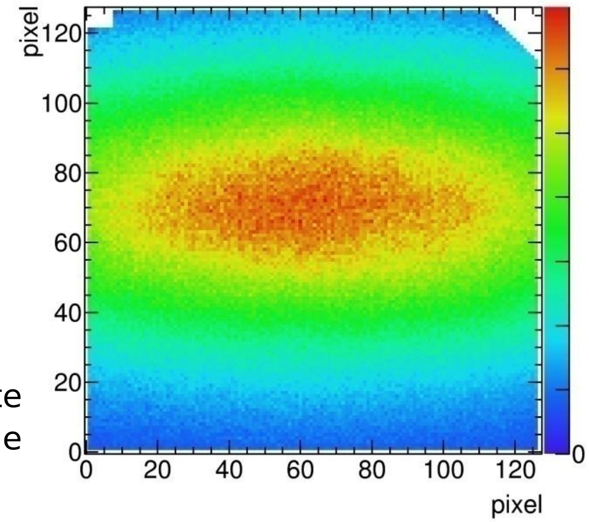

Graphite Sample

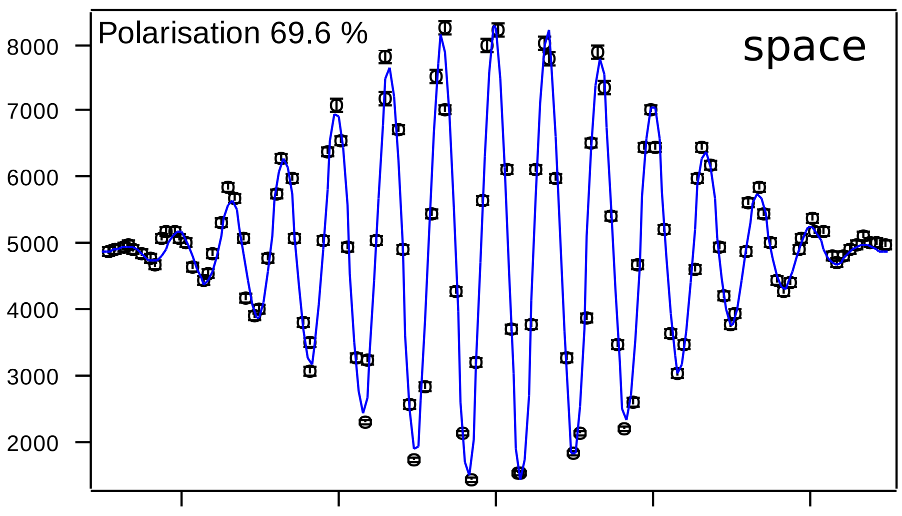

Typical Spin Echo group

Spin Echo Measurements

100 kHz x16

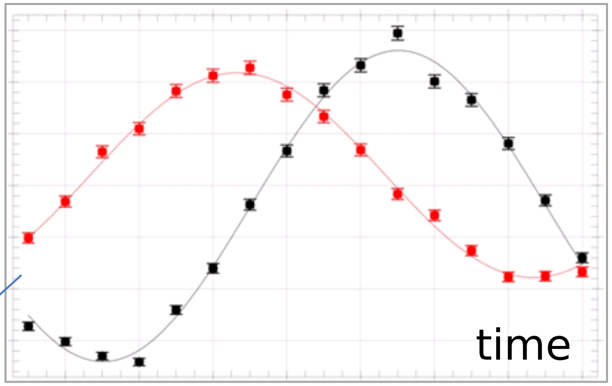

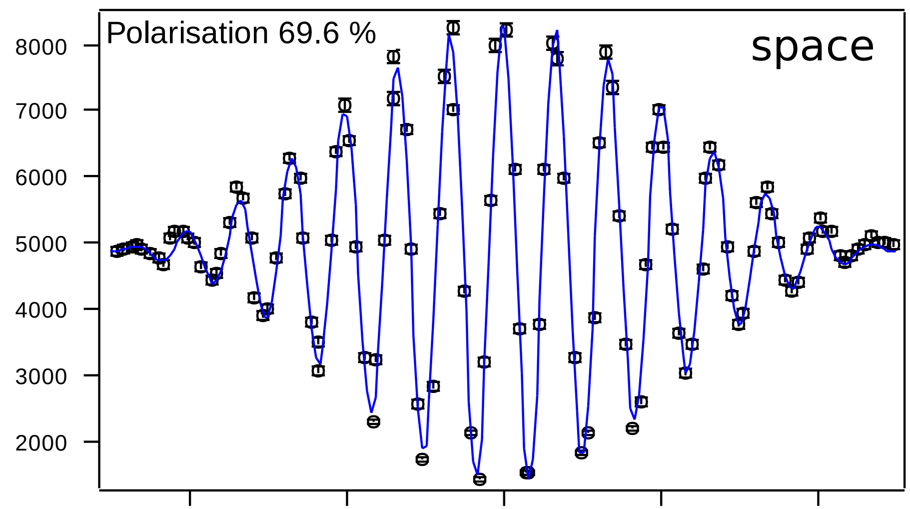

Typical Spin Echo group

Graphite Sample

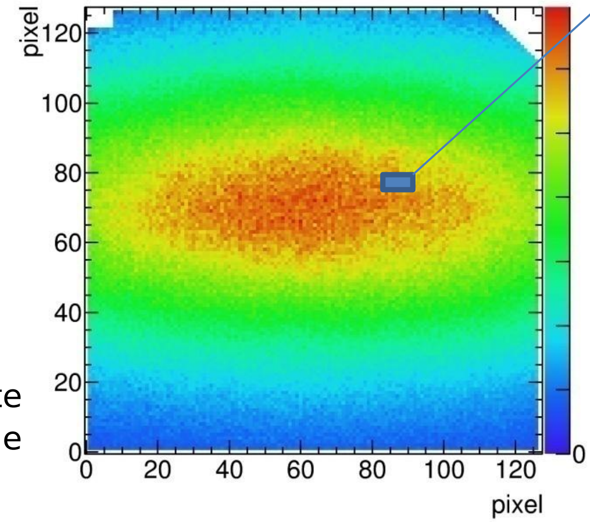

Spin Echo Measurements

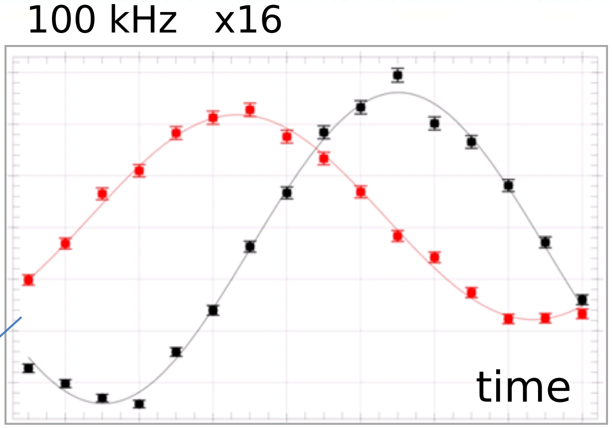

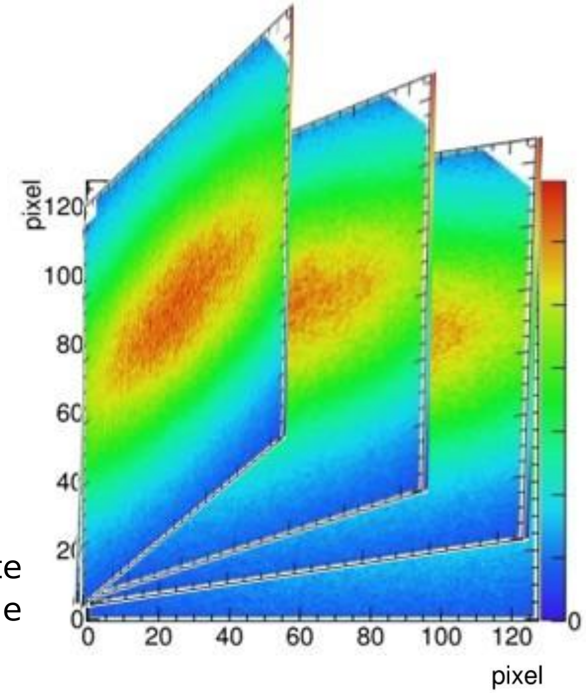

Graphite Sample

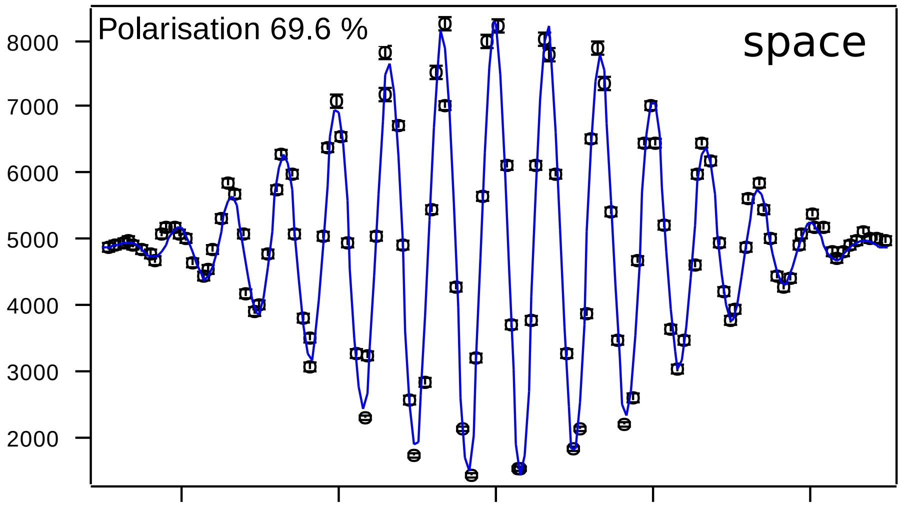

Typical Spin Echo group

Spin Echo Measurements

100 kHz x16

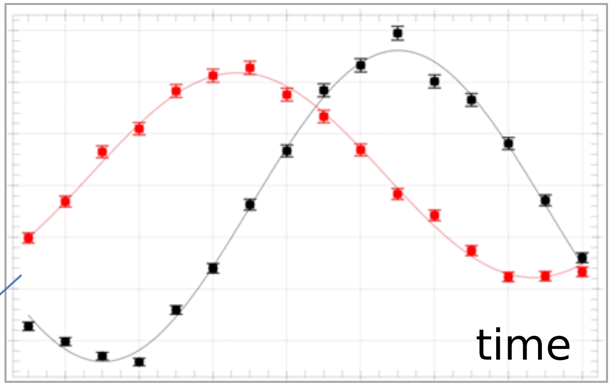

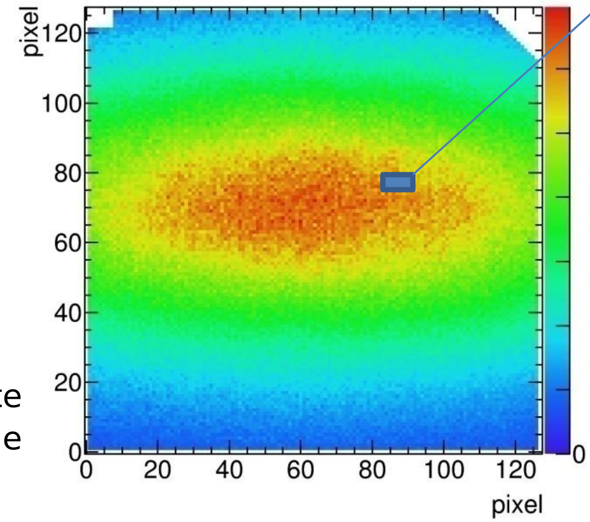

Graphite Sample

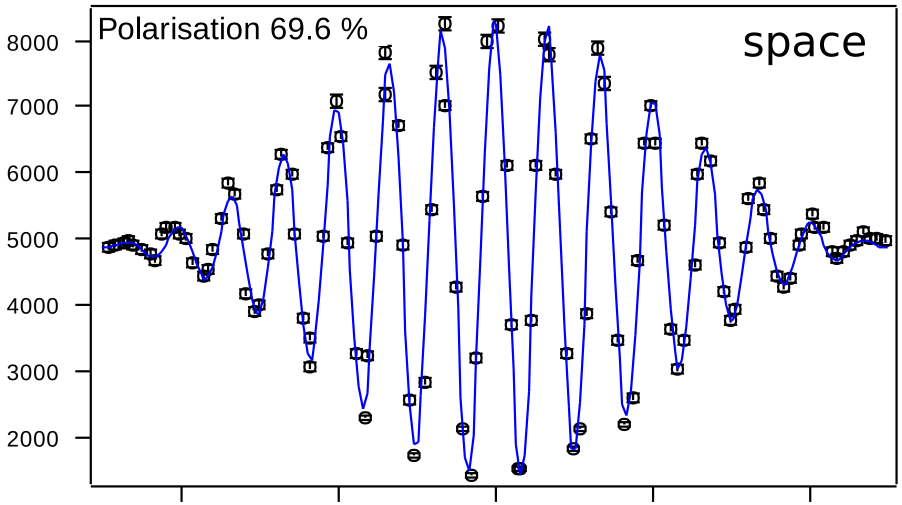

Typical Spin Echo group

Spin Echo Measurements

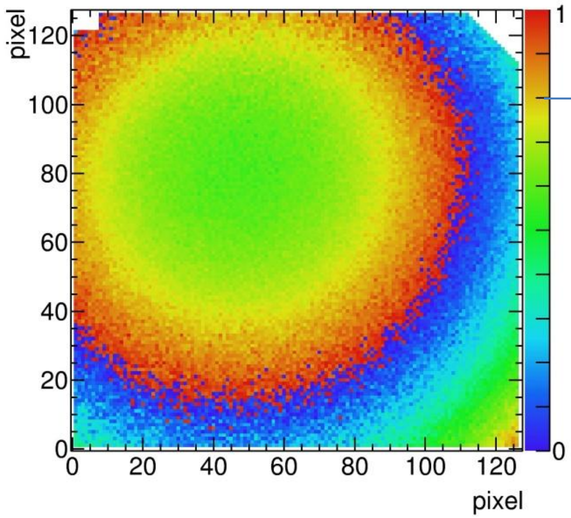

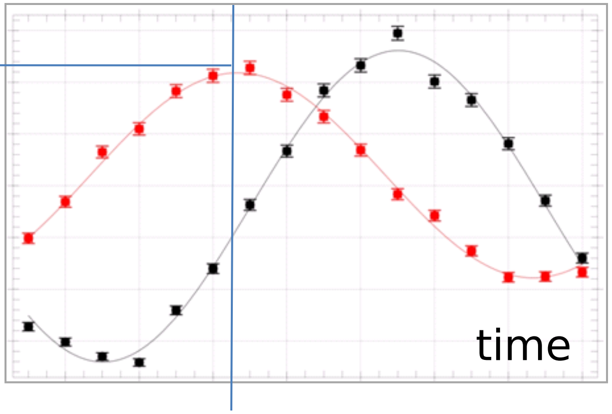

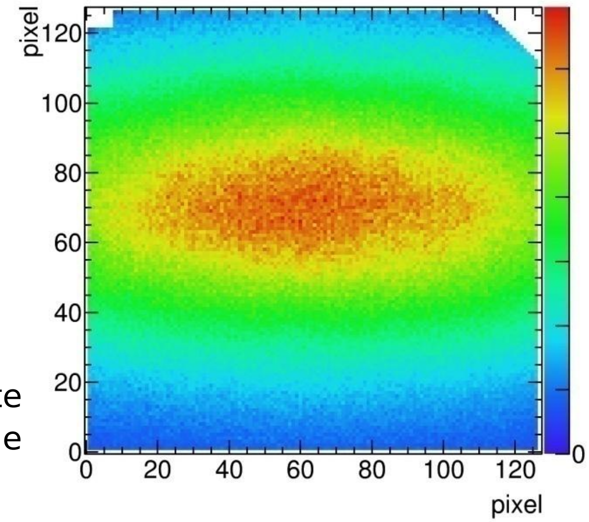

Graphite Sample

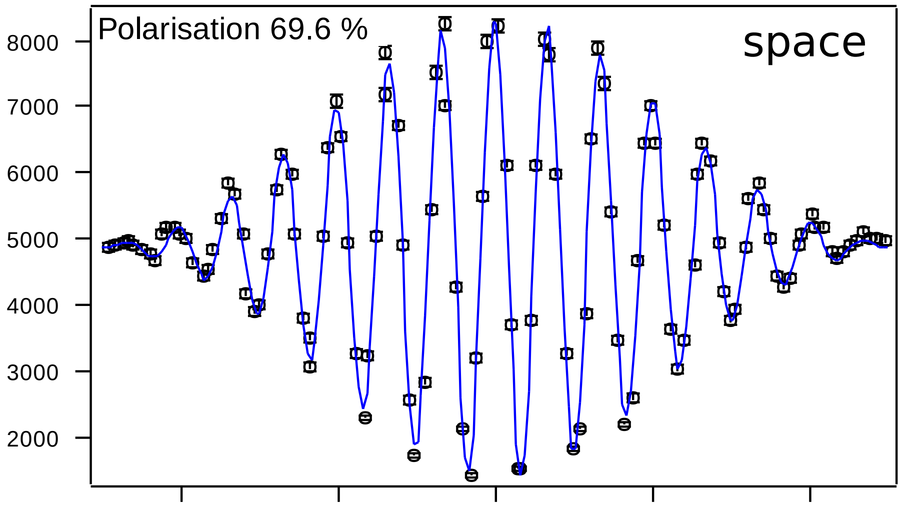

Typical Spin Echo group

Spin Echo Measurements

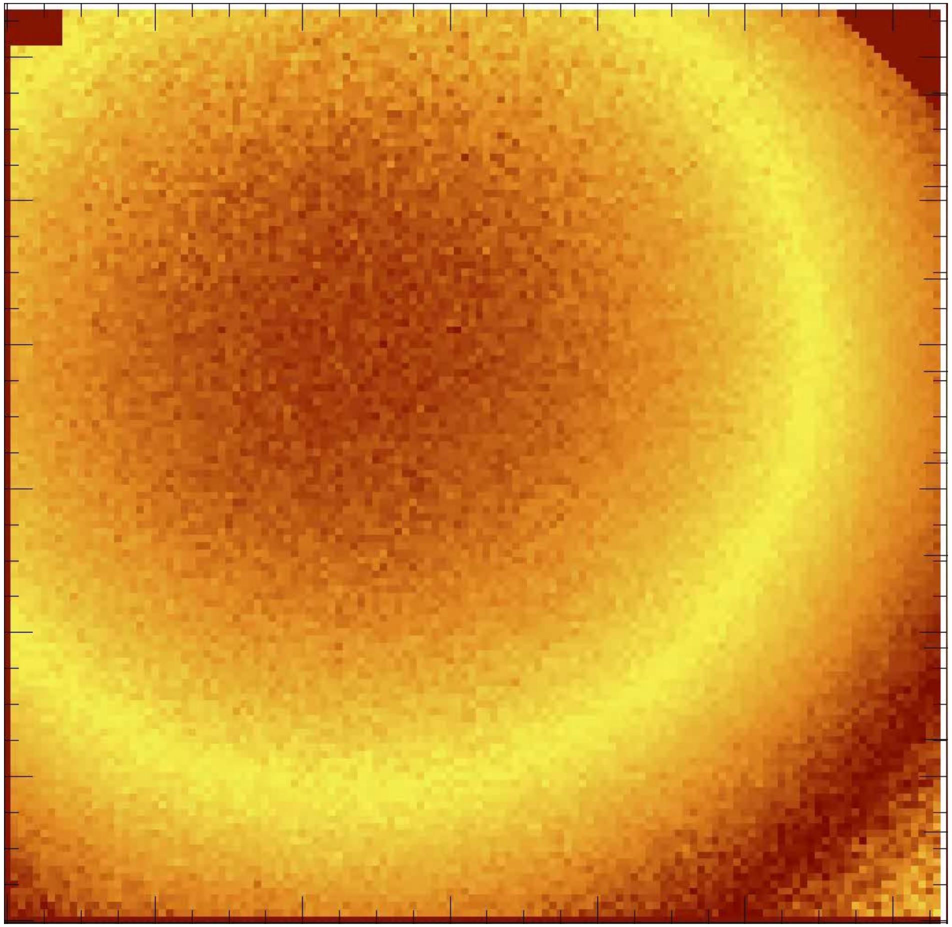

100 kHz x16

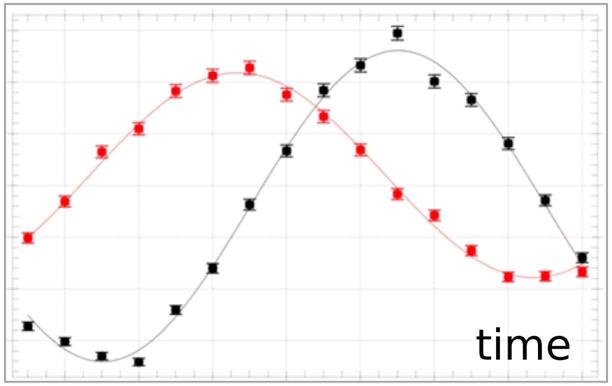

Spin Echo Measurements

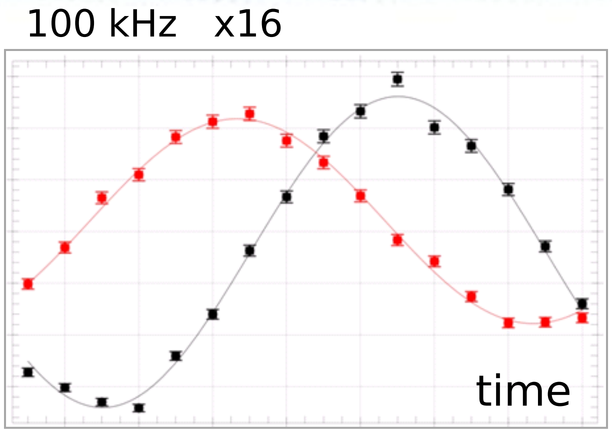

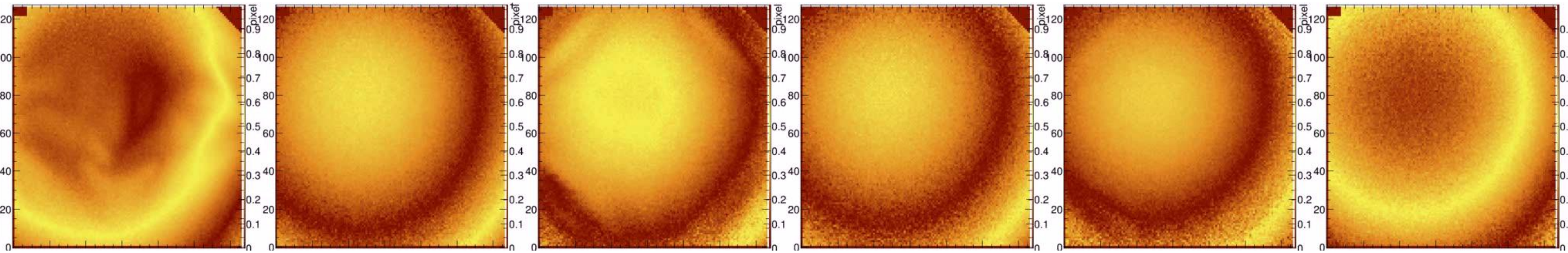

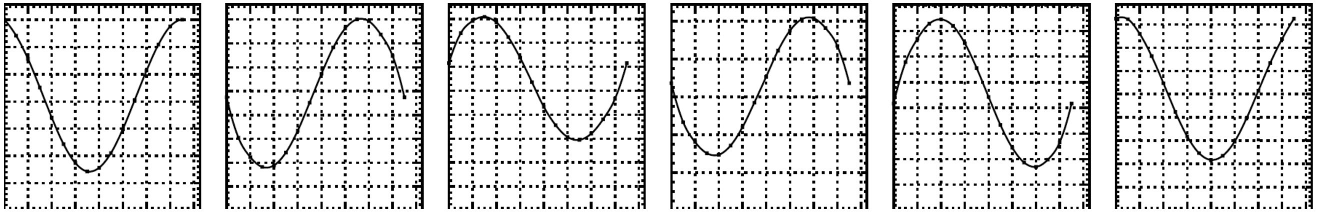

Spin Echo Measurements

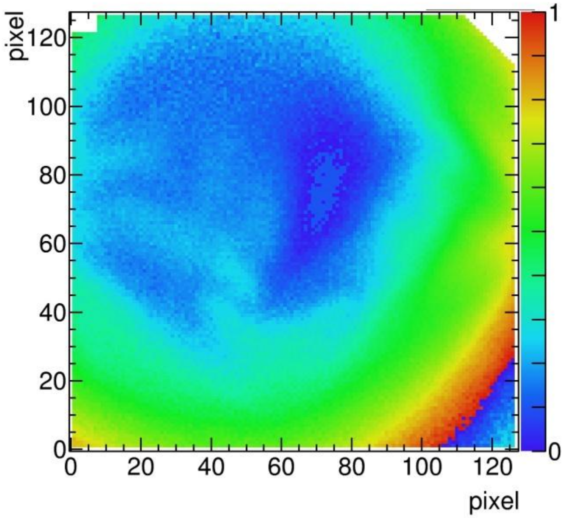

Graphite Sample

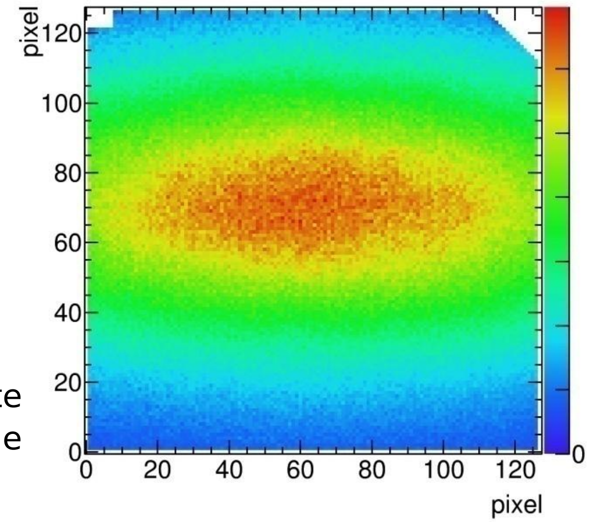

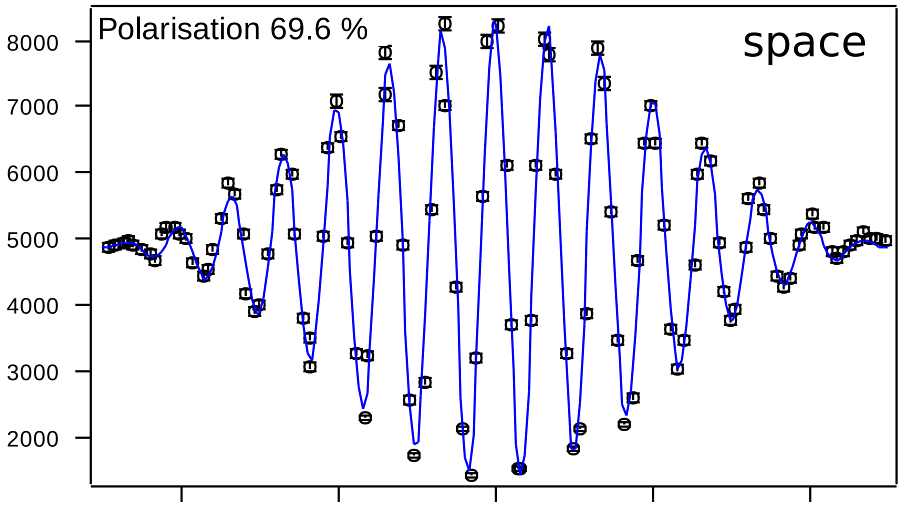

Typical Spin Echo group

Spin Echo Measurements

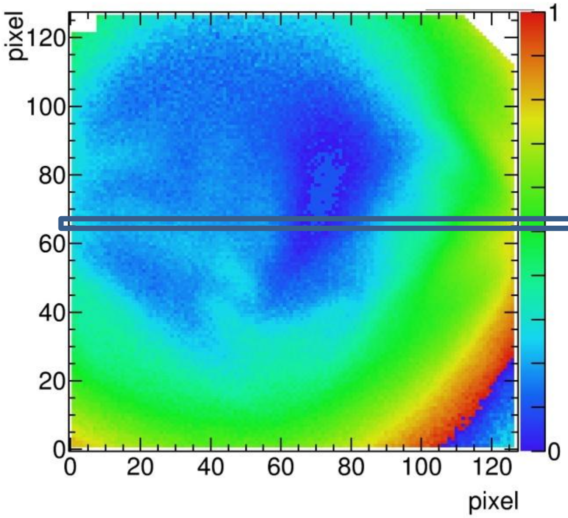

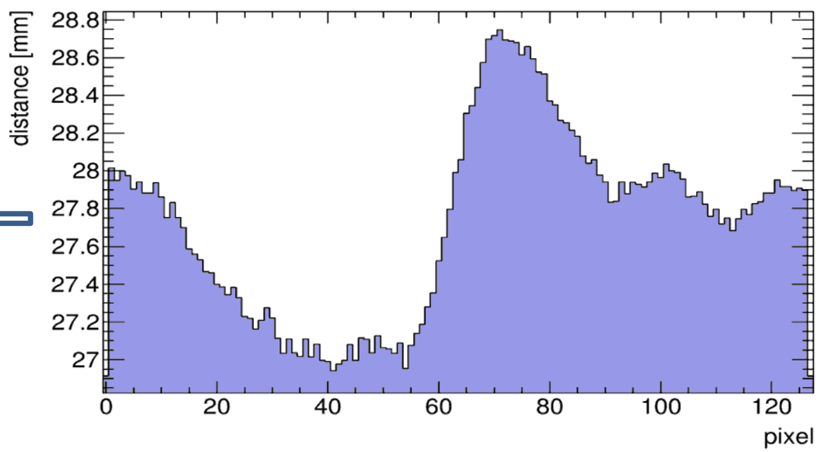

Graphite
Sample

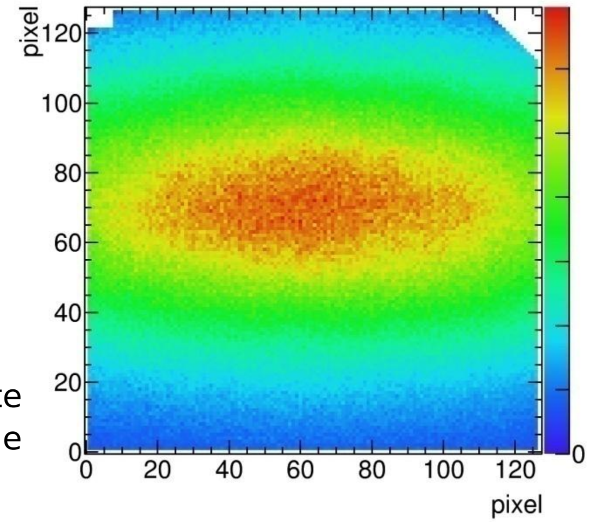

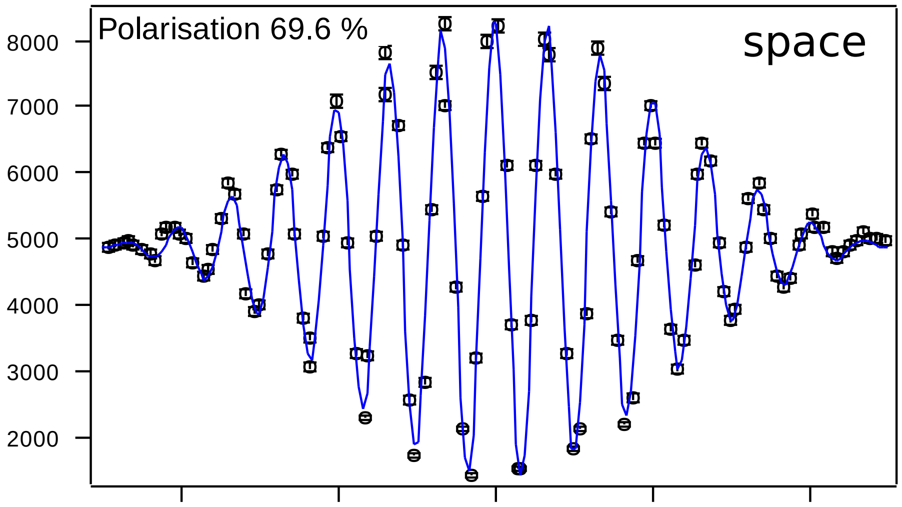

Typical Spin Echo group

CASCADE

Boron-10 technology

a high rate, spatially and time resolved detector for Spin Echo applications

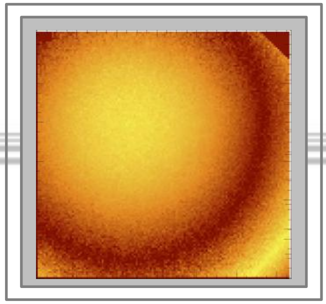

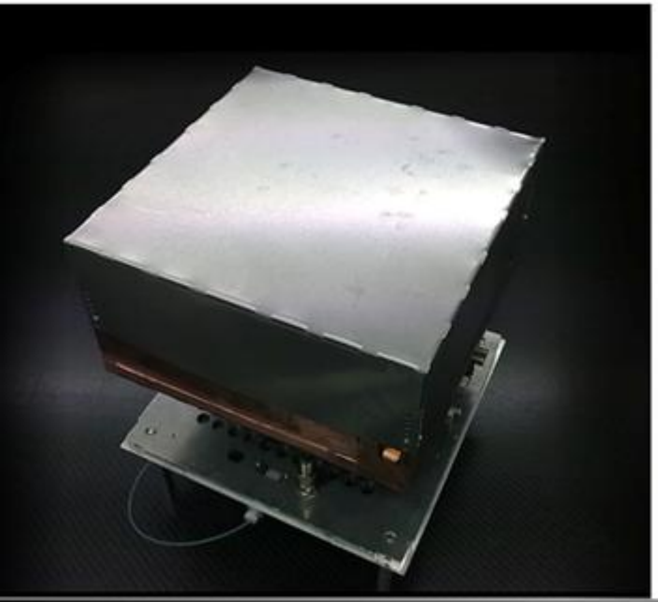

- conversion layer identification
- high TOF resolution (100 ns readout)
- 2.4 mm FWHM spatial resolution
- 2 MHz rate capability
- 21% thermal neutron efficiency @ 6 layers